DISSERTATION

submitted to the
Combined Faculties for the Natural Sciences and for Mathematics
of the Ruperto-Carola University of Heidelberg, Germany
for the degree of
Doctor of Natural Sciences

presented by

Diplom-Physiker Björn Feuerbacher,
born in Heidenheim

Oral examination: June 25, 2003

Perturbative Check of the Action and Energy Lattice Sum Rules

Referees: Prof. Dr. Heinz-Jürgen Rothe
and Prof. Dr. Dieter Gromes

Perturbative Überprüfung der Wirkungs- und Energie-Gittersummenregeln

Zusammenfassung

Gittersummenregeln werden mittels Störungstheorie auf dem Gitter überprüft. Die Wirkungssummenregel liefert eine Beziehung zwischen dem Quark-Antiquark-Potential, dessen logarithmischer Ableitung nach dem Abstand und dem Erwartungswert der Wirkung; die Energiesummenregel drückt das Potential als Summe der Energie in den Gluonenfeldern und eines anomalen Terms aus. Zwei verschiedene unabhängige Berechnungen des Quark-Antiquark-Potentials werden vorgestellt, und die Transversalität der gluonischen Vakuumpolarisation auf dem Gitter wird bewiesen. Der wesentliche Teil der Wirkungssummenregel ist eine Identität, deren explizite Überprüfung Methoden und Ergebnisse zur Verfügung stellt, die bei der Behandlung der Energiesummenregel nützlich werden. Zusätzlich wird die Eichinvarianz des Erwartungswertes des Wilson-Loops bis zur nächstführenden Ordnung bewiesen. Die Möglichkeit, den Erwartungswert der Wirkung auf den Erwartungswert der Summe der Plaketten zu einer festen Zeit einzuschränken, wird diskutiert. Die Energiesummenregel wird störungstheoretisch bis zur nächstführenden Ordnung überprüft, und es wird gezeigt, dass sie mit guter numerischer Genauigkeit erfüllt ist. Die einzelnen Beiträge zum Quark-Antiquark-Potential werden analysiert, und die Einschränkung des Erwartungswertes der Summe über alle räumlichen Plaketten (die Energie in den magnetischen Feldern) auf den Erwartungswert der Summe der räumlichen Plaketten zu einer festen Zeit wird untersucht.

Perturbative Check of the Action and Energy Lattice Sum Rules

Abstract

Lattice sum rules are checked using lattice perturbation theory. The action sum rule gives a relation between the quark-antiquark potential, its logarithmic derivative with respect to distance and the expectation value of the action; the energy sum rule expresses the potential as the sum of the energy in the gluon fields and of an anomalous term. Two different independent calculations of the quark-antiquark potential are presented, and the transversality of the gluonic vacuum polarization on the lattice is proven. The crucial part of the action sum rule is an identity whose explicit check using perturbation theory provides methods and results which are useful for checking the energy sum rule. Additionally, the gauge invariance of the expectation value of the Wilson loop up to next-to-leading order is proven. The possibility of restricting the expectation value of the action to one fixed time slice is discussed. The energy sum rule is checked perturbatively up to next-to-leading order and shown to be satisfied with good numerical accuracy. The various contributions to the quark-antiquark potential are analyzed, and the restriction of the expectation value of the sum over all spatial plaquettes (the energy in the magnetic fields) to one fixed time slice is examined.

There are very beautiful and elegant ways of getting these things these days; but suppose that you were inventing it, what would you do to find [it]? You fiddle around. All the elegant stuff is found later; the way to learn is not to learn elegant things, it's to fiddle around blind and stupid. Later you see how it works; polish it up; remove the scaffolding and publish the result for other students to be amazed at your ingenuity.

Richard Feynman

Contents

Chapter 1

Introduction

1.1 Quantum Chromodynamics

Only 40 years ago, protons and neutrons were still assumed to be elementary particles. But already in the fifties of the 20th century, more and more new so-called "elementary" particles had been found at high energy colliders (see, for example, [1]); eventually dozens were known, most of them with very short life times.

The turning point came 1964 with the invention of the quark model [2, 3], which postulates that all of these particles (nowadays known as *hadrons*) are composed of sub-particles, the *quarks*. With this model, the variety of hadrons could be sorted in a systematic way: the particles with integer spin, the *mesons*, consist of a quark-antiquark-pair, the particles with half-integer spin, the *baryons*, are bound states of three quarks or three antiquarks. Today hundreds of hadrons are known, and most of them fit well into the quark model. The few exceptions can be attributed to so-called *glueballs* and other exotic states.

Early experimental support came from high-energy scattering experiments, which showed that there are sub-particles, called *partons*, in the proton [4]. The scale invariance which was observed in these experiments was well explained by the quark model [5]. Based on these and many other experimental results, nowadays the quark model is universally accepted; a good introduction can be found in [6], for instance.

The theoretical description of the quarks and their interactions is provided by Quantum Chromodynamics (QCD) [7, 8]. In this quantum field theory, the quarks are described by Dirac spinors with an additional degree of freedom called *color*; they are coupled to $SU(3)$ gauge fields. The quantization of the bosonic gauge fields leads to the eight spin-one particles called *gluons* which mediate the interactions of the quarks. A prediction of QCD is the existence of bound states from these gluon fields, the already above mentioned glueballs. An early theoretical review of QCD can be found in [9]; for a review of the experimental support see, for instance, [10] and [11].

A large problem remains, however: no free quarks or gluons ever have been observed, despite all efforts taken in the years following the invention of the

quark model [12]. The standard explanation for this is that quarks and gluons can only exist in bound states; this phenomenon is called *confinement*.

It can be explained if one assumes that the force between the quark-antiquark pair does not decrease with increasing distance as in electrodynamics, but instead stays constant—a flux tube or *string* of gluons forms between the quarks. Therefore, if the distance is increased, a point will be reached at which the gluon string contains enough energy for the generation of a new quark-antiquark pair out of the vacuum, breaking the string. Hence instead of separating the original quark-antiquark-pair, one has produced two new pairs (this effect is called *screening* of the color charge). Recent Monte Carlo simulations on the lattice (see below) confirm this picture [13].

1.2 Lattice Gauge Theory

The most commonly used method in Quantum Field Theory is perturbation theory. But for many important problems, unfortunately including quark confinement, perturbative expansions fail: In QCD, the coupling constant is small at high energies, corresponding to small separations of the quarks (this is known as *asymptotic freedom* and is based on the non-abelian nature of the gauge group), but large at the low energies and relatively large distances occuring in hadronic bound states. Therefore many non-perturbative methods have been developed in the past decades in order to treat confinement.

Most promising is the formulation of QCD on a space-time lattice: space and time are discretized, so that the number of degrees of freedom is reduced drastically. Usually one works in euclidean space-time. If additionally one only looks at a finite volume and a finite time interval, there is only a finite number of degrees of freedom left, and the generating functional for this discretized version of QCD can in principle be calculated on a computer. In the limit of infinitely small lattice spacing, the results one obtains should reduce to the continuum results.

Lattice formulations of QCD where first suggested 1974 by Wilson [14], Kogut and Susskind [15]. In the three decades since these proposals, lattice gauge theory has become a branch of particle physics in its own right. Additionally, it is closely connected to statistical mechanics and therefore of interest not only to particle physicist, but also to physicists working on solid state physics and other many-particle problems. Today, there are lots of encouraging results from lattice calculations, including the quark-antiquark potential, the string tension, hadron masses, the QCD phase transition from the hadronic bound states to a quark-gluon plasma and so on. An introduction to all of these concepts and a summary of the results can be found in [16], for example.

But one still has to use a very large number of degrees of freedom in order to get a reasonable approximation to continuum, infinite volume QCD. Because of this, very high-dimensional integrals have to be computed. For example, if one uses a lattice with an extension of only 10 in each of the four directions and for simplicity considers only the gauge fields, there are already 320.000 degrees of freedom ($10^4 \cdot 4$ (polarization) $\cdot\, 8$ (color)). Hence a 320.000-dimensional integral

has to be performed. Using only 10 points in every direction in this 320.000-dimensional space in order to evaluate this integral numerically, one would have to compute and add 10^{320000} terms!

Obviously this is not feasible; hence the numerical integrals are usually done by Monte Carlo methods. Most gauge field configurations have a large action and thus only contribute very little to the generating functional. Therefore the functional integral can be approximated by generating a sequence of gauge field configurations with a probability distribution given by the Boltzmann factor; this technique is called *importance sampling*. Then the expectation values of operators can be approximated by their ensemble average over these representative configurations.

Simulating the gauge fields is relatively simple; the quarks pose bigger problems—for example, *fermion doubling* [17] and the sign of the fermionic determinant. Therefore one often works in the so-called *quenched* approximation: one neglects the effects of dynamical quarks. Obviously the screening and the string breaking due to the creation of quark-antiquark pairs can not be observed in such simulations, but they still can give valuable results on the short distance behaviour of bound states.

For a description of the commonly used Monte Carlo algorithms and a review of the most important results, see e. g. [16].

1.3 Sum Rules for the Quark-Antiquark-Potential

Although the lattice results reproduce the expected behaviour of the quark-antiquark potential, including the confinement, quite nicely and give good estimates for the string tension, an analytic description would be preferable instead of these solely numerical results. In order to gain some insight into the quark-antiquark potential and the corresponding energy densities of the gluon fields, in 1987 C. Michael invented *lattice sum rules* [21]. These connect the quark-antiquark potential with the expectation values of the energy in the gluon fields; even a separation of the electric and magnetic contributions is possible.

However, Michael's derivation was partly incorrect (see below); this was pointed out by Dosch, Nachtmann and Rueter in 1995 [22]. Shortly afterwards H. J. Rothe published a corrected version [23], and when Michael extended his sum rules in 1996 [25], he took this correction into account. Additionally, Rothe discovered that the trace anomaly of the energy momentum tensor gives an important contribution to the quark-antiquark potential [24].

The main goal of this dissertation is a perturbative check of these sum rules. In the following subsections, their derivations will be presented, based on [23], [24] and [16]; then I will outline the problems with the sum rules which will be investigated using perturbation theory and give an overview of my approach to solve these problems. Some results will be presented for a general gauge group G, but in most cases I will restrict myself to the commonly used group $SU(N)$.

1.3.1 The Wilson Loop and Wilson's Action

The starting point for the derivation of both sum rules is the standard formula for the quark-antiquark potential $\hat{V}$:

$$\hat{V}(\hat{R}) = -\lim_{\hat{T}\to\infty} \frac{1}{\hat{T}} \ln < W(\hat{R},\hat{T}) > . \tag{1.1}$$

The Wilson loop $W(\hat{R},\hat{T})$ is the path ordered product of the link variables U_l along a closed rectangle C with spatial and temporal size $\hat{R}$ and $\hat{T}$, respectively:

$$W(\hat{R},\hat{T}) = \frac{1}{d(R)} \mathrm{Tr} \prod_{l\in C} U_l. \tag{1.2}$$

The link variables U_l are elements of the gauge group, and $d(R)$ is the dimension of the representation R of the group in which the sources of the gauge field are. Usually the fundamental representation F is used; then $d(R) = d(F) = N$ for the group $SU(N)$.

Wilson introduced this loop in 1974 as an order parameter for Quantum Chromodynamics [14]; a similar structure was already used in 1971 by F. J. Wegner for the Ising model [18]. The derivation of the formula (1.1) which connects the quark-antiquark-potential to the expectation value of the Wilson loop can be found in [19] and in the review article [20], for example.

The potential and the size parameters of the Wilson loop are measured in lattice spacings a:

$$\begin{aligned} \hat{R} &= \frac{R}{a} \\ \hat{T} &= \frac{T}{a} \\ \hat{V} &= V \cdot a. \end{aligned} \tag{1.3}$$

The expectation value in (1.1) is calculated with Wilson's action (the sum over all plaquettes) in the quenched approximation (no dynamical fermions):

$$S = \hat{\beta} \sum_{n,\mu,\nu} \left(1 - \frac{1}{2d(F)} \mathrm{Tr}(U_{\mu\nu}(n) + U^{\dagger}_{\mu\nu}(n)) \right) =: \hat{\beta}\mathcal{P} \tag{1.4}$$

with the lattice coupling constant

$$\hat{\beta} = \frac{2d(F)}{g_0^2} \tag{1.5}$$

and the plaquette variables

$$U_{\mu\nu}(n) = U_\mu(n) U_\nu(n+\hat{\mu}) U^{\dagger}_\mu(n+\hat{\nu}) U^{\dagger}_\nu(n), \tag{1.6}$$

where $\hat{\mu}$ resp. $\hat{\nu}$ are unit vectors pointing in the corresponding direction. The sum in the action runs over all lattice sites n and all possible orientations of the plaquettes.

1.3.2 Action Sum Rule

Taking the derivative of (1.1) with respect to the logarithm of the coupling constant, one arrives at:

$$\frac{\partial \hat{V}}{\partial \ln \hat{\beta}} = \hat{\beta}\frac{\partial \hat{V}}{\partial \hat{\beta}} = \lim_{\hat{T}\to\infty} \frac{1}{\hat{T}} < S >_{q\bar{q}-0}, \tag{1.7}$$

where for a general operator O, the expectation value in the quark-antiquark state with respect to the vacuum state is defined as

$$< O >_{q\bar{q}-0} = \frac{< OW >}{< W >} - < O > . \tag{1.8}$$

Now the scaling behaviour (1.3) of the potential can be used. In the continuum limit $a \to 0$, the physical potential V obviously should be independent of the lattice spacing. This gives:

$$\frac{d}{da}\left(\frac{\hat{V}\left(\frac{R}{a}, \hat{\beta}\right)}{a}\right) = 0 \qquad \text{for } a \to 0. \tag{1.9}$$

Carrying out the differentation, using the scaling behaviour of $\hat{R}$, the definition (1.5) and introducing the lattice beta function

$$\beta_L(g_0) = -a\frac{\partial g_0}{\partial a}, \tag{1.10}$$

one arrives at

$$\frac{2\beta_L}{g_0}\hat{\beta}\frac{\partial \hat{V}}{\partial \hat{\beta}} = \hat{V} + \hat{R}\frac{\partial \hat{V}}{\partial \hat{R}}. \tag{1.11}$$

Using this in (1.7), the result is:

$$\boxed{\hat{V} + \hat{R}\frac{\partial \hat{V}}{\partial \hat{R}} = \frac{2\beta_L}{g_0} \lim_{\hat{T}\to\infty} \frac{1}{\hat{T}} < S >_{q\bar{q}-0} .} \tag{1.12}$$

This is essentially the action sum rule for the quark-antiquark potential which was derived by H. J. Rothe in 1995 [23].

As already pointed out, Michael derived this sum rule first (in 1987, [21]), but instead of (1.11), he used a wrong scaling behaviour for the potential, and therefore in his final formula, the logarithmic derivative of the potential with respect to $\hat{R}$ was missing. For a confining potential, $\hat{V} \equiv \sigma\hat{R}$, this is crucial: using the correct sum rule, the left hand side gives $2\hat{V}$, whereas Michael's wrong sum rule only had $\hat{V}$ and therefore was wrong by a factor of 2.

On the other hand, in his 1987 paper, Michael claimed that the expectation value $< S >_{q\bar{q}-0}$ on the right hand side can be further simplified in the limit $\hat{T} \to \infty$ (for a more detailed derivation, using transfer matrix methods, see [29]): plaquettes on different time slices should give the *same* contribution to the expectation value, so that

$$< S >_{q\bar{q}-0} \to \hat{T} < L(t) >_{q\bar{q}-0}, \tag{1.13}$$

where $L(t)$ is the sum over all plaquettes at a *fixed* time slice t:

$$L(t) = \hat{\beta} \sum_{\vec{n},\mu,\nu} \left(1 - \frac{1}{2d(F)} \mathrm{Tr}(U_{\mu\nu}(\vec{n},t) + U^{\dagger}_{\mu\nu}(\vec{n},t))\right). \tag{1.14}$$

Obviously this is the Lagrangian at time t.

Therefore the action sum rule becomes:

$$\hat{V} + \hat{R}\frac{\partial \hat{V}}{\partial \hat{R}} = \frac{2\beta_L}{g_0} \lim_{\hat{T}\to\infty} < L(t) >_{q\bar{q}-0} . \tag{1.15}$$

Rothe noticed 1995 [24] that this can be rewritten using the trace anomaly of the energy momentum tensor. This was motivated by Ji's observation that this trace anomaly contributes 1/4 of the hadron masses [26]. Already in 1977 it had been shown by Collins, Dunkan and Joglekar [27] that the trace of the energy momentum tensor in the continuum formulation of $SU(N)$ gauge theory is given by

$$T^{\mu}_{\ \mu} = \frac{\beta(g)}{2g} F^{A}_{\mu\nu} F^{\mu\nu,A} = \frac{2\beta(g)}{g}\mathcal{L} \tag{1.16}$$

in the quenched approximation, where $\mathcal{L}$ is the Lagrangian density, which is exactly the combination appearing in the formula above. In 1992, Caracciolo, Menotti and Pelisetto showed that this is also true in lattice perturbation theory [28]. Using this one finally gets for the action sum rule:

$$\hat{V} + \hat{R}\frac{\partial \hat{V}}{\partial \hat{R}} = \lim_{\hat{T}\to\infty} \sum_{\vec{x},\mu} < T_{\mu\mu}(\vec{x},t) >_{q\bar{q}-0} . \tag{1.17}$$

1.3.3 Energy Sum Rule

In order to derive the energy sum rule, one has to use an anisotropic lattice with lattice spacing a_t in the temporal direction. The anisotropy parameter is defined as

$$\xi := a_t/a.$$

Then the action has to be rewritten:

$$\begin{aligned} S &= \hat{\beta}_s \sum_{n,j,k} \left(1 - \frac{1}{2d(F)} \mathrm{Tr}(U_{jk}(n) + U^{\dagger}_{jk}(n))\right) \\ &\quad + \hat{\beta}_t \sum_{n,j} \left(1 - \frac{1}{2d(F)} \mathrm{Tr}(U_{j4}(n) + U^{\dagger}_{j4}(n) + U_{4j}(n) + U^{\dagger}_{4j}(n))\right) \\ &=: \hat{\beta}_s \mathcal{P}_s + \hat{\beta}_t \mathcal{P}_t, \end{aligned} \tag{1.18}$$

where one has to use different coupling constants for the spatial and the temporal plaquettes.

In the continuum limit, the expectation value of the Wilson loop should be independent of the asymmetry, as long as the extension in the temporal direction is the same:

$$< W(\hat{R},\hat{T}) >_{\xi=1} = < W(\hat{R},\xi\hat{T}) >_{\xi} \qquad \text{for } a \to 0,$$

and accordingly

$$\hat{V}(\hat{R},\hat{\beta}) = \xi\tilde{V}(\hat{R},\hat{\beta}_s(\xi),\hat{\beta}_t(\xi))$$

with

$$\tilde{V}(\hat{R},\hat{\beta}_s(\xi),\hat{\beta}_t(\xi)) = -\lim_{\xi\hat{T}\to\infty}\frac{1}{\xi\hat{T}}\ln < W(\hat{R},\xi\hat{T}) > .$$

It follows that in the continuum limit

$$\frac{d}{d\xi}\left[\xi\tilde{V}(\hat{R},\hat{\beta}_s(\xi),\hat{\beta}_t(\xi))\right] = 0 \tag{1.19}$$

should be satisfied. Carrying out the differentation and then returning to the isotropic lattice by setting $\xi = 1$, one arrives at:

$$\hat{V}(\hat{R},\hat{\beta}) = -\lim_{\hat{T}\to\infty}\frac{1}{\hat{T}}\left[\frac{\partial\hat{\beta}_t}{\partial\xi} < \mathcal{P}_t >_{q\bar{q}-0} + \frac{\partial\hat{\beta}_s}{\partial\xi} < \mathcal{P}_s >_{q\bar{q}-0}\right]_{\xi=1} . \tag{1.20}$$

With the abbreviations

$$\eta_\pm := \frac{1}{2}\left[\frac{\partial\hat{\beta}_t}{\partial\xi} \pm \frac{\partial\hat{\beta}_s}{\partial\xi}\right]_{\xi=1} , \tag{1.21}$$

this can be rewritten as

$$\hat{V}(\hat{R},\hat{\beta}) = \lim_{\hat{T}\to\infty}\frac{1}{\hat{T}}\left[\eta_- < -\mathcal{P}_t + \mathcal{P}_s >_{q\bar{q}-0} - \eta_+ < \mathcal{P}_t + \mathcal{P}_s >_{q\bar{q}-0}\right].$$

In [42], Karsch had shown that

$$\eta_+ = -\frac{1}{4}\frac{2\beta_L(g_0)}{g_0}\hat{\beta} \tag{1.22}$$

by requiring that the string tension calculated from space-time-like Wilson loops should be identical to the one calculated from purely spatial ones. Hence the potential becomes:

$$\hat{V}(\hat{R},\hat{\beta}) = \lim_{\hat{T}\to\infty}\frac{1}{\hat{T}}\left[\eta_- < -\mathcal{P}_t + \mathcal{P}_s >_{q\bar{q}-0} + \frac{1}{4}\frac{2\beta_L(g_0)}{g_0}\hat{\beta} < \mathcal{P}_t + \mathcal{P}_s >_{q\bar{q}-0}\right],$$

where obviously the second term contains the expectation value of the action:

$$\boxed{\hat{V}(\hat{R},\hat{\beta}) = \lim_{\hat{T}\to\infty}\frac{1}{\hat{T}}\left[\eta_- < -\mathcal{P}_t + \mathcal{P}_s >_{q\bar{q}-0} + \frac{1}{4}\frac{2\beta_L(g_0)}{g_0} < S >_{q\bar{q}-0}\right].} \tag{1.23}$$

This is essentially the energy sum rule which Rothe derived in [23]. Using the relation between the action and the trace of the energy momentum tensor, it can be rewritten as

$$\hat{V}(\hat{R},\hat{\beta}) = \lim_{\hat{T}\to\infty}\left[\eta_-\frac{1}{\hat{T}} < -\mathcal{P}_t + \mathcal{P}_s >_{q\bar{q}-0} + \frac{1}{4}\sum_{\vec{x},\mu} < T_{\mu\mu}(\vec{x},t) >_{q\bar{q}-0}\right].$$

On the other hand, Karsch [42] showed that in the continuum limit ($g_0 \to 0$):

$$\eta_- \to \hat{\beta},$$

and if one again assumes that the expectation value for plaquettes on different time slices is identical for large $\hat{T}$, one can rewrite the first expectation value:

$$\lim_{\hat{T}\to\infty} \frac{1}{\hat{T}} < -\mathcal{P}_t + \mathcal{P}_s >_{q\bar{q}-0} = \lim_{\hat{T}\to\infty} < -\mathcal{P}'_t(t) + \mathcal{P}'_s(t) >_{q\bar{q}-0},$$

where $\mathcal{P}'_{s,t}(t)$ is the sum over all spatial respectively temporal plaquettes on the *fixed* time slice t. Therefore in the continuum limit, the first term on the right hand side of (1.23) reduces to:

$$\lim_{\hat{T}\to\infty} \eta_- \frac{1}{\hat{T}} < -\mathcal{P}_t + \mathcal{P}_s >_{q\bar{q}-0} \to a \sum_{\vec{x}} a^3 \frac{1}{2} \lim_{\hat{T}\to\infty} < -\vec{E}^2(\vec{x}) + \vec{B}^2(\vec{x}) >_{q\bar{q}-0}, \tag{1.24}$$

which is just the euclidean version of the energy in the gluon fields. Hence the energy sum rule tells us that the potential energy of the quark-antiquark pair is given by:

$$\text{energy in the gluon fields} + \frac{1}{4}\text{trace anomaly of the energy momentum tensor.}$$

An especially interesting case to look at is a purely confining potential:

$$\hat{V}(\hat{R}) = \sigma \hat{R}.$$

From the action sum rule, one can deduce that

$$\lim_{\hat{T}\to\infty} \sum_{\vec{x},\mu} < T_{\mu\mu}(\vec{x}, t) >_{q\bar{q}-0} = \hat{V} + \hat{R}\frac{\partial \hat{V}}{\partial \hat{R}} = 2\hat{V};$$

hence the energy sum rule gives:

$$\frac{1}{2}\hat{V} = -\lim_{\hat{T}\to\infty} \eta_- \frac{1}{\hat{T}} < -\mathcal{P}_t + \mathcal{P}_s >_{q\bar{q}-0} .$$

Therefore for a confining potential, the contributions from the energy in the gluon fields and from the trace anomaly of the energy-momentum-tensor have the same magnitude: both account for exactly one half of the total potential energy.

1.4 Problems with the Sum Rules

The main goal of this work is to check the lattice sum rules. This is necessary because of several reasons: first, neither for the argument leading to the restriction to one fixed time slice, nor for the scaling arguments on the anisotropic lattice, it is known if they are justified. Hence their validity should be checked.

But beyond these validity doubts, there are also other reasons to take a closer look at the sum rules. Because of the opposite signs of the magnetic

and electric field energies in the euclidean formulation, cancellations between these two contributions can occur when their expectation values are calculated in Monte Carlo simulations. These cancellations are a possible source of errors; a more thorough investigation of what happens there exactly should be helpful. Additionally, it would be interesting to see how do the contributions of the trace anomaly of the energy-momentum tensor look like.

There are in principle two ways to check the sum rules and to examine these interesting details. On the one hand, one could perform Monte Carlo simulations. Using these, one could investigate the physically interesting region where the coupling constant is large. But there are some drawbacks, too: much computer power and time is needed for these simulations, and the results are not very enlightening in general; numerical results do not tell as much about the underlying physics than analytical calculations.

Because of these reasons, in this work lattice perturbation theory is used to study the sum rules. Obviously this is only possible for weak coupling, hence the physically interesting and relevant region is missed. But this is countered by the fact that much less computer power and time is needed (only some low-dimensional numerical integrals in momentum space have to be done). Additionally, one gets analytical results, which are expected to shed some light on the problems mentioned above.

The Feynman rules for lattice perturbation theory are well-known and can be taken, for example, from [16]; there the necessary weak coupling expansion of the action is also explained in detail. The consistency of these perturbative calculations, a general power counting theorem, and considerations about the continuum limit can be found in [38]. The last necessary ingredient for the check of the sum rules in the weak coupling approximation is an expression for the potential up to next-to-leading order, which is provided in [39].

The outline of the check is as follows: first, I will explain how one obtains a weak coupling expansion of the quark-antiquark potential in lattice perturbation theory; I will outline an approach by Kovacs to this problem [30] as well as the methods used by Heller and Karsch, already mentioned above [39]. In the same chapter, I will prove additionally the transversality of the gluonic vacuum polarization, which appears in the calculation of the potential.

Then I will turn to the check of the action sum rule. In principle the validity of this sum rule is clear - after all, it is more or less an identity. Nevertheless, it seemed to be an easier task to check it rather than the energy sum rule, and it provides an opportunity to demonstrate some of the necessary methods. Additionally, it will turn out that this sum rule is closely connected with the gauge invariance of the Wilson loop—only some small additional calculations will be needed to check this gauge invariance, too. And there is one part of the action sum rule for which a check is really needed: the validity of the restriction to one time slice, which was already mentioned above, is not clear at all even for the action sum rule.

Finally the energy sum rule also has to be checked. Many results of the check of the action sum rule will become useful there (a further reason to check that sum rule first), hence this check will be easier than the check of the action sum rule, although it looks more complicated at first sight. After the check, I will

explain how one can derive results about the sizes of the various contributions to the potential (electric, magnetic, anomal) from my calculations and the energy sum rule. I will close that chapter again with a section on the restriction to one time slice.

The last chapter contains a summary and the conclusions. In the appendix, useful formulas are summarized, and some basic calculations are presented. A detailed account of the Fourier transformation needed in chapter 2 for calculating the potential can also be found there.

Chapter 2

The Quark-Antiquark Potential

In this chapter, I will line out how one can calculate the static quark-antiquark potential on the lattice, which is needed in order to check the sum rules. First I will give a general derivation, based on the running of the coupling constant and renormalization group arguments (for more details, see [30]), then I will discuss how one can derive these results directly by a perturbative lattice calculation. Additionally, I will prove that the gluonic vacuum polarization is transversal in leading order of the lattice perturbation theory.

2.1 The running coupling constant

In leading order, the quark-antiquark potential is given by:

$$V(R) = -\frac{g^2}{4\pi R} C_2(F), \tag{2.1}$$

where g is the coupling constant of the strong interaction and $C_2(F)$ the quadratic Casimir operator of fundamental representation F; for $SU(N)$:

$$C_2(F) = \frac{N^2 - 1}{2N}. \tag{2.2}$$

If one takes into account that the coupling constant depends also on the distance between the quark and the anti-quark ("running coupling constant"), then the formula above needs corrections:

$$V(R) = -\frac{g^2(R)}{4\pi R} C_2(F) = -\frac{g^2}{4\pi R} C_2(F) + O(g^4). \tag{2.3}$$

There are various methods to calculate these corrections. In [35], they were determined in momentum space, using dimensional regularization and the $\bar{MS}$ renormalization scheme (modified minimial subtraction: not only the pole in ϵ is subtracted, but also terms of $\ln 4\pi$). The result is:

$$V(\vec{q}^2) = -\frac{g^2_{\bar{MS}}(\mu^2)}{\vec{q}^2} C_2(F) \left[1 + g^2_{\bar{MS}}(\mu^2) \beta_0 \left(\ln \frac{\mu^2}{\vec{q}^2} - \gamma + \frac{31}{33} \right) \right]. \tag{2.4}$$

Here the Feynman gauge (gauge parameter $\alpha = 1$) and the quenched approximation (number of dynamic fermions $n_f = 0$) was used. $g_{\bar{MS}}$ is the coupling constant defined in the $\bar{M}S$ scheme, μ a mass parameter which has to be introduced during renormalization, $\gamma \approx 0.577216$ is the Euler-Mascheroni constant and β_0 the first coefficient in the expansion of the beta function:

$$\beta_0 = \frac{11 C_2(G)}{48\pi^2}, \tag{2.5}$$

where $C_2(G) = N$ is the quadratic Casimir operator of $SU(N)$ in the adjoint representation.

From this one can get an expression for the potential which should result from lattice calculations by using the relation between $g_{\bar{MS}}$ and the coupling constant $g_0(a)$ appearing in perturbative calculations on the lattice. This is done in two steps; first the following relation can be used:

$$g^2_{MS}(\mu^2) = g^2_{MOM}(\mu^2)\left[1 - \frac{A(\alpha, n_f, N)}{4\pi} g^2_{MOM}(\mu^2) + O(g^4)\right],$$

where g_{MS} and g_{MOM} are the coupling constants defined in the MS and MOM (momentum-space subtraction) renormalization scheme, respectively. $A(\alpha, n_f, N)$ was determined in [31] for various values of the gauge parameter α and numbers of dynamical fermions n_f; the value $A(1, 0, N)$ which is relevant here is given by:

$$A(1,0,N) = \frac{C_2(G)}{2\pi}\left(-\frac{11}{6}\gamma + \frac{11}{6}\ln 4\pi + \frac{23}{6} + \frac{1}{36} I\right)$$

with

$$I = -2\int_0^1 \frac{\ln x}{x^2 - x + 1} \approx 2.3439072.$$

But here $g_{\bar{MS}}$ is needed; for this one obtains:

$$g^2_{\bar{MS}}(\mu^2) = g^2_{MOM}(\mu^2)\left[1 - \frac{\bar{A}(1,0,N)}{4\pi} g^2_{MOM}(\mu^2) + O(g^4)\right] \tag{2.6}$$

with

$$\bar{A}(1,0,N) = A(1,0,N) - \frac{11 C_2(G)}{12\pi}\ln 4\pi = \frac{C_2(G)}{2\pi}\left(-\frac{11}{6}\gamma + \frac{23}{6} + \frac{1}{36} I\right). \tag{2.7}$$

The second step is to connect $g_{MOM}(\mu^2)$ with $g_0(a)$ in the continuum limit $a \to 0$ [32, 33]:

$$g^2_{M\bar{O}M}(\mu^2) = g_0^2(a)\left[1 + g_0^2(a)\left(\beta_0 \ln \frac{\pi^2}{a^2\mu^2} + R(N)\right) + O(g^4)\right], \tag{2.8}$$

with

$$\begin{aligned} R(N) &= C_2(G)\left[\frac{1}{48\pi^2}\left(23 - 22\ln\pi + \frac{1}{6} I\right) + 2P\right] - \frac{1}{8N} \\ &= C_2(G)\left[\frac{1}{48\pi^2}\left(23 - 22\ln\pi + \frac{1}{6} I\right) + 2P - \frac{1}{8}\right] + \frac{1}{4} C_2(F), \end{aligned} \tag{2.9}$$

where I is defined as above and $P \approx 0.0849780$.

Putting everything together, the result for the potential in momentum space is:

$$\begin{aligned} V(\vec{q}^2) &= -\frac{g_0^2(a)}{\vec{q}^2} C_2(F) \\ &\quad \cdot \left[1 + g_0^2(a) \left[\beta_0 \left(\ln \frac{\pi^2}{a^2 \vec{q}^2} - \gamma + \frac{31}{33} \right) - \frac{\bar{A}(1,0,N)}{4\pi} + R(N) \right] \right]. \end{aligned}$$

In order to get the potential in coordinate space, one has to do a Fourier transformation (for details, see appendix D):

$$\begin{aligned} V(R) &= -\frac{g_0^2(a)}{4\pi R} C_2(F) \\ &\quad \cdot \left[1 + g_0^2(a) \left[\beta_0 \left(\ln \frac{\pi^2 R^2}{a^2} + \gamma + \frac{31}{33} \right) - \frac{\bar{A}(1,0,N)}{4\pi} + R(N) \right] \right]; \end{aligned}$$

hence the potential, measured in lattice spacings, is:

$$\begin{aligned} \hat{V}(\hat{R}) &= -\frac{g_0^2(a)}{4\pi \hat{R}} C_2(F) \\ &\quad \cdot \left[1 + g_0^2(a) \left[2\beta_0 \ln \left(\pi e^{\gamma/2 + 31/66} \hat{R} \right) - \frac{\bar{A}(1,0,N)}{4\pi} + R(N) \right] \right]. \end{aligned} \tag{2.10}$$

Inserting the explicit expressions for $\bar{A}(1,0,N)$ and $R(N)$ given above, one finally arrives at:

$$\begin{aligned} \hat{V}(\hat{R}) &= -\frac{g_0^2(a)}{4\pi \hat{R}} C_2(F) \\ &\quad \cdot \left[1 + g_0^2(a) \left[2\beta_0 \ln \left(e^{\gamma + 31/66 + 48\pi^2 P/11 - 3\pi^2/11} \hat{R} \right) + \frac{1}{4} C_2(F) \right] \right] \\ &\approx -\frac{g_0^2(a)}{4\pi \hat{R}} C_2(F) \left[1 + g_0^2(a) \left[\frac{11}{24\pi^2} C_2(G) \ln \left(7.501 \hat{R} \right) + \frac{1}{4} C_2(F) \right] \right] \end{aligned} \tag{2.11}$$

or

$$\begin{aligned} \hat{V}(\hat{R}) &\approx -\frac{g_0^2(a)}{4\pi \hat{R}} C_2(F) \left[1 + 2 g_0^2(a) \beta_0 \ln \left(7.501 e^{C_2(F)/8\beta_0} \hat{R} \right) \right] \\ &= -\frac{g_0^2(a)}{4\pi \hat{R}} C_2(F) \left[1 + 2 g_0^2(a) \beta_0 \ln \left(7.501 e^{3\pi^2 (N^2-1)/11N^2} \hat{R} \right) \right] \\ &= -\frac{g_0^2(a)}{4\pi \hat{R}} \begin{cases} \frac{3}{4} \left[1 + 2 g_0^2(a) \beta_0 \ln \left(56.47 \hat{R} \right) \right] & SU(2) \\ \frac{4}{3} \left[1 + 2 g_0^2(a) \beta_0 \ln \left(82.07 \hat{R} \right) \right] & SU(3) \end{cases} \end{aligned} \tag{2.12}$$

Alternatively, one can express these results by using the QCD scale parameters Λ of the different renormalization schemes; the following relations hold [31, 32, 33]:

$$\begin{aligned} \frac{\bar{A}(1,0,N)}{4\pi} &= 2\beta_0 \ln \frac{\Lambda_{MOM}}{\Lambda_{\bar{M}S}} \\ R(N) &= 2\beta_0 \ln \frac{\Lambda_{MOM}}{\pi \Lambda_L}. \end{aligned} \tag{2.13}$$

With this, one can write for the potential

$$\begin{aligned}\hat{V}(\hat{R}) &= -\frac{g_0^2(a)}{4\pi\hat{R}}C_2(F)\left[1+2g_0^2(a)\beta_0\ln\left(\frac{e^{\gamma/2+31/66}\Lambda_{\bar{M}S}}{\Lambda_L}\hat{R}\right)\right] \\ &\approx -\frac{g_0^2(a)}{4\pi\hat{R}}C_2(F)\left[1+2g_0^2(a)\beta_0\ln\left(2.135\frac{\Lambda_{\bar{M}S}}{\Lambda_L}\hat{R}\right)\right]. \qquad (2.14)\end{aligned}$$

The ratio of the scale parameters is:

$$\frac{\Lambda_{\bar{M}S}}{\Lambda_L} \approx \begin{cases} 26.45 & SU(2) \\ 38.45 & SU(3) \end{cases} \qquad (2.15)$$

These expressions for the potential agree with results from Monte Carlo simulations [30], as well as with a perturbative calculation on the lattice [39]. Additionally, the potential shows the right scaling behaviour, compared with (1.11).

In some older publications, one can find the following simpler expression for the potential instead of the one derived above [34]:

$$\hat{V}(\hat{R}) = -\frac{g_0^2(a)}{4\pi\hat{R}}C_2(F)\left[1+2g_0^2(a)\beta_0\ln\hat{R}\right], \qquad (2.16)$$

the (big) factor $2.135\frac{\Lambda_{\bar{M}S}}{\Lambda_L}$ in the logarithm is missing there completely! There are two reasons for this:

1. The contribution from the tadpole graph in the gluonic vacuum polarization was left out by these authors; therefore the term proportional to $C_2(F)^2$ is missing. That term contributes a factor 7.529 ($SU(2)$) or 10.942 ($SU(3)$), respectively, in the logarithm.

2. For the ultraviolet and infrared cutoffs, they used only rough approximations, choosing them idential to a and R, respectively; hence the ratio of the cutoffs is identical to $\hat{R}$ in their results. In contrast, the correct calculation yields an additional factor of 7.501 in the logarithm.

2.2 Weak coupling expansion on the lattice

A weak coupling expansion of the quark-antiquark potential on the lattice was done first by Heller and Karsch in 1985 [39]. Their methods and results are summarized in this section for future reference.

As already mentioned in the introduction, the quark-antiquark potential can be derived from the expectation value of the Wilson loop:

$$\hat{V}(\hat{R},\hat{\beta}) = -\lim_{\hat{T}\to\infty}\frac{1}{\hat{T}}\ln < W(\hat{R},\hat{T}) >_{subtr}, \qquad (2.17)$$

with

$$W = \frac{1}{d(F)}\mathrm{Tr}\prod_{l\in C}U_l. \qquad \text{(path ordered)} \qquad (2.18)$$

The subscript "subtr" means that in order to get the correct potential from the formula above, one has to subtract the self energy contributions to the quarks. This subscript will be omitted in most places in the following.

The rectangular curve C is chosen to have the corners n_0, $n_0 + \hat{R}\hat{\mu}$, $n_0 + \hat{R}\hat{\mu} + \hat{T}\hat{\nu}$, $n_0 + \hat{T}\hat{\nu}$, where $\hat{\mu}$ and $\hat{\nu}$ are the unit vectors in one spatial and the temporal direction of the lattice, respectively. The link variables are connected with the vector potential by the following relation:

$$U_l = e^{ig_0 A_l}. \tag{2.19}$$

Using the Baker-Hausdorf formula repeatedly, one then arrives at the following expression for W:

$$\begin{aligned} W \;=\; & \frac{1}{d(F)}\mathrm{Tr}\exp\left[ig_0\sum_l A_l - \frac{1}{2}g_0^2\sum_{l_1<l_2}[A_{l_1},A_{l_2}] - \frac{1}{4}ig_0^3\sum_{l_1<l_2<l_3}[[A_{l_1},A_{l_2}],A_{l_3}]\right. \\ & \left. -\frac{1}{12}ig_0^3\sum_{(l_1,l_2)<l_3}[A_{l_1},[A_{l_2},A_{l_3}]] - \frac{1}{12}ig_0^3\sum_{l_1<l_2}[[A_{l_1},A_{l_2}],A_{l_2}] + O(g_0^4)\right], \end{aligned}$$

where A_l is given by:

$$\begin{aligned} A_l &= A_\mu(n) \qquad \text{for } l = (n, n+\hat{\mu}) \\ A_l &= -A_\mu(n-\hat{\mu}) \qquad \text{for } l = (n, n-\hat{\mu}). \end{aligned}$$

Expanding the exponential and taking the trace, one obtains the perturbative expansion for the Wilson loop:

$$W = 1 - g_0^2\omega^{(2)} - g_0^3\omega^{(3)} - g_0^4\omega^{(4)} + O(g_0^5) \tag{2.20}$$

with

$$\omega^{(2)} = \frac{1}{4d(F)}\left(\sum_l A_l^A\right)^2 \tag{2.21}$$

$$\omega^{(3)} = \frac{i}{6d(F)}\mathrm{Tr}\left(\sum_l A_l\right)^3 + \frac{i}{2d(F)}\mathrm{Tr}\left(\sum_l A_l \sum_{l_1<l_2}[A_{l_1},A_{l_2}]\right) \tag{2.22}$$

$$\begin{aligned} \omega^{(4)} = & -\frac{1}{24d(F)}\mathrm{Tr}\left(\sum_l A_l\right)^4 - \frac{1}{8d(F)}\mathrm{Tr}\left(\sum_{l_1<l_2}[A_{l_1},A_{l_2}]\right)^2 \\ & -\frac{1}{4d(F)}\mathrm{Tr}\left(\sum_l A_l \sum_{l_1<l_2<l_3}[[A_{l_1},A_{l_2}],A_{l_3}]\right) \\ & -\frac{1}{12d(F)}\mathrm{Tr}\left(\sum_l A_l \sum_{(l_1,l_2)<l_3}[A_{l_1},[A_{l_2},A_{l_3}]]\right) \\ & -\frac{1}{12d(F)}\mathrm{Tr}\left(\sum_l A_l \sum_{l_1<l_2}[[A_{l_1},A_{l_2}],A_{l_2}]\right) \\ & -\frac{1}{4d(F)}\mathrm{Tr}\left(\left(\sum_l A_l\right)^2 \sum_{l_1<l_2}[A_{l_1},A_{l_2}]\right). \end{aligned} \tag{2.23}$$

For doing explicit calculations with these expressions, it is convenient to split $\omega^{(4)}$ up into its parts in the following way:

$$\omega^{(4)} = -\omega^{(4A)} - \ldots - \omega^{(4F)}. \tag{2.24}$$

Additionally, in order to calculate the expectation value of the Wilson loop, one needs a perturbative expansion for the action. Expectation values are calculated in the usual way:

$$< O >= \frac{\int DUOe^{-S}}{\int DUe^{-S}}, \tag{2.25}$$

where S is Wilson's action (1.4) and the integral runs over all elements U of the gauge group. Carrying out the Faddeev-Popov gauge fixing and rewriting the integration measure using the vector potential A^A_μ, one arrives at the following perturbative expansion (see, for example, [16]):

$$S_{eff} = S^{(0)} + g_0 S^{(1)} + g_0^2 S^{(2)} + g_0^2 S^{(2)}_{FP} + g_0^2 S^{(2)}_{meas} + O(g_0^3). \tag{2.26}$$

$S^{(1)}$ gives the three-gluon, $S^{(2)}$ the four-gluon vertex; $S^{(FP)}$ comes from the Fadeev-Popov determinant, and $S^{(meas)}$ from the transformation of the integration measure. $S^{(0)}$ is the term of order g_0^0, which is quadratic in the gauge fields:

$$S^{(0)} = -\frac{1}{2} \int\limits_{BZ} \sum_{\mu,\nu} \frac{d^4p}{(2\pi)^4} \hat{A}^A_\mu(-p) \left(\hat{p}^2 \delta_{\mu\nu} - \left(1 - \frac{1}{\alpha}\right) \hat{p}_\mu \hat{p}_\nu \right) \hat{A}^A_\nu(p). \tag{2.27}$$

Here, α is the usual gauge parameter; for all the results summarized below, the Feynman gauge $\alpha = 1$ had been used. The subscript BZ denotes the region of integration: the first Brillouin zone, all components of p run from $-\pi$ to $+\pi$. Additionally, the following standard abbreviations were introduced above:

$$\begin{aligned} \hat{p}_\mu &= 2\sin(p_\mu/2) \\ \hat{p}^2 &= \sum_{\mu=1}^{4} \hat{p}^2_\mu. \end{aligned} \tag{2.28}$$

Note also that the sum over the Lorentz indices μ and ν was explicitly written out, i. e. the usual sum convention is not used in this work: *Repeated indices only have to be summed if this is explicitly denoted.*

Now the expectation value of an operator becomes:

$$\begin{aligned} < O > &= \frac{\int DA\; O\; e^{-S_{eff}}}{\int DA\; e^{-S_{eff}}} = \frac{\int DA\; O\; e^{-S^{(0)}}}{\int DA\; e^{-S^{(0)}}} (1 + O(g_0)) \\ &=: < O >_0 + O(g_0), \end{aligned} \tag{2.29}$$

and the free gluon propagator is given by

$$\begin{aligned} < A^A_\mu(p) A^B_\nu(q) >_0 &= \delta^{AB} (2\pi)^4 \delta(p+q) \frac{\delta_{\mu\nu} - \left(1 - \frac{1}{\alpha}\right) \frac{\hat{p}_\mu \hat{p}_\nu}{\hat{p}^2}}{\hat{p}^2} \\ &= \delta^{AB} (2\pi)^4 \delta(p+q) \frac{\delta_{\mu\nu}}{\hat{p}^2} \quad \text{(Feynman gauge)}. \end{aligned} \tag{2.30}$$

The explicit expressions for the other coefficients in the expansion of the action can also be found partly in [39] (but notice that the action is defined there with just the opposite sign in comparison to the convention here!); for the three- and four-gluon vertices, see [36] or [37]. A more modern version, better suited for calculations, is given in [16].

2.2.1 Leading order

Using the formula (1.1) and the expansion of the Wilson loop outlined above, one gets in leading order:

$$\hat{V} = g_0^2 \lim_{\hat{T}\to\infty} \frac{1}{\hat{T}} < \omega^{(2)} >_{0,subtr}, \tag{2.31}$$

with

$$\begin{aligned} & < \omega^{(2)} >_0 \qquad (2.32)\\ = \; & 2C_2(F) \int\limits_{BZ} \frac{d^4p}{(2\pi)^4} \frac{\sin^2(p_\mu \hat{R}/2)\sin^2(p_\nu \hat{T}/2)}{\hat{p}^2} \left(\frac{1}{\sin^2(p_\mu/2)} + \frac{1}{\sin^2(p_\nu/2)} \right). \end{aligned}$$

For a detailed derivation of this expression, see appendix B. As mentioned above, *subtr* means that the self-energy contributions have to be subtracted. μ and ν represent here the spatial respectively temporal direction of the Wilson loop; these are different, *fixed* indizes and are *not* summed over. Because of the symmetry of the lattice, these two indices can be chosen arbitrarily without changing the result.

In this order, the potential can be calculated exactly. First, perform the limit $\hat{T} \to \infty$. The following relations hold:

$$\begin{aligned} \lim_{\hat{T}\to\infty} \frac{1}{\hat{T}} \frac{\sin^2(p_\mu \hat{R}/2)\sin^2(p_\nu \hat{T}/2)}{\sin^2(p_\mu/2)} &= 0 \\ \lim_{\hat{T}\to\infty} \frac{1}{\hat{T}} \frac{\sin^2(p_\mu \hat{R}/2)\sin^2(p_\nu \hat{T}/2)}{\sin^2(p_\nu/2)} &= 2\pi\delta(p_\nu). \end{aligned}$$

With this one gets:

$$\hat{V} = 2C_2(F) g_0^2 \int\limits_{BZ} \frac{d^3p}{(2\pi)^3} \frac{\sin^2(p_\mu \hat{R}/2)}{\hat{\vec{p}}^2}, \tag{2.33}$$

where

$$\hat{\vec{p}}^2 = \sum_{\lambda\neq\nu} \hat{p}_\lambda^2;$$

hence

$$\begin{aligned} V &= \frac{2C_2(F)g_0^2}{a} \int\limits_{BZ} \frac{d^3p}{(2\pi)^3} \frac{\sin^2(p_\mu \hat{R}/2)}{\hat{\vec{p}}^2} \\ &= 2C_2(F) g_0^2 \int\limits_{-\pi/a}^{\pi/a} \frac{d^3p'}{(2\pi)^3} \frac{\sin^2(p'_\mu R/2)}{\frac{4}{a^2}\sum_{\lambda\neq\nu}\sin^2(p'_\lambda a/2)}. \end{aligned}$$

In the continuum limit $a \to 0$, the integral gets its main contributions for $p'_\lambda a \approx 0$. Hence one can expand the sines in the denominator: $\sin^2(p'_\lambda a/2)) \approx \frac{1}{4} p'^2_\lambda a^2$. The integration limits $\pm\pi/a$ go to $\pm\infty$ in the limit $a \to 0$. Therefore one gets:

$$V = 2C_2(F)g_0^2 \int_{-\infty}^{\infty} \frac{d^3p'}{(2\pi)^3} \frac{\sin^2(p'_\mu R/2)}{\sum_{\lambda\neq\nu} p'^2_\lambda}. \tag{2.34}$$

Now use the relation

$$\int_0^\infty dt e^{-tx} = \frac{1}{x};$$

with this one can write:

$$\begin{aligned}
V &= 2C_2(F)g_0^2 \int_{-\infty}^{\infty} \frac{d^3p'}{(2\pi)^3} \int_0^\infty dt \sin^2(p'_\mu R/2) e^{-t\sum_{\lambda\neq\nu} p'^2_\lambda} \\
&= 2C_2(F)g_0^2 \int_0^\infty dt \int_{-\infty}^{\infty} \frac{dp'_\mu}{2\pi} \sin^2(p'_\mu R/2) e^{-tp'^2_\mu} \left(\int_{-\infty}^{\infty} \frac{dx}{2\pi} e^{-tx^2} \right)^2 \\
&= \frac{1}{2\pi} C_2(F)g_0^2 \int_0^\infty \frac{dt}{t} \int_{-\infty}^{\infty} \frac{dp'_\mu}{2\pi} \sin^2(p'_\mu R/2) e^{-tp'^2_\mu} \\
&= \frac{1}{4\pi} C_2(F)g_0^2 \int_0^\infty \frac{dt}{t} \int_{-\infty}^{\infty} \frac{dp'_\mu}{2\pi} (1 - e^{ip'_\mu R}) e^{-tp'^2_\mu}.
\end{aligned}$$

After completing the square in the exponent, the integral over p'_μ can be done:

$$V = \frac{1}{8\pi^{3/2}} C_2(F)g_0^2 \int_0^\infty \frac{dt}{t^{3/2}} (1 - e^{-R^2/4t}).$$

Only the second term depends on R; the first gives an infinite contribution which is independent of R—hence it is the self energy contribution (this can also be seen by a close inspection of the graphs contributing to $< \omega^{(2)} >_0$). After subtracting it, what remains is:

$$\begin{aligned}
V &= -\frac{g_0^2}{8\pi^{3/2}} C_2(F) \int_0^\infty \frac{dt}{t^{3/2}} e^{-R^2/4t} \\
&= -\frac{g_0^2}{4\pi^{3/2}R} C_2(F) \int_0^\infty dx e^{-x^2} = -\frac{g_0^2}{4\pi^{3/2}R} C_2(F) \int_{-\infty}^\infty dx e^{-x^2} \\
&= -\frac{g_0^2}{4\pi R} C_2(F).
\end{aligned} \tag{2.35}$$

Hence indeed one recovers the correct formula for the potential in leading order from lattice perturbation theory.

2.2.2 Next-to-leading order

In next-to-leading order, there are several different contributions to the expectation value of the Wilson loop:

$$< W >= 1 - g_0^2 \ldots + g_0^4 < \omega^{(3)} S^{(1)} >_{conn} - g_0^4 < \omega^{(4)} >_0 - g_0^4 W_{VP} + O(g_0^6), \tag{2.36}$$

(note the different sign for the $\omega^{(3)}$-term, compared to [39]) where the subscript "conn" means that one has to consider only the connected graphs contributing to the expectation value, and W_{VP} stands for the contributions to $< W >$ coming from the vacuum polarization graphs:

$$\begin{aligned} W_{VP} &= - < \omega^{(2)} S^{(2)} >_{conn} + < \omega^{(2)} \frac{1}{2} \left(S^{(1)} \right)^2 >_{conn} - < \omega^{(2)} S^{(2)}_{FP} >_{conn} \\ &\quad - < \omega^{(2)} S^{(2)}_{meas} >_{conn} \qquad (2.37) \\ &= 2C_2(F) \int\limits_{BZ} \frac{d^4p}{(2\pi)^4} \frac{\sin^2(p_\mu \hat{R}/2) \sin^2(p_\nu \hat{T}/2)}{(\hat{p}^2)^2} \\ &\quad \cdot \left(\frac{\Pi_{\mu\mu}(p)}{\sin^2(p_\mu/2)} - 2 \frac{\Pi_{\mu\nu}(p)}{\sin(p_\mu/2)\sin(p_\nu/2)} + \frac{\Pi_{\nu\nu}(p)}{\sin^2(p_\nu/2)} \right). \qquad (2.38) \end{aligned}$$

Again, the signs of three of the terms are opposite to the ones in [39] because of the different sign convention for the action.

The explicit contributions are, given here for future reference:

$$\begin{aligned} & < \omega^{(3)} S^{(1)} >_{conn} \\ = \; & -C_2(G)C_2(F) \int\limits_{BZ} \frac{d^4p}{(2\pi)^4} \int\limits_{BZ} \frac{d^4k}{(2\pi)^4} \frac{1}{\hat{p}^2 \hat{k}^2 \widehat{(p+k)^2}} \\ & \left[\left\{ \frac{\sin^2(p_\mu \hat{R}/2)}{\sin(p_{\mu/2})} \sin(p_\nu \hat{T}/2) \cos(p_\nu/2) \sin((2p+k)_\mu/2) \right. \right. \\ & \cdot \left(\frac{\sin(p_\nu \hat{T}/2) \sin((2p+k)_\nu/2)}{\sin(p_\nu/2)\sin(k_\nu/2)\sin((p+k)_\nu/2)} - \frac{\sin((2p+k)_\nu \hat{T}/2)}{\sin(k_\nu/2)\sin((p+k)_\nu/2)} \right) \\ & + 4 \frac{\sin((k-p)_\nu/2)\cos((p+k)_\mu/2)}{\sin(p_\mu/2)\sin(k_\mu/2)\sin((p+k)_\nu/2)} \\ & \cdot \sin(p_\mu \hat{R}/2) \sin(p_\nu \hat{T}/2) \sin((p+k)_\nu \hat{T}/2) \sin(k_\mu \hat{R}/2) \\ & \left. \left. \cdot \cos((p+k)_\mu \hat{R}/2) \cos(k_\nu \hat{T}/2) \right\} + \left\{ (\mu, \hat{R}) \leftrightarrow (\nu, \hat{T}) \right\} \right] \qquad (2.39) \end{aligned}$$

Here again the same comment with respect to the sign as above applies.

For the calculation of $< \omega^{(4)} >$, use the decomposition (2.24) and determine each of the six contributions separately [40]:

$$\begin{aligned} < \omega^{(4A)} >_0 &= \left(2C_2(F)^2 - \frac{1}{3} C_2(G) C_2(F) \right) \qquad (2.40) \\ & \left[\int\limits_{BZ} \frac{d^4p}{(2\pi)^4} \frac{\sin^2(p_\mu \hat{R}/2) \sin^2(k_\nu \hat{T}/2)}{\hat{p}^2} \left(\frac{1}{\sin^2(p_\mu)} + \frac{1}{\sin^2(p_\nu)} \right) \right]^2 \end{aligned}$$

$$< \omega^{(4B)} >_0 = -\frac{1}{2} C_2(G) C_2(F) g_0^4 \int\limits_{BZ} \frac{d^4p}{(2\pi)^4} \int\limits_{BZ} \frac{d^4k}{(2\pi)^4}$$

$$
\begin{aligned}
&\frac{1}{\hat{p}^2\hat{k}^2}\left[\left\{\frac{\sin^2(p_\mu\hat{R}/2)\sin^2(k_\nu\hat{T}/2)}{\sin^2(p_{\mu/2})\sin^2(k_\nu/2)}\right\}+\left\{(\mu,\hat{R})\leftrightarrow(\nu,\hat{T})\right\}\right]\\
&-\frac{N^2-1}{16}g_0^4\int\limits_{BZ}\frac{d^4p}{(2\pi)^4}\int\limits_{BZ}\frac{d^4k}{(2\pi)^4}\frac{1}{\hat{p}^2\hat{k}^2}\left[\left\{\frac{1}{2}\frac{\sin^2((p_\mu+k_\mu)\hat{R}/2)}{\sin^2(p_{\mu/2})}\right.\right.\\
&\frac{\sin^2((p_\nu+k_\nu)\hat{T}/2)}{\sin^2(k_\mu/2)}\left[\frac{\sin((p_\mu-k_\mu)\hat{R}/2)}{\sin((p_\mu+k_\mu)\hat{R}/2)}-\frac{\sin((p_\mu-k_\mu)/2)}{\sin((p_\mu+k_\mu)/2)}\right]^2\\
&\left.+2\frac{\sin^2((k_\nu-p_\nu)\hat{T}/2)\sin^2(p_\mu\hat{R}/2)\sin^2(k_\mu\hat{R}/2)}{\sin^2(p_\mu/2)\sin^2(k_\mu/2)}\right\}\\
&\left.+\left\{(\mu,\hat{R})\leftrightarrow(\nu,\hat{T})\right\}\right] \qquad (2.41)
\end{aligned}
$$

$$
\begin{aligned}
<\omega^{(4C)}>_0 \;=\;& \frac{1}{2}C_2(G)C_2(F)g_0^4\int\limits_{BZ}\frac{d^4p}{(2\pi)^4}\int\limits_{BZ}\frac{d^4k}{(2\pi)^4}\frac{1}{\hat{p}^2\hat{k}^2}\\
&\left[\left\{\frac{\sin(p_\mu\hat{R}/2)}{\sin(p_\mu/2)}2\sin^2(p_\nu\hat{T}/2)(\Sigma_1-\Sigma_2)\right.\right.\\
&-\frac{\sin(p_\mu\hat{R}/2)\sin^2(p_\nu\hat{T}/2)}{\sin(p_\mu/2)}\frac{\sin(k_\mu\hat{R}/2)\cos(k_\nu\hat{T})}{\sin(k_\mu/2)}\\
&\cdot(\Sigma_R(-p_\mu,k_\mu)-\Sigma_R(k_\mu,-p_\mu))\\
&+\frac{\sin^2(p_\mu\hat{R}/2)\sin^2(p_\nu\hat{T}/2)}{\sin^2(p_\mu/2)}\Sigma_R(k_\mu,-k_\mu)\\
&+\frac{\sin(p_\mu\hat{R}/2)\sin^2(p_\nu\hat{T}/2)}{\sin(p_\mu/2)}\frac{\sin(k_\mu\hat{R}/2)\cos(k_\nu\hat{T})}{\sin(k_\mu/2)}\Sigma_R(-k_\mu,-p_\mu)\\
&\left.+\frac{\sin^2(p_\mu\hat{R}/2)\sin^2(p_\nu\hat{T}/2)}{\sin^2(p_\nu/2)}\Sigma_R(k_\mu,-k_\mu)\right\}+\left\{(\mu,\hat{R})\leftrightarrow(\nu,\hat{T})\right\}\\
&+2\frac{\sin^2(p_\mu\hat{R}/2)\sin^2(p_\nu\hat{T}/2)}{\sin^2(p_\mu/2)}\Sigma_T(k_\nu,-k_\nu)\\
&\left.+\frac{\sin^2(p_\mu\hat{R}/2)\sin^2(p_\nu\hat{T}/2)}{\sin^2(p_\nu/2)}\frac{\sin^2(k_\mu\hat{R}/2)\cos(k_\nu\hat{T})}{\sin^2(k_\mu/2)}\right] \qquad (2.42)
\end{aligned}
$$

$$
\begin{aligned}
<\omega^{(4D)}>_0 \;=\;& \frac{1}{6}C_2(G)C_2(F)g_0^4\int\limits_{BZ}\frac{d^4p}{(2\pi)^4}\int\limits_{BZ}\frac{d^4k}{(2\pi)^4}\frac{1}{\hat{p}^2\hat{k}^2}\\
&\left[\left\{\frac{\sin(p_\mu\hat{R}/2)}{\sin(p_\mu/2)}\sin^2(p_\nu\hat{T}/2)\right.\right.\\
&\cdot(\Sigma_R(0,-p_\mu)+\Sigma_1-\Sigma_2-\Sigma_R(k_\mu-p_\mu,-k_\mu))\\
&\left.+\frac{\sin(p_\mu\hat{R}/2)}{\sin(p_\mu/2)}\sin^2(p_\nu T/2)\right.\\
&\cdot(\Sigma_R(-p_\mu,0)+\Sigma_1-\Sigma_2-\Sigma_R(-k_\mu,k_\mu-p_\mu))
\end{aligned}
$$

$$
\begin{aligned}
&+\frac{\sin^2(p_\mu\hat{R}/2)}{\sin^2(p_\mu/2)}\sin^2(p_\nu\hat{T}/2)\frac{\sin^2(k_\nu\hat{T}/2)}{\sin(k_\nu/2)}\\
&+\frac{\sin(p_\mu\hat{R}/2)}{\sin^2(p_\mu/2)}\sin^2(p_\nu\hat{T}/2)\frac{\sin^2(k_\mu\hat{R}/2)}{\sin^2(k_\mu/2)}\left(1+\cos(k_\nu\hat{T})\right)\\
&-\frac{\sin(p_\mu\hat{R}/2)}{\sin(p_\mu/2)}\sin^2(p_\nu\hat{T}/2)\frac{\sin(k_\mu\hat{R}/2)}{\sin(k_\mu/2)}\cos(k_\nu\hat{T})\\
&(\Sigma_R(-p_\mu,-k_\mu)-\Sigma_R(-k_\mu,-p_\mu))\\
&-\frac{\sin(p_\mu\hat{R}/2)}{\sin(p_\mu/2)}\sin^2(p_\nu\hat{T}/2)\frac{\sin(k_\mu\hat{R}/2)}{\sin(k_\mu/2)}\cos(k_\nu\hat{T})\Sigma_R(-p_\mu,k_\mu)\\
&-\frac{\sin(p_\mu^2\hat{R}/2)}{\sin^2(p_\mu/2)}\sin^2(p_\nu\hat{T}/2)\Sigma_R(k_\mu,-k_\mu)\\
&-\frac{\sin^2(p_\mu\hat{R}/2)}{\sin^2(p_\nu/2)}\sin^2(p_\nu\hat{T}/2)\Sigma_R(k_\mu,-k_\mu)\Bigg\}+\Big\{(\mu,\hat{R})\leftrightarrow(\nu,\hat{T})\Big\}\\
&+2\frac{\sin^2(p_\mu\hat{R}/2)}{\sin^2(p_\nu/2)}\sin^2(p_\nu\hat{T}/2)\frac{\sin^2(k_\mu\hat{R}/2)}{\sin^2(k_\mu/2)}\\
&-2\frac{\sin^2(p_\mu\hat{R}/2)}{\sin^2(p_\mu/2)}\sin^2(p_\nu\hat{T}/2)\Sigma_T(k_\nu,-k_\nu)\\
&-\frac{\sin^2(p_\mu\hat{R}/2)}{\sin^2(p_\nu/2)}\sin^2(p_\nu\hat{T}/2)\frac{\sin^2(k_\mu\hat{R}/2)}{\sin^2(k_\mu/2)}\cos(k_\nu\hat{T})\\
&+2\frac{\sin^2(p_\mu\hat{R}/2)}{\sin^2(p_\mu/2)}\sin^2(p_\nu\hat{T}/2)\frac{\sin^2(k_\nu\hat{T}/2)}{\sin^2(k_\nu/2)}\cos(k_\mu\hat{R})\Bigg]
\end{aligned}
\tag{2.43}
$$

$$
\begin{aligned}
<\omega^{(4E)}>_0 \;=\;& \frac{1}{6}C_2(G)C_2(F)g_0^4\int_{BZ}\frac{d^4p}{(2\pi)^4}\int_{BZ}\frac{d^4k}{(2\pi)^4}\frac{1}{\hat{p}^2\hat{k}^2}\\
&\Bigg[\Bigg\{\frac{\sin(p_\mu\hat{R}/2)}{\sin(p_\mu/2)}\sin^2(p_\nu\hat{T}/2)\Sigma_R(-p_\mu,0)\\
&-\frac{\sin(p_\mu\hat{R}/2)}{\sin(p_\mu/2)}\sin^2(p_\nu\hat{T}/2)\Sigma_R(k_\mu,-p_\mu-k_\mu)\\
&+\frac{\sin(p_\mu\hat{R}/2)}{\sin(p_\mu/2)}\sin^2(p_\nu\hat{T}/2)\Sigma_R(0,-p_\mu)\\
&-\frac{\sin(p_\mu\hat{R}/2)}{\sin(p_\mu/2)}\sin^2(p_\nu\hat{T}/2)\Sigma_R(-p_\mu-k_\mu,k_\mu)\\
&+\frac{\sin^2(p_\mu\hat{R}/2)\sin^2(p_\nu\hat{T}/2)}{\sin^2(p_\mu/2)}\hat{R}+\frac{\sin^2(p_\mu\hat{R}/2)\sin^2(p_\nu\hat{T}/2)}{\sin^2(p_\nu/2)}\hat{R}\\
&+\frac{\sin(p_\mu\hat{R}/2)}{\sin(p_\mu/2)}\sin^2(p_\nu\hat{T}/2)\frac{\sin(k_\mu\hat{R}/2)}{\sin(k_\mu/2)}\frac{\sin((p_\mu+k_\mu)\hat{R}/2)}{\sin((p_\mu+k_\mu)/2)}\\
&\cdot\cos(k_\nu\hat{T})\Bigg\}
\end{aligned}
$$

$$+\left\{(\mu,\hat{R})\leftrightarrow(\nu,\hat{T})\right\}+2\frac{\sin^2(p_\mu\hat{R}/2)}{\sin^2(p_\mu/2)}\sin^2(p_\nu\hat{T}/2)\hat{T}\Bigg] \quad (2.44)$$

and finally, due to symmetry properties in the colour indices

$$<\omega^{(4F)}>_0=0. \quad (2.45)$$

Here the functions Σ are the parts of the following functions $\tilde{\Sigma}$ which are even in $p_\mu\to -p_\mu, k_\mu\to -k_\mu$:

$$\begin{aligned}
\tilde{\Sigma}_1 &= e^{ip_\mu(\hat{R}-1)/2}\sum_{x_1=0}^{\hat{R}-3}\sum_{x_2=x_1+1}^{\hat{R}-2}\sum_{x_3=x_2+1}^{\hat{R}-1}e^{-ip_\mu x_1}e^{ik_\mu(x_2-x_3)}\\
\tilde{\Sigma}_2 &= e^{ip_\mu(\hat{R}-1)/2}\sum_{x_1=0}^{\hat{R}-3}\sum_{x_2=x_1+1}^{\hat{R}-2}\sum_{x_3=x_2+1}^{\hat{R}-1}e^{-ip_\mu x_2}e^{ik_\mu(x_1-x_3)}\\
\tilde{\Sigma}_R(p_\mu,k_\mu) &= e^{-ip_\mu(\hat{R}-1)/2}e^{-ik_\mu(\hat{R}-1)/2}\sum_{x_1=0}^{\hat{R}-2}\sum_{x_2=x_1+1}^{\hat{R}-1}e^{ip_\mu x_1}e^{ik_\mu x_2}.
\end{aligned}$$

The explicit expressions are for $\hat{R}>2$ [40]:

$$\begin{aligned}
\Sigma_1 &= -\frac{1}{4}(\hat{R}-2)\frac{\sin(p_\mu\hat{R}/2)}{\sin(p_\mu/2)}+\frac{1}{4}\frac{\sin(p_\mu(\hat{R}-2)/2)}{\sin(p_\mu/2)}\\
&\quad -\frac{1}{4}\frac{\sin((k_\mu-p_\mu)(\hat{R}-2)/2)\cos(k_\mu(\hat{R}+1)/2-p_\mu)}{\sin((k_\mu-p_\mu)/2)\sin^2(k_\mu/2)}\\
&\quad +\frac{1}{4}\frac{\sin(p_\mu(\hat{R}-2)/2)\cos(p_\mu-k_\mu)}{\sin(p_\mu/2)\sin^2(k_\mu/2)} \qquad (2.46)\\
\Sigma_2 &= -\frac{1}{4}\frac{\sin(p_\mu(\hat{R}-2)/2)}{\sin(p_\mu/2)}\frac{\cos(k_\mu-p_\mu/2)}{\sin(k_\mu/2)\sin((p_\mu+k_\mu)/2)}\\
&\quad +\frac{1}{4}\frac{\sin(k_\mu(\hat{R}-2)/2)}{\sin^2(k_\mu/2)}\frac{\cos((p_\mu+k_\mu)\hat{R}/2+k_\mu/2-p_\mu)}{\sin((p_\mu+k_\mu)/2)}\\
&\quad +\frac{1}{4}\frac{\sin((k_\mu-p_\mu)(\hat{R}-2)/2)\cos(k_\mu(\hat{R}+2)/2-p_\mu/2)}{\sin(p_\mu/2)\sin(k_\mu/2)\sin((k_\mu-p_\mu)/2)}\\
&\quad -\frac{1}{4}\frac{\sin(k_\mu(\hat{R}-2)/2)\cos((p_\mu+k_\mu)\hat{R}/2+k_\mu-p_\mu)}{\sin(p_\mu/2)\sin^2(k_\mu/2)} \qquad (2.47)
\end{aligned}$$

For $\hat{R}\leq 2$, both of these functions vanish because of the constraints in the sums. Additionally for $\hat{R}>1$ one has:

$$\begin{aligned}
\Sigma_R(p_\mu,k_\mu) &= \mathrm{Re}\,\tilde{\Sigma}_R(p_\mu,k_\mu)\\
&= \frac{1}{2}\frac{\sin(p_\mu(\hat{R}-1)/2)\sin(k_\mu\hat{R}/2-p_\mu/2)}{\sin(p_\mu/2)\sin(k_\mu/2)}\\
&\quad +\frac{1}{2}\frac{\sin((p_\mu+k_\mu)(\hat{R}-1)/2)\sin(p_\mu/2)}{\sin((p_\mu+k_\mu)/2)\sin(k_\mu/2)}\\
&= \frac{1}{2}\frac{\sin(p_\mu\hat{R}/2)}{\sin(p_\mu/2)}\frac{\sin(k_\mu\hat{R}/2)}{\sin(k_\mu/2)}-\frac{1}{2}\frac{\sin((p_\mu+k_\mu)\hat{R}/2)}{\sin((p_\mu+k_\mu)/2)} \qquad (2.48)
\end{aligned}$$

For $\hat{R} = 1$, this function also vanishes, again because of the constraints in the sums. Obviously the function is also even under $p_\mu \leftrightarrow k_\mu$; therefore terms like

$$\Sigma_R(p_\mu, k_\mu) - \Sigma_R(k_\mu, p_\mu)$$

in the expressions (2.41) to (2.44) vanish.

Additionally, the part of $\tilde{\Sigma}_R$ which is odd under $p_\mu \to -p_\mu, k_\mu \to -k_\mu$ appears also several times in the expressions above (in $< \omega^{4B)} >_0$ and in $< \omega^{(3)} S^{(1)} >$). It is given by:

$$\begin{aligned} & O_R(p_\mu, k_\mu) = \mathrm{Im}\, \tilde{\Sigma}_R(p_\mu, k_\mu) \qquad (2.49)\\ = \;& \frac{1}{2}\left[\frac{\sin((p_\mu+k_\mu)(\hat{R}-1)/2)}{\sin((p_\mu+k_\mu)/2)}\frac{\cos(p_\mu/2)}{\sin(k_\mu/2)}\right.\\ & \left.-\frac{\cos(k_\mu\hat{R}/2-p_\mu/2)}{\sin(k_\mu/2)}\frac{\sin(p_\mu(\hat{R}-1)/2)}{\sin(p_\mu/2)}\right]\\ = \;& \frac{1}{4}\frac{\sin((p_\mu-k_\mu)/2)}{\sin(p_\mu/2)\sin(k_\mu/2)}\left[\frac{\sin((p_\mu+k_\mu)\hat{R}/2)}{\sin((p_\mu+k_\mu)/2)}-\frac{\sin((p_\mu-k_\mu)\hat{R}/2)}{\sin((p_\mu-k_\mu)/2)}\right]. \end{aligned}$$

Obviously, $O_R(p_\mu, k_\mu)$ is also odd under $p_\mu \leftrightarrow k_\mu$.

Finally, the vacuum polarization is given by the sum of the following five contributions, where the fourth and the fifth are unique to lattice perturbation theory:

$$\begin{aligned} \Pi_{\mu\nu}^{gluonloop} = \;& \frac{1}{2}C_2(G)\int_{BZ}\frac{d^dk}{(2\pi)^d}\frac{1}{\hat{p}^2\left(\widehat{p+k}\right)^2}\left[2\delta_{\mu\nu}\cos^2(k_\nu/2)\left(2\widehat{p+k}\right)^2\right.\\ & +\left(2\widehat{k+p}\right)_\mu\left(2\widehat{k+p}\right)_\nu\sum_{\rho\neq\mu,\nu}\cos^2(p_\rho/2)\\ & \left.+2\left(2\widehat{p+k}\right)_\mu\left(\widehat{k-p}\right)_\nu\cos((p_\mu+k_\mu)/2)\cos(k_\nu/2)\right] \qquad (2.50)\\ \Pi_{\mu\nu}^{gluontadpole} = \;& \frac{1}{2d}\left(2C_2(F)-\frac{1}{3}C_2(G)\right)\left(\delta_{\mu\nu}\hat{p}^2-\hat{p}_\mu\hat{p}_\nu\right)\\ & +\frac{1}{6}C_2(G)\delta_{\mu\nu}\left[(d+3)\Delta_0+1-\frac{2}{d}+3\left(\Delta_0-\frac{1}{2d}\right)\cos(p_\mu)\right.\\ & \left.-\left(7\Delta_0-\frac{5}{2d}\right)\sum_\rho\cos(p_\rho)\right] \qquad (2.51)\\ \Pi_{\mu\nu}^{ghostloop} = \;& -\frac{1}{2}C_2(G)\int_{BZ}\frac{d^dk}{(2\pi)^d}\frac{1}{\hat{p}^2\left(\widehat{p+k}\right)^2}\\ & \left[2\left(\widehat{p+k}\right)_\mu\hat{k}_\nu\cos(k_\mu/2)\cos((p_\nu+k_\nu)/2)\right] \qquad (2.52)\\ \Pi_{\mu\nu}^{ghosttadpole} = \;& -\frac{1}{4d}C_2(G)\delta_{\mu\nu} \qquad (2.53)\\ \Pi_{\mu\nu}^{measure} = \;& -\frac{1}{12}C_2(G)\delta_{\mu\nu}. \qquad (2.54) \end{aligned}$$

For later convenience, the results are given here for an arbitrary numbers of dimensions d. Additonally, the abbreviation

$$\Delta_0 = \int\limits_{BZ} \frac{d^d k}{(2\pi)^d} \frac{1}{\hat{k}^2} \tag{2.55}$$

has been introduced (compare appendix C).

It is not obvious how one could get an explicit expression for the potential from these eight-dimensional integrals in momentum space, reproducing the result (2.12). One way is to evaluate the integrals numerically; Heller and Karsch did this already in their original paper [39] and fitted their results to the following formula:

$$\hat{V}(\hat{R}) = V_{self} - \frac{4}{3}\frac{g_0^2}{4\pi\hat{R}}\left(1 + \frac{11}{16\pi^2} g_0^2 \ln(\hat{R}M)^2\right).$$

Here the factor $\frac{4}{3}$ comes from the quadratic Casimir operator $C_2(F)$ for $SU(3)$ in the fundamental representation, the factor $\frac{11}{16\pi^2}$ comes from the first coefficient of the beta function, and V_{self} denotes the contributions from the self energy. Comparing with (2.12), one should get:

$$M = 82.07$$

respectively

$$\ln M = 4.408.$$

The results Heller and Karsch obtained for $\ln M$ for $\hat{R} \gg 1$ are consistent with this prediction - a further verification that (2.12) indeed gives the right result for the quark-antiquark potential.

2.2.3 Transversality of the gluonic vacuum polarization

Using the results Heller and Karsch obtained for the vacuum polarization [39], one can show that it is transversal even for finite lattice spacing. This is not crucial for this work, but an interesting result in itself. So far, the transversality of the vacuum polarization, calculated in lattice perturbation theory, only had been checked in the continuum limit [37].

The contribution proportional to $C_2(F)$ of the vacuum polarization is obviously transversal. For the contributions proportional to $C_2(G)$ it has to be shown that

$$\sum_{\mu,\nu} \hat{p}_\mu \hat{p}_\nu \Pi_{\mu\nu} = 0, \tag{2.56}$$

which proves the transversality. In order to show this, look at the various contributions separately:

$$\sum_{\mu,\nu} \hat{p}_\mu \hat{p}_\nu \Pi_{\mu\nu}^{gluonloop} = C_2(G) g_0^2 \left[\hat{p}^2 \left(\left(d - \frac{1}{2}\right)\Delta_0 - \frac{1}{2} + \frac{1}{2d}\right)\right.$$

$$+\left(\hat{p}^2\right)^2\left(-\frac{1}{4}\left(\Delta_0-\frac{1}{2d}\right)-\frac{1}{4}I\right)+\hat{p}^4\frac{1}{4}\left(\Delta_0-\frac{1}{2d}\right)\Big] \tag{2.57}$$

$$\sum_{\mu,\nu}\hat{p}_\mu\hat{p}_\nu\Pi^{gluontadpole}_{\mu\nu} = C_2(G)g_0^2\left[\hat{p}^2\left((1-d)\Delta_0+\frac{7}{12}-\frac{7}{12d}\right)\right.$$
$$\left.+\left(\hat{p}^2\right)^2\frac{1}{4}\left(\Delta_0-\frac{1}{2d}\right)-\hat{p}^4\frac{1}{4}\left(\Delta_0-\frac{1}{2d}\right)\right] \tag{2.58}$$

$$\sum_{\mu,\nu}\hat{p}_\mu\hat{p}_\nu\Pi^{ghostloop}_{\mu\nu} = C_2(G)g_0^2\left[\hat{p}^2\left(-\frac{1}{2}\Delta_0+\frac{1}{4d}\right)+\left(\hat{p}^2\right)^2\frac{1}{4}I\right] \tag{2.59}$$

$$\sum_{\mu,\nu}\hat{p}_\mu\hat{p}_\nu\Pi^{ghosttadpole}_{\mu\nu} = C_2(G)g_0^2\left[\hat{p}^2\left(-\frac{1}{6d}\right)\right] \tag{2.60}$$

$$\sum_{\mu,\nu}\hat{p}_\mu\hat{p}_\nu\Pi^{measure}_{\mu\nu} = C_2(G)g_0^2\left[\hat{p}^2\left(-\frac{1}{12}\right)\right]. \tag{2.61}$$

Here the abbreviation

$$I := \int_{BZ}\frac{d^dk}{(2\pi)^d}\int_{BZ}\frac{d^dq}{(2\pi)^d}\frac{\delta^{(d)}(p+k+q)}{\hat{q}^2\hat{k}^2}$$

was introduced. In the calculation, the following Ward identity for the three-gluon vertex was used:

$$\sum_\mu\hat{p}_\mu\Gamma_{\mu\nu\lambda}(p,q,k) = ig_0(2\pi)^d\delta^{(d)}(p+q+k) \tag{2.62}$$
$$\cdot\left[\cos(p_\lambda/2)(\hat{q}^2\delta_{\nu\lambda}-\hat{q}_\nu\hat{q}_\lambda)-\cos(p_\nu/2)(\hat{k}^2\delta_{\nu\lambda}-\hat{k}_\nu\hat{k}_\lambda)\right].$$

Another useful formula which was needed here is:

$$\hat{p}\,\hat{k}\,\cos((p+k)/2) = \frac{1}{2}\left(\widehat{(p+k)}^2-\hat{p}^2-\hat{k}^2\right). \tag{2.63}$$

For the evaluation of the other integrals appearing in the derivation, see appendix C.

Adding up all these contributions, everything cancels, and one arrives indeed at the result that the vacuum polarization is transversal. Hence it can be written in the following form:

$$\Pi_{\mu\nu}(p) = \left(\delta_{\mu\nu}\hat{p}^2-\hat{p}_\mu\hat{p}_\nu\right)\Pi(p). \tag{2.64}$$

Additionally, one should show that the function $\Pi(p)$ is regular at $p=0$ or alternatively that $\Pi_{\mu\nu}(0)=0$. For the contribution proportional to $C_2(F)$ this is again obvious; and again the contributions proportional to $C_2(G)$ are determined separately:

$$\Pi^{gluonloop}_{\mu\nu}(0) = C_2(G)g_0^2\delta_{\mu\nu}\left[\left(d-\frac{1}{2}\right)\Delta_0+\frac{1}{2d}-\frac{1}{2}\right] \tag{2.65}$$

$$\Pi^{gluontadpole}_{\mu\nu}(0) = C_2(G)g_0^2\delta_{\mu\nu}\left[(d-1)\left(-\Delta_0+\frac{7}{12d}\right)\right] \tag{2.66}$$

$$\Pi_{\mu\nu}^{ghostloop}(0) = C_2(G)g_0^2\delta_{\mu\nu}\left[-\frac{1}{2}\Delta_0 + \frac{1}{4d}\right] \tag{2.67}$$

$$\Pi_{\mu\nu}^{ghosttadpole}(0) = C_2(G)g_0^2\delta_{\mu\nu}\left[-\frac{1}{6d}\right] \tag{2.68}$$

$$\Pi_{\mu\nu}^{measure}(0) = C_2(G)g_0^2\delta_{\mu\nu}\left[-\frac{1}{12}\right]. \tag{2.69}$$

Again, some of the integrals listed in appendix C were used. Adding everything, one indeed arrives at the claimed result

$$\Pi_{\mu\nu}(0) = 0. \tag{2.70}$$

Chapter 3

Action Sum Rule

In order to derive the action sum rule

$$\hat{V} + \hat{R}\frac{\partial \hat{V}}{\partial \hat{R}} = \frac{2\beta_L}{g_0} \lim_{\hat{T}\to\infty} < L(t) >_{q\bar{q}-0}, \tag{3.1}$$

essentially three steps were needed:

1. Taking the logarithmic derivative of (1.1); this led to the identity (1.7).
2. Using the scaling behaviour of the potential; the result was (1.12).
3. Taking the limit of large $\hat{T}$ and thereby restricting the sum over all plaquettes to one fixed time slice.

The explicit form of the potential up to next-to-leading order was already derived in chapter 2; its easy to see that it has indeed the right scaling behaviour. Hence only the first and the third step remain to be checked. As already pointed out, the first step gives essentially an identity, so that in principle a check for this is not needed.

Nevertheless, it is instructive to see how this identity looks like on the level of Feynman graphs, and the results derived here will be helpful later. Additionally, it will turn out that this identity is closely connected with the gauge invariance of the Wilson loop, so that this invariance can also be checked perturbatively.

The first section will give an introduction and contains the necessary expansions; the second section will deal with the perturbative check of (1.7) up to next-to-leading order. Then I will point out the connections to the gauge invariance of the Wilson loop, and how this can be checked. Finally the restriction to one fixed time slice will be examined.

3.1 Preliminaries

The identity (1.7), when inserting the definition (1.8) and the formula (1.1), becomes

$$-\hat{\beta}\frac{\partial}{\partial\hat{\beta}} \lim_{\hat{T}\to\infty} \frac{1}{\hat{T}} \ln < W(\hat{R},\hat{T}) >= \lim_{\hat{T}\to\infty} \frac{1}{\hat{T}} \left(\frac{< SW >}{< W >} - < S > \right). \tag{3.2}$$

Obviously, this identity has to be satisfied even for all finite $\hat{T}$:

$$-\hat{\beta}\frac{\partial}{\partial\hat{\beta}}\ln < W(\hat{R},\hat{T}) >= \frac{< SW >}{< W >} - < S > . \tag{3.3}$$

Carrying out the derivative and multiplying by $< W >$ gives:

$$-\hat{\beta}\frac{\partial}{\partial\hat{\beta}} < W >=< SW > - < S >< W > . \tag{3.4}$$

Now insert the relation (1.5) between the lattice coupling constant $\hat{\beta}$ and the coupling constant $g_0(a)$ appearing in perturbative lattice calculations; this finally leads to:

$$g_0^2\frac{\partial}{\partial g_0^2} < W >=< SW > - < S >< W >=< SW >_{conn} . \tag{3.5}$$

That is the formula which will be checked perturbatively in the next section.

3.2 Perturbative check

3.2.1 Leading order

Using the expansions

$$S = S^{(0)} + O(g_0). \tag{3.6}$$

and

$$W = 1 - g_0^2\omega^{(2)} + O(g_0^3), \tag{3.7}$$

(3.5) becomes

$$< \omega^{(2)} >_0 =< \omega^{(2)} S^{(0)} >_{conn} . \tag{3.8}$$

The expectation value on the left hand side was already given in section 2.2.1:

$$\begin{aligned} & < \omega^{(2)} >_0 \qquad (3.9)\\ = \; & 2C_2(F)\int\limits_{BZ}\frac{d^4p}{(2\pi)^4}\frac{\sin^2(\frac{1}{2}p_\mu\hat{R})\sin^2(\frac{1}{2}p_\nu\hat{T})}{\hat{p}^2}\left(\frac{1}{\sin^2(\frac{1}{2}p_\mu)}+\frac{1}{\sin^2(\frac{1}{2}p_\nu)}\right); \end{aligned}$$

this result was derived using Feynman gauge $\alpha = 1$. In the following, if it is not explicitly indicated otherwise, all expectation values will be calculated in that gauge.

The easiest way to calculate the correlator on the right hand side of (3.8) is to compute the correlator between two gauge fields and the action first; this is equivalent to the insertion of the action into a gluon line:

$$< A_\mu^A(p)A_\nu^B(q)S >_{conn} = \delta^{AB}\frac{\delta_{\mu\nu} - \frac{\hat{p}_\mu\hat{p}_\nu}{\hat{p}^2}}{\hat{p}^2}(2\pi)^4\delta(p+q). \tag{3.10}$$

This results hold for every gauge parameter α—hence inserting the action into a gluon line with arbitrary gauge parameter simply gives a propagator in Landau gauge $\alpha = \infty$! Therefore the calculation of the correlator $< \omega^{(2)}S^{(0)} >_{conn}$ gives

exactly the same result as if one would calculate the expectation value $< \omega^{(2)} >_0$ using the propagator in Landau gauge. For convenience, this expectation value will now be calculated in an arbitrary gauge.

First, $\omega^{(2)}$ is given by:

$$\omega^{(2)} = \frac{1}{4d(F)} \left(\sum_l A_l^A \right)^2 , \tag{3.11}$$

with the sum along the Wilson loop:

$$\begin{aligned} \sum_l A_l^A &= \sum_{l=0}^{\hat{R}-1} A_\mu^A(n_0 + l\hat{\mu}) + \sum_{l=0}^{\hat{T}-1} A_\nu^A(n_0 + \hat{\mu}\hat{R} + l\hat{\nu}) \\ &\quad - \sum_{l=0}^{\hat{R}-1} A_\mu^A(n_0 + \hat{\mu}\hat{R} + \hat{\nu}\hat{T} - l\hat{\mu}) - \sum_{l=0}^{\hat{T}-1} A_\nu^A(n_0 + \hat{\nu}\hat{T} - l\hat{\nu}). \end{aligned} \tag{3.12}$$

Expressing this in Fourier space, one gets:

$$\sum_l A_l^A = -2i \int_{BZ} \frac{d^4p}{(2\pi)^4} \sin(p_\mu \hat{R}/2) \sin(p_\nu \hat{T}/2) e^{ipn_c} \frac{A_\alpha^A(p)(\delta_{\mu\alpha} - \delta_{\nu\alpha})}{\sin(p_\alpha/2)}, \tag{3.13}$$

where

$$n_c = n_0 + \hat{\mu}\hat{R}/2 + \hat{\nu}\hat{T}/2$$

is the center of the Wilson loop.

Hence calculating the expectation value, using the propagator (2.30), the result is:

$$\begin{aligned} & < \omega^{(2)} >_{0,\alpha} \\ = \; & -\frac{1}{d(F)} \sum_{\alpha,\beta} \int_{BZ} \frac{d^4p}{(2\pi)^4} \int_{BZ} \frac{d^4q}{(2\pi)^4} < A_\alpha^A(p) A_\beta^A(q) >_{0,\alpha} e^{i(p+q)n_c} \frac{\delta_{\mu\alpha} - \delta_{\nu\alpha}}{\sin(p_\alpha/2)} \\ & \frac{\delta_{\mu\beta} - \delta_{\nu\beta}}{\sin(q_\beta/2)} \sin(p_\mu \hat{R}/2) \sin(p_\nu \hat{T}/2) \sin(q_\mu \hat{R}/2) \sin(q_\nu \hat{T}/2) \\ = \; & 2C_2(F) \sum_{\alpha,\beta} \int_{BZ} \frac{d^4p}{(2\pi)^4} \frac{\sin^2(p_\mu \hat{R}/2) \sin^2(p_\nu \hat{T}/2)}{\hat{p}^2} \\ & \frac{\delta_{\mu\alpha} - \delta_{\nu\alpha}}{\sin(p_\alpha/2)} \frac{\delta_{\mu\beta} - \delta_{\nu\beta}}{\sin(p_\beta/2)} \left(\delta_{\mu\nu} - \left(1 - \frac{1}{\alpha}\right) \frac{\hat{p}_\mu \hat{p}_\nu}{\hat{p}^2} \right) \\ = \; & 2C_2(F) \int_{BZ} \frac{d^4p}{(2\pi)^4} \frac{\sin^2(\frac{1}{2}p_\mu \hat{R}) \sin^2(\frac{1}{2}p_\nu \hat{T})}{\hat{p}^2} \\ & \cdot \left(\frac{1}{\sin^2(\frac{1}{2}p_\mu)} + \frac{1}{\sin^2(\frac{1}{2}p_\nu)} \right) \\ = \; & < \omega^{(2)} >_{0,\alpha=1} . \end{aligned} \tag{3.14}$$

Therefore the expectation value $< \omega^{(2)} >_0$ does not depend on the gauge parameter α, i. e., it is gauge invariant! Naively one could have expected this

result, because the Wilson loop is defined in a gauge-invariant way. But gauge transformations on the lattice are defined with respect to the link variables, and it is not entirely clear what effects this can have in a weak-coupling expansion. Hence it is nice to see that even in the limit of small coupling, the gauge invariance is preserved. The close connection between the action sum rule and the gauge invariance of the Wilson loop which becomes apparent here will be discussed further in section 3.3.
Additionally, using this gauge invariance, it is obvious that indeed

$$< \omega^{(2)} >_0 = < \omega^{(2)} S^{(0)} >_{conn}$$

holds—hence the action sum rule is valid in leading order.

This validity as well as the gauge invariance of the Wilson loop in leading order can also be expressed in diagrammatical form in the following way:

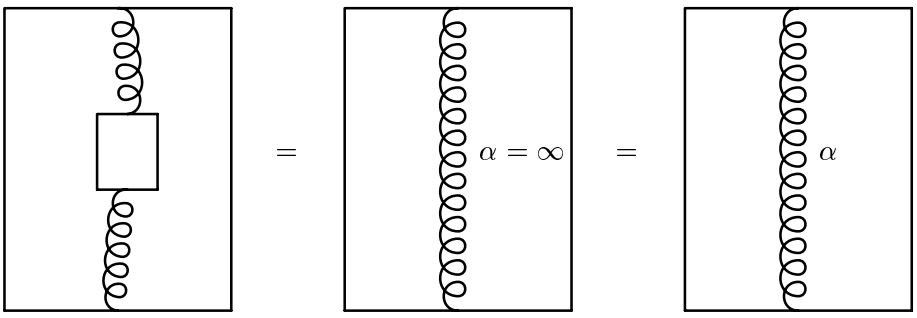

In these diagrams, a sum of the end points of the gluon line along the Wilson loop as well as along the plaquette, and a sum over all possible positions and orientations of the plaquette is to be understood. In the third graph, the gauge parameter α can be arbitrary. Gluon lines without an explicit index α are in Feynman gauge.

Another way to express this more concisely is to introduce the operator

$$G := \frac{1}{2} \int_{BZ} A^A_\mu(p) \hat{p}_\mu \hat{p}_\nu A^A_\nu(-p); \tag{3.15}$$

then one can write:

$$< A^A(p) A^B(q) >_{0,\alpha} = < A^A(p) A^B(q) >_0 - \left(1 - \frac{1}{\alpha}\right) < A^A(p) A^B(q) G >_{conn} . \tag{3.16}$$

If one denotes the insertion of this operator into a gluon line by a cross, one can also express this diagrammatically:

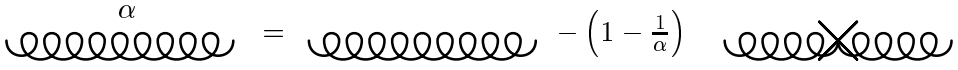

where again a gluon line without an explicit index represents a propagator in Feynman gauge.

Now, using this notation, the gauge invariance of the Wilson loop in leading order can be expressed in the following concise way:

$$< \omega^{(2)} G >_{conn} = 0, \tag{3.17}$$

or again diagrammatically:

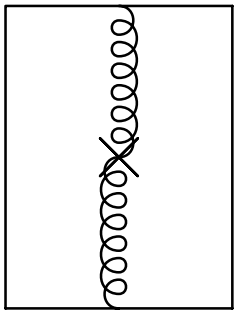

$= 0.$

3.2.2 Next-to-leading order

Taking the higher terms in the expansions of the Wilson loop

$$W = 1 - g_0^2 \omega^{(2)} - g_0^3 \omega^{(3)} - g_0^4 \omega^{(4)} + O(g_0^5) \tag{3.18}$$

into account, one gets:

$$\begin{aligned} & g_0^2 \frac{\partial}{\partial g_0^2} < W > \\ = \; & -g_0^2 < \omega^{(2)} >_0 + 2g_0^4 < \omega^{(2)} S^{(2)} >_{conn} - g_0^4 < \omega^{(2)} \left(S^{(1)} \right)^2 >_{conn} \\ & + 2g_0^4 < \omega^{(2)} S^{(2)}_{FP} >_{conn} + 2g_0^4 < \omega^{(2)} S^{(2)}_{meas} >_{conn} - 2g_0^4 < \omega^{(4)} >_0 \\ & + 2g_0^4 < \omega^{(3)} S^{(1)} >_0 + O(g_0^5). \end{aligned} \tag{3.19}$$

For the right side of (3.5), the higher terms in the expansion of the action have also to be used:

$$S = S^{(0)} + g_0 S^{(1)} + g_0^2 S^{(2)} + O(g_0^3).$$

The result is:

$$\begin{aligned} & < WS > - < W >< S > \\ = \; & -g_0^2 < S^{(0)} \omega^{(2)} >_{conn} + g_0^4 < S^{(0)} S^{(2)} \omega^{(2)} >_{conn} \\ & -\frac{1}{2} g_0^4 < S^{(0)} \left(S^{(1)} \right)^2 \omega^{(2)} >_{conn} + g_0^4 < S^{(0)} S^{(2)}_{FP} \omega^{(2)} >_{conn} \\ & + g_0^4 < S^{(0)} S^{(2)}_{meas} \omega^{(2)} >_{conn} - g_0^4 < S^{(2)} \omega^{(2)} >_{conn} \\ & + g_0^4 < \left(S^{(1)} \right)^2 \omega^{(2)} >_{conn} - g_0^4 < S^{(1)} \omega^{(3)} >_0 + g_0^4 < S^{(0)} S^{(1)} \omega^{(3)} >_{conn} \\ & - g_0^4 < S^{(0)} \omega^{(4)} >_{conn} + O(g_0^6). \end{aligned} \tag{3.20}$$

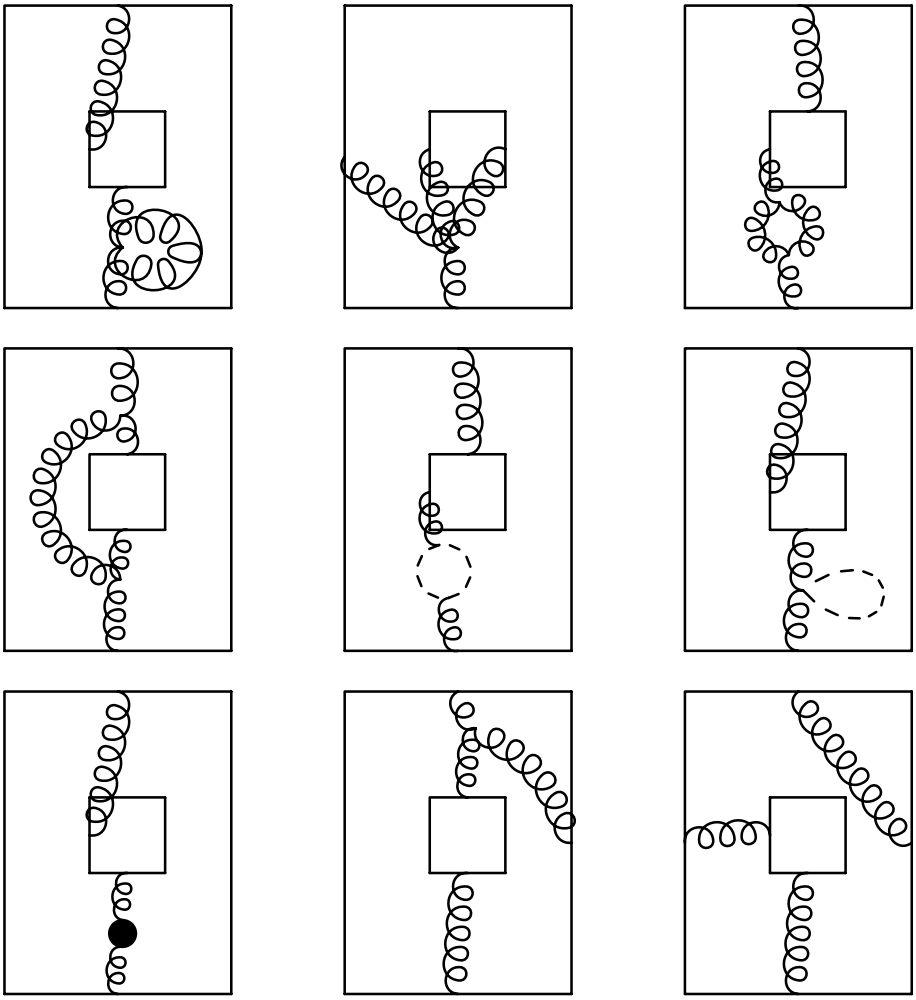

Figure 3.1: Contributions to the l.h.s. of (3.21)

Inserting this into the formula (3.5) and using the validity of the action sum rule in leading order, one arrives at the following formula which has to be shown to be true:

$$
\begin{aligned}
&< S^{(0)} S^{(2)} \omega^{(2)} >_{conn} - \frac{1}{2} < S^{(0)} \left(S^{(1)} \right)^2 \omega^{(2)} >_{conn} + < S^{(0)} S^{(2)}_{FP} \omega^{(2)} >_{conn} \\
&+ < S^{(0)} S^{(2)}_{meas} \omega^{(2)} >_{conn} + < S^{(0)} S^{(1)} \omega^{(3)} >_{conn} - < S^{(0)} \omega^{(4)} >_{conn} \\
&= \\
&+3 < \omega^{(2)} S^{(2)} >_{conn} -2 < \omega^{(2)} \left(S^{(1)} \right)^2 >_{conn} +2 < \omega^{(2)} S^{(2)}_{FP} >_{conn} \\
&+2 < \omega^{(2)} S^{(2)}_{meas} >_{conn} +3 < \omega^{(3)} S^{(1)} >_0 -2 < \omega^{(4)} >_0 \, . \qquad (3.21)
\end{aligned}
$$

Now one can use that the insertion of $S^{(0)}$ into a gluon line transforms the propagator into Landau gauge. For every graph, one has to count the numbers of gluons lines into which $S^{(0)}$ can be inserted; then one gets the following simple results:

$$< S^{(0)} \omega^{(2)} S^{(2)} >_{conn,\alpha=\infty} = 3 < \omega^{(2)} S^{(2)} >_{conn,\alpha=\infty}$$

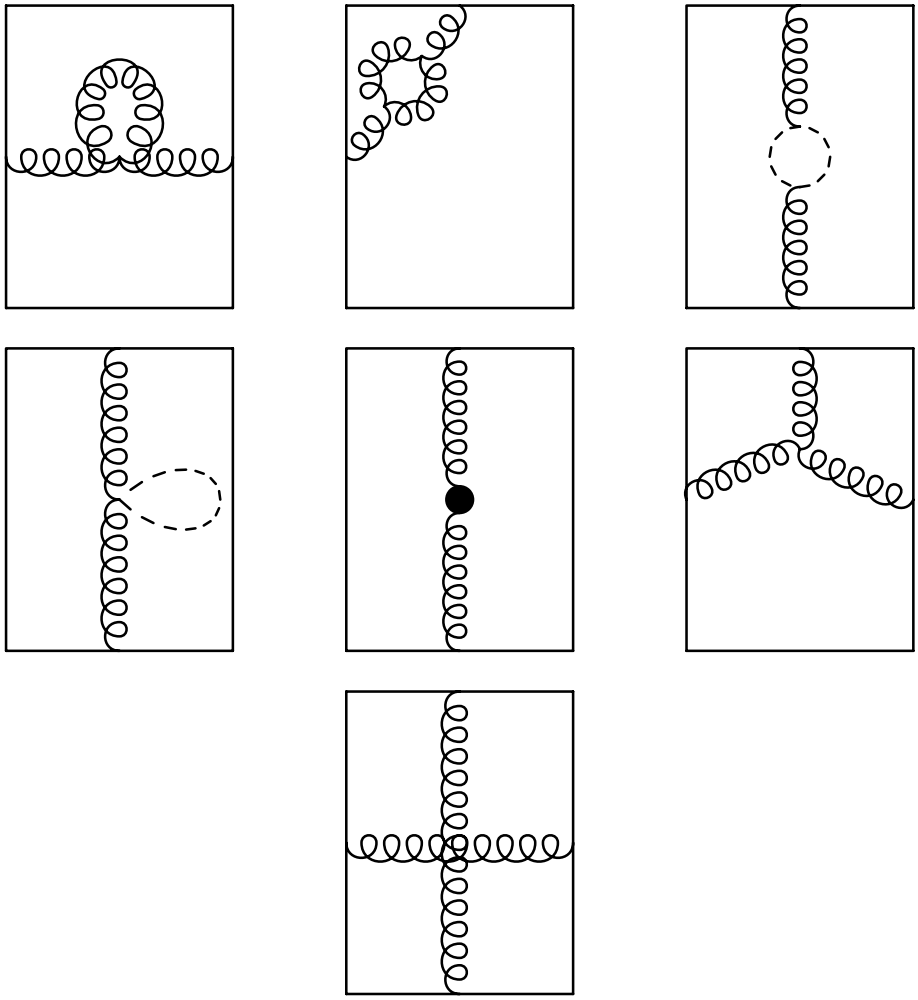

Figure 3.2: Contributions to the r.h.s. of (3.21)

$$
\begin{aligned}
&< S^{(0)}\omega^{(2)}(S^{(1)})^2 >_{conn,\alpha=\infty} = 4 < \omega^{(2)}(S^{(1)})^2 >_{conn,\alpha=\infty} \\
&< S^{(0)}\omega^{(2)}S^{(2)}_{FP} >_{conn,\alpha=\infty} = 2 < \omega^{(2)}S^{(2)}_{FP} >_{conn,\alpha=\infty} \\
&< S^{(0)}\omega^{(2)}S^{(2)}_{meas} >_{conn,\alpha=\infty} = 2 < \omega^{(2)}S^{(2)}_{meas} >_{conn,\alpha=\infty} \\
&< S^{(0)}\omega^{(3)}S^{(1)} >_{conn,\alpha=\infty} = 3 < \omega^{(3)}S^{(1)} >_{conn,\alpha=\infty} \\
&< S^{(0)}\omega^{(4)} >_{conn,\alpha=\infty} = 2 < \omega^{(4)} >_{\alpha=\infty} \ . \qquad (3.22)
\end{aligned}
$$

Inserting these expressions into (3.21), one sees that indeed the left hand side is equal to the right hand side. Hence if one calculates every graph in Landau gauge, the action sum rule is obviously valid up to next-to-leading order. But this is not entirely satisfying, because the results for the potential in chapter 2, taken from [39], were calculated in Feynman gauge instead of Landau gauge; and it will turn out later that checking the energy sum rule can also be done much more easily in Feynman gauge.

Hence what is needed is either a check that the expectation value of the Wilson loop is gauge invariant up to next-to-leading order, or an explicit check

of (3.21) in the Feynman gauge. As will be explained in section 3.3, these two are closely related; checking (3.21) will provide more than half of the check of the gauge invariance already.

Therefore now (3.21) has to be checked. The relevant Feynman diagrams contributing to the left and right hand side, respectively, are given in the figures 3.1 and 3.2. There are essentially three types of graphs: vacuum polarization graphs, one with a three-gluon vertex and one with two independent gluon lines. For the last two, the end points of the gluon lines are not summed over the entire Wilson loop; there are constraints: see the explicit form of $\omega^{(3)}$ and $\omega^{(4)}$ given in section 2.2. In contrast, in the vacuum polarization graphs both gluon end points are summed over the complete Wilson loop. Additionally, in all of the graphs, a sum over all possible positions and orientations of the plaquette is to be understood.

The vacuum polarization graphs can be grouped into two types again: the ones where the action is inserted into an *internal* gluon line (the second and fourth graph in figure 3.1), and the ones where it is inserted into an *external* line (the first, third, fifth, sixth and seventh graph). The second class includes a gluon loop, a gluon tadpole, a ghost loop, a ghost tadpole and a contribution coming from the integration measure; the latter two are special for lattice perturbation theory. These graphs can be dealt with easily if one uses the following observation:

$$\sum_l < A_l A^A_\mu(x) S^{(0)} >_{conn} = \sum_l < A_l A^A_\mu(x) >_{0,\alpha} . \tag{3.23}$$

This means that even if only one end of the gluon line into which the action is inserted is summed over the whole Wilson loop, while the other end is entirely arbitrary, the result will be the same as if one would have used a gluon line in an arbitrary gauge, but without the insertion. This can also be expressed diagrammatically:

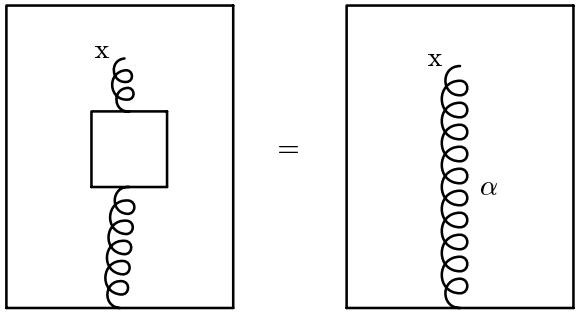

Using this, it becomes obvious that

$$\begin{aligned}
< S^{(0)}\omega^{(2)}S^{(2)} >_{conn} &= 2 < \omega^{(2)}S^{(2)} >_{conn} + \text{insertions into internal lines} \\
< S^{(0)}\omega^{(2)}(S^{(1)})^2 >_{conn} &= 2 < \omega^{(2)}(S^{(1)})^2 >_{conn} + \text{ins. into internal lines} \\
< S^{(0)}\omega^{(2)}S^{(2)}_{FP} >_{conn} &= 2 < \omega^{(2)}S^{(2)}_{FP} >_{conn} \\
< S^{(0)}\omega^{(2)}S^{(2)}_{meas} >_{conn} &= 2 < \omega^{(2)}S^{(2)}_{meas} >_{conn}
\end{aligned} \tag{3.24}$$

or, again with diagrams:

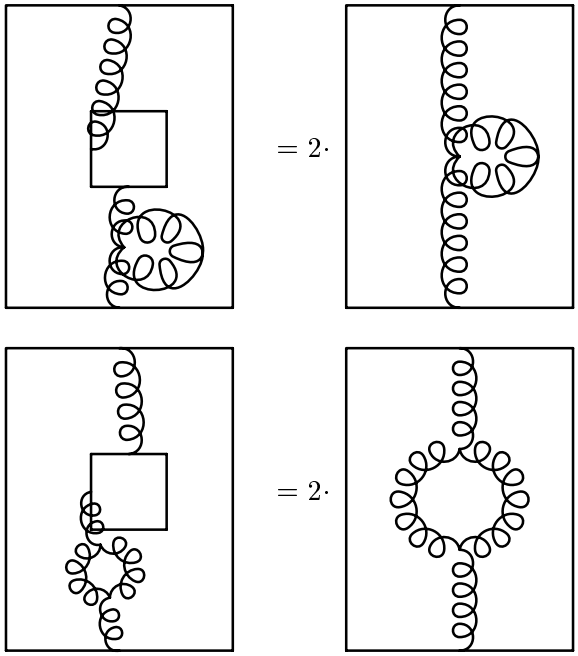

and the same for the graphs with ghost lines and the graph with the insertion of the contribution of the integration measure.

Then there are the graphs where the action is inserted into *internal* gluon lines of the vacuum polarization. Taking them also into account, one can write:

$$\begin{aligned} &< S^{(0)}\omega^{(2)}(S^{(1)})^2 >_{conn} = 4 < (S^{(1)})^2\omega^{(2)} >_{conn} + \Delta < (S^{(1)})^2\omega^{(2)} > \\ &< S^{(0)}\omega^{(2)}S^{(2)} >_{conn} = 3 < S^{(2)}\omega^{(2)} >_{conn} + \Delta < S^{(2)}\omega^{(2)} >, \end{aligned} \tag{3.25}$$

where the Δ-terms come from the operator G contained in the action. The explicit results are:

$$\begin{aligned} &\Delta < (S^{(1)})^2\omega^{(2)} > \\ = \;& -4C_2(G)C_2(F)\sum_{\alpha,\beta}\int_{BZ}\frac{d^4p}{(2\pi)^4}\frac{\sin^2(p_\mu\hat{R}/2)\sin^2(p_\nu\hat{T}/2)}{\hat{p}^4}\frac{\delta_{\mu\alpha}-\delta_{\nu\alpha}}{\sin(p_\alpha/2)}\frac{\delta_{\mu\beta}-\delta_{\nu\beta}}{\sin(p_\beta/2)} \\ & \int_{BZ}\frac{d^4k}{(2\pi)^4}\frac{1}{\hat{k}^4(\widehat{p+k})^2}\Bigg[(\widehat{p+2k})_\alpha(\widehat{p+2k})_\beta\sum_\gamma\hat{k}_\gamma^2\cos^2(p_\gamma/2) \\ + \;& \delta_{\alpha\beta}\cos(k_\alpha/2)\cos(k_\beta/2)((2\widehat{p+k})\hat{k})^2 \\ + \;& \hat{k}_\alpha\hat{k}_\beta\cos((k+p)_\alpha/2)\cos((p+k)_\beta/2)(\widehat{k-p})^2 \\ - \;& \sum_\gamma\hat{k}_\gamma(\widehat{k-p})_\gamma\cos(p_\gamma/2)[(\widehat{p+2k})_\alpha\hat{k}_\beta\cos((p+k)_\beta/2)+\alpha\leftrightarrow\beta] \\ - \;& \hat{k}(2\widehat{p+k})[(\widehat{p+2k})_\alpha\hat{k}_\beta\cos(k_\beta/2)\cos(p_\beta/2)+\alpha\leftrightarrow\beta] \\ + \;& \hat{k}(2\widehat{p+k})[(\widehat{k-p})_\alpha\cos(k_\alpha/2)\hat{k}_\beta\cos((p+k)_\beta/2)+\alpha\leftrightarrow\beta]\Bigg] \end{aligned} \tag{3.26}$$

and

$$\Delta < \omega^{(2)}S^{(2)} >$$

$$
\begin{aligned}
= \quad & -C_2(G)C_2(F)\sum_{\alpha,\beta}\int_{BZ}\frac{d^4p}{(2\pi)^4}\frac{\sin^2(p_\mu\hat{R}/2)\sin^2(p_\nu\hat{T}/2)}{\hat{p}^4}\frac{\delta_{\mu\alpha}-\delta_{\nu\alpha}}{\sin(p_\alpha/2)}\frac{\delta_{\mu\beta}-\delta_{\nu\beta}}{\sin(p_\beta/2)} \\
& \int_{BZ}\frac{d^4k}{(2\pi)^4}\frac{1}{\hat{k}^4}\Bigg[\delta_{\alpha\beta}\Bigg\{2\sum_{\rho\neq\alpha}\hat{k}_\rho^2\cos^2(k_\alpha/2)-4\cos^2(k_\alpha/2)\sum_\rho\sin^2(p_\rho/2)\hat{k}_\rho^2 \\
- \quad & \frac{2}{3}\sin^2(k_\alpha/2)\hat{p}^2+2\hat{k}_\alpha^2\cos^2(k_\alpha/2)\sin^2(p_\alpha/2)\Bigg\} \\
+ \quad & \hat{p}_\alpha\hat{p}_\beta\Bigg\{\frac{4}{3}\sin^2(k_\alpha/2)+\frac{4}{3}\sin^2(k_\beta/2)-2\sin^2(k_\alpha/2)\sin^2(k_\beta/2)\Bigg\}\Bigg] \qquad (3.27)
\end{aligned}
$$

For the graph with the three-gluon vertex (the so-called "spider graph"), one can make use of the fact that in $\omega^{(3)}$, one of the end points of the three gluon lines is summed over the entire gluon loop, without any constraints. Therefore, according to (3.23), an insertion of the action into this line just reproduces the normal spider graph without the insertion, and one has to consider only the effect of inserting the action into the other two lines. The result is, the Δ-term again coming from the operator G contained in the action:

$$
< S^{(0)}\omega^{(3)}S^{(1)} >_{conn} = 3 < \omega^{(3)}S^{(1)} >_{conn} + \Delta < \omega^{(3)}S^{(1)} >, \qquad (3.28)
$$

with

$$
\begin{aligned}
& \Delta < \omega^{(3)}S^{(1)} > \\
= \quad & -2C_2(G)C_2(F)\int_{BZ}\frac{d^4p}{(2\pi)^4}\int_{BZ}\frac{d^4q}{(2\pi)^4}\frac{\sin(p_\mu R/2)\sin(p_\nu T/2)}{\hat{p}^2\hat{q}^4\widehat{(p+q)^2}} \\
& \cdot\Bigg[\Bigg\{\frac{1}{\sin((p_\mu+q_\mu)/2)}\Bigg(\frac{\cos(q_\mu/2)}{\sin(p_\mu/2)}\sum_{\rho\neq\mu}\widehat{(2p+q)}_\rho\hat{q}_\rho \\
& +\frac{\hat{q}_\mu\widehat{(q+p)}_\nu\cos(q_\nu/2)\cos(p_\mu/2)}{\sin(p_\nu/2)}+\frac{\cos(q_\mu/2)\cos((q_\nu+p_\nu)/2)\hat{q}_\nu\hat{p}_\mu}{\sin(p_\nu/2)}\Bigg) \\
& \cdot\Bigg(\sin(p_\nu T/2)\sin((p_\mu+2q_\mu)/2)\Bigg[\frac{\sin((p_\mu+2q_\mu)R/2)}{\sin((p_\mu+2q_\mu)/2)}-\frac{\sin(p_\mu R/2)}{\sin(p_\mu/2)}\Bigg] \\
& +2\sin(q_\nu T/2)\sin((p_\mu+q_\mu)R/2)\cos((p_\nu+q_\nu)T/2)\cos(q_\mu R/2)\Bigg)\Bigg\} \\
& +\Bigg\{(\mu,R)\leftrightarrow(\nu,T)\Bigg\}\Bigg]. \qquad (3.29)
\end{aligned}
$$

For calculating the effect of inserting the action into the graph with two independent gluon lines, it is convenient to split up $\omega^{(4)}$ as shown already in (2.24) and treat the various terms separately. In $\omega^{(4A)}$, all end points of gluon lines are summed over the entire Wilson loop, hence using (3.23), one gets:

$$
< \omega^{(4A)}S^{(0)} >_{conn} = 2 < \omega^{(4A)} >_0 . \qquad (3.30)
$$

The other contributions are much more complicated. In $\omega^{(4C)}$ to $\omega^{(4F)}$, at least one of the end points of the gluon lines is summed over the entire Wilson loop,

and therefore (3.23) can be used to simplify the calculation: insertions of the action in that gluon line simply reproduce the same result as for the graph without any insertions. In $\omega^{(4B)}$, even this simplification is not possible.

The end result is, where again the Δ-terms come from the insertion of G

$$< \omega^{(4)} S^{(0)} >_{conn} = 2 < \omega^{(4)} > + \Delta < \omega^{(4)} >, \tag{3.31}$$

respectively

$$\begin{aligned} < \omega^{(4B)} S^{(0)} >_{conn} &= 2 < \omega^{(4B)} >_0 + \Delta < \omega^{(4B)} >; \\ < \omega^{(4C)} S^{(0)} >_{conn} &= 2 < \omega^{(4C)} >_0 + \Delta < \omega^{(4C)} >; \\ &\dots \end{aligned} \tag{3.32}$$

with:

$$\begin{aligned} & \Delta < \omega^{(4B)} > \\ = \; & -\frac{C_2(G)C_2(F)}{8} g_0^4 \int_{BZ} \frac{d^4p}{(2\pi)^4} \int_{BZ} \frac{d^4k}{(2\pi)^4} \frac{1}{\hat{p}^2 \hat{k}^2} \\ & \cdot \Bigg[\Bigg\{ -4 \frac{\hat{k}_\mu^2}{\hat{k}^2} \Bigg(\Big(\sin^2(p_\nu T/2) \cos^2(k_\nu T/2) + \sin^2(k_\nu T/2) \cos^2(p_\nu T/2) \Big) \\ & \cdot \frac{\sin^2(p_\mu R/2)}{\sin^2(p_\mu/2)} \frac{\sin^2(k_\mu R/2)}{\sin^2(k_\mu/2)} \\ & + \frac{\sin^2(k_\mu R/2)}{\sin^2(k_\mu/2)} \frac{\sin^2(p_\nu T/2)}{\sin^2(p_\nu/2)} + \frac{1}{4} \frac{\sin^2((p_\nu + k_\nu)T/2) \sin^2((p_\mu - k_\mu)/2)}{\sin^2(p_\mu/2) \sin^2(k_\mu/2)} \\ & \cdot \left[\frac{\sin((p_\mu + k_\mu)R/2)}{\sin((p_\mu + k_\mu)/2)} - \frac{\sin((p_\mu - k_\mu)R/2)}{\sin((p_\mu - k_\mu)/2)} \right]^2 \Bigg) \\ & + 8 \frac{\hat{k}_\mu \hat{k}_\nu}{\hat{k}^2} \Bigg(\frac{\sin^2(p_\mu R/2)}{\sin^2(p_\mu/2)} \frac{\sin^2(k_\mu R/2)}{\sin(k_\mu/2)} \frac{\sin^2(k_\nu T/2)}{\sin(k_\nu/2)} \cos^2(p_\nu T/2) \\ & - \frac{1}{2} \frac{\sin((p_\nu + k_\nu)T/2) \sin((p_\mu - k_\mu)/2)}{\sin(p_\mu/2) \sin(k_\mu/2)} \\ & \cdot \left[\frac{\sin((p_\mu + k_\mu)R/2)}{\sin((p_\mu + k_\mu)/2)} - \frac{\sin((p_\mu - k_\mu)R/2)}{\sin((p_\mu - k_\mu)/2)} \right] \Bigg) \Bigg\} + \Big\{ (\mu, R) \leftrightarrow (\nu, T) \Big\} \Bigg] \end{aligned} \tag{3.33}$$

$$\begin{aligned} & \Delta < \omega^{(4C)} > \\ = \; & -\frac{C_2(G)C_2(F)}{4} g_0^4 \int_{BZ} \frac{d^4p}{(2\pi)^4} \int_{BZ} \frac{d^4k}{(2\pi)^4} \frac{1}{\hat{p}^2 \hat{k}^2} \\ & \cdot \Bigg[\Bigg\{ 4 \frac{\hat{k}_\mu^2}{\hat{k}^2} \frac{\sin(p_\mu R/2)}{\sin(p_\mu/2)} \sin^2(p_\nu T/2)(\Sigma_1 - \Sigma_2) \\ & + \frac{\sin^2(p_\mu R/2) \sin^2(p_\nu T/2)}{\sin^2(p_\alpha/2)} (\delta_{\alpha\mu} + \delta_{\alpha\nu}) \frac{\hat{k}_\mu^2}{\hat{k}^2} \left(\frac{\sin^2(k_\mu R/2)}{\sin^2(k_\mu/2)} - R \right) \\ & + 2 \frac{\sin(p_\mu R/2)}{\sin(p_\mu/2)} \sin^2(p_\nu T/2) \frac{\sin(k_\mu R/2)}{\sin(k_\mu/2)} \cos(k_\nu T) \frac{\hat{k}_\mu^2}{\hat{k}^2} \Sigma_R(p_\mu, k_\mu) \end{aligned}$$

$$
\begin{aligned}
&-\frac{\sin(p_\mu R/2)}{\sin(p_\mu/2)}\sin^2(p_\nu T/2)\frac{\sin^2(k_\nu T/2)}{\sin(k_\nu/2)}\frac{\hat{k}_\mu\hat{k}_\nu}{\hat{k}^2}\\
&\cdot\Bigg(\frac{\sin(p_\mu(R-1)/2)}{\sin(p_\mu/2)}\frac{\cos(p_\mu/2)}{\sin(k_\mu/2)}\\
&-\frac{\cos(k_\mu R/2+p_\mu/2)}{\sin(k_\mu/2)}\frac{\sin((p_\mu+k_\mu)(R-1)/2)}{\sin((p_\mu+k_\mu)/2)}\\
&-2\frac{\sin(k_\mu(R-1)/2)\sin(k_\mu(R+1)/2)}{\sin(k_\mu/2)}\frac{\sin(p_\mu R/2)}{\sin(p_\mu/2)}\\
&+2\frac{\cos(k_\mu(R+1)/2)}{\sin(p_\mu/2)}\frac{\sin((p_\mu+k_\mu)(R-1)/2)}{\sin((p_\mu+k_\mu)/2)}\Bigg)\Bigg\}+\Big\{(\mu,R)\leftrightarrow(\nu,T)\Big\}\\
&+2\sin^2(p_\mu R/2)\frac{\sin^2(p_\nu T/2)}{\sin^2(p_\nu/2)}\frac{\hat{k}_\mu^2}{\hat{k}^2}\frac{\sin^2(k_\mu R/2)}{\sin^2(k_\mu/2)}\cos(k_\nu T)\\
&+2\sin^2(p_\nu T/2)\frac{\sin^2(p_\mu R/2)}{\sin^2(p_\mu/2)}\frac{\hat{k}_\nu^2}{\hat{k}^2}\left(\frac{\sin^2(k_\nu T/2)}{\sin^2(k_\nu/2)}-T\right)\\
&-2\frac{\sin^2(p_\mu R/2)}{\sin^2(p_\mu/2)}\sin^2(p_\nu T/2)\frac{\hat{k}_\mu\hat{k}_\nu}{\hat{k}^2}\frac{\sin^2(k_\mu R/2)}{\sin(k_\mu/2)}\frac{\sin^2(k_\nu T/2)}{\sin(k_\nu/2)}\\
&+2\sin^2(p_\mu R/2)\frac{\sin(p_\nu T/2)}{\sin(p_\nu/2)}\frac{\sin^2(k_\mu R/2)}{\sin(k_\mu/2)}\sin(k_\nu T/2)\frac{\hat{k}_\mu\hat{k}_\nu}{\hat{k}^2}\\
&\cdot\left(\frac{\sin(p_\nu T/2)}{\sin(p_\nu/2)}\frac{\sin(k_\nu T/2)}{\sin(k_\nu/2)}-\frac{\sin((p_\nu+k_\nu)T/2)}{\sin((p_\nu+k_\nu)/2)}\right)\Bigg] \qquad (3.34)\\
&\Delta<\omega^{(4D)}>\\
=\;&-\frac{C_2(G)C_2(F)}{12}g_0^4\int\limits_{BZ}\frac{d^4p}{(2\pi)^4}\int\limits_{BZ}\frac{d^4k}{(2\pi)^4}\frac{1}{\hat{p}^2\hat{k}^2}\Bigg[\Bigg\{4\frac{\hat{k}_\mu^2}{\hat{k}^2}\frac{\sin(p_\mu R/2)}{\sin(p_\mu/2)}\sin^2(p_\nu T/2)\\
&\cdot\left(\Sigma_1-\Sigma_2+\frac{1}{2}\frac{\sin(p_\mu R/2)}{\sin(p_\mu/2)}R-\frac{1}{2}\frac{\sin(k_\mu R/2)}{\sin(k_\mu/2)}\frac{\sin((p_\mu+k_\mu)R/2)}{\sin((p_\mu+k_\mu)/2)}\right)\\
&-\frac{\sin^2(p_\mu R/2)\sin^2(p_\nu T/2)}{\sin^2(p_\alpha/2)}(\delta_{\alpha\mu}+\delta_{\alpha\nu})\frac{\hat{k}_\mu^2}{\hat{k}^2}\left(\frac{\sin^2(k_\mu R/2)}{\sin^2(k_\mu/2)}-R\right)\\
&+2\sin^2(p_\mu R/2)\frac{\sin^2(p_\nu T/2)}{\sin^2(p_\nu/2)}\frac{\sin^2(k_\mu R/2)}{\sin^2(k_\mu/2)}\frac{\hat{k}_\mu^2}{\hat{k}^2}\\
&+2\sin^2(p_\nu T/2)\frac{\sin^2(p_\mu R/2)}{\sin^2(p_\mu/2)}\frac{\sin^2(k_\mu R/2)}{\sin^2(k_\mu/2)}\frac{\hat{k}_\mu^2}{\hat{k}^2}(1+\cos(k_\nu T))\\
&-2\sin^2(p_\nu T/2)\frac{\sin(p_\mu R/2)}{\sin(p_\mu/2)}\frac{\sin(k_\mu R/2)}{\sin(k_\mu/2)}\frac{\hat{k}_\mu^2}{\hat{k}^2}\cos(k_\nu T)\Sigma_R(p_\mu,k_\mu)\\
&+2\sin^2(p_\nu T/2)\frac{\sin^2(p_\mu R/2)}{\sin^2(p_\mu/2)}\frac{\sin^2(k_\mu R/2)}{\sin(k_\mu/2)}\frac{\sin^2(k_\nu T/2)}{\sin(k_\nu/2)}\frac{\hat{k}_\mu\hat{k}_\nu}{\hat{k}^2}\\
&-\sin^2(p_\nu T/2)\frac{\sin(p_\mu R/2)}{\sin(p_\mu/2)}\frac{\sin^2(k_\nu T/2)}{\sin(k_\nu/2)}\frac{\hat{k}_\mu\hat{k}_\nu}{\hat{k}^2}\left(2\frac{\sin(p_\mu(R-1)/2)}{\sin(p_\mu/2)}\frac{\cos(p_\mu/2)}{\sin(k_\mu/2)}\right.
\end{aligned}
$$

$$
\begin{aligned}
&-2\frac{\cos(k_\mu R/2+p_\mu/2)}{\sin(k_\mu/2)}\frac{\sin((p_\mu+k_\mu)(R-1)/2)}{\sin((p_\mu+k_\mu)/2)}\\
&-\frac{\sin(k_\mu(R-1)/2)\sin(k_\mu(R+1)/2)}{\sin(k_\mu/2)}\frac{\sin(p_\mu R/2)}{\sin(p_\mu/2)}\\
&+\frac{\cos(k_\mu(R+1)/2)}{\sin(p_\mu/2)}\frac{\sin((p_\mu+k_\mu)(R-1)/2)}{\sin((p_\mu+k_\mu)/2)}\Bigg)\Bigg\}+\Bigg\{(\mu,R)\leftrightarrow(\nu,T)\Bigg\}\\
&-2\sin^2(p_\mu R/2)\frac{\sin(p_\nu T/2)}{\sin(p_\nu/2)}\frac{\sin^2(k_\mu R/2)}{\sin(k_\mu/2)}\sin(k_\nu T/2)\frac{\hat{k}_\mu\hat{k}_\nu}{\hat{k}^2}\\
&\cdot\left(\frac{\sin(p_\nu T/2)}{\sin(p_\nu/2)}\frac{\sin(k_\nu T/2)}{\sin(k_\nu/2)}-\frac{\sin((p_\nu+k_\nu)T/2)}{\sin((p_\nu+k_\nu)/2)}\right)\\
&-2\sin^2(p_\nu T/2)\frac{\sin^2(p_\mu R/2)}{\sin^2(p_\mu/2)}\frac{\hat{k}_\nu^2}{\hat{k}^2}\left(\frac{\sin^2(k_\nu T/2)}{\sin^2(k_\nu/2)}-T\right)\\
&+4\frac{\sin^2(p_\nu T/2)\sin^2(p_\mu R/2)}{\sin^2(p_\alpha/2)}(\delta_{\alpha\mu}-\delta_{\alpha\nu})\frac{\sin^2(k_\mu R/2)}{\sin(k_\mu/2)}\frac{\sin^2(k_\nu T/2)}{\sin(k_\nu/2)}\frac{\hat{k}_\mu\hat{k}_\nu}{\hat{k}^2}\\
&+4\sin^2(p_\mu R/2)\frac{\sin^2(p_\nu T/2)}{\sin^2(p_\nu/2)}\frac{\sin^2(k_\mu R/2)}{\sin^2(k_\mu/2)}\frac{\hat{k}_\mu^2}{\hat{k}^2}\\
&+4\sin^2(p_\nu T/2)\frac{\sin^2(p_\mu R/2)}{\sin^2(p_\mu/2)}\frac{\sin^2(k_\nu T/2)}{\sin^2(k_\nu/2)}\cos(k_\mu R)\frac{\hat{k}_\nu^2}{\hat{k}^2}\\
&-2\sin^2(p_\mu R/2)\frac{\sin^2(p_\nu T/2)}{\sin^2(p_\nu/2)}\frac{\sin^2(k_\mu R/2)}{\sin^2(k_\mu/2)}\cos(k_\nu T)\frac{\hat{k}_\mu^2}{\hat{k}^2}\\
&+2\sin^2(p_\nu T/2)\frac{\sin^2(p_\mu R/2)}{\sin^2(p_\mu/2)}\frac{\sin^2(k_\mu R/2)}{\sin(k_\mu/2)}\frac{\sin^2(k_\nu T/2)}{\sin(k_\nu/2)}\frac{\hat{k}_\mu\hat{k}_\nu}{\hat{k}^2}\Bigg] \qquad (3.35)
\end{aligned}
$$

$$
\begin{aligned}
&\Delta<\omega^{(4E)}>\\
=\;&-\frac{C_2(G)C_2(F)}{6}g_0^4\int\limits_{BZ}\frac{d^4p}{(2\pi)^4}\int\limits_{BZ}\frac{d^4k}{(2\pi)^4}\frac{1}{\hat{p}^2\hat{k}^2}\Bigg[\Bigg\{\frac{\sin(p_\mu R/2)}{\sin(p_\mu/2)}\sin^2(p_\nu T/2)\\
&\cdot\left(\frac{1}{4}\frac{\sin(p_\mu R/2)}{\sin(p_\mu/2)}(2R+T)+\frac{\hat{k}_\mu^2}{\hat{k}^2}\frac{\sin(k_\mu R/2)}{\sin(k_\mu/2)}\frac{\sin((p_\mu+k_\mu)R/2)}{\sin((p_\mu+k_\mu)/2)}\right.\\
&\left.\cdot(\cos(k_\nu T)-1)+\frac{\hat{k}_\mu\hat{k}_\nu}{\hat{k}^2}\frac{\sin^2(k_\nu T/2)}{\sin(k_\nu/2)}\sin(k_\mu R/2)\frac{\sin((p_\mu+k_\mu)R/2)}{\sin((p_\mu+k_\mu)/2)}\right)\Bigg\}\\
&+\Bigg\{(\mu,R)\leftrightarrow(\nu,T)\Bigg\}+\frac{1}{2}\sin^2(p_\nu T/2)\frac{\sin^2(p_\mu R/2)}{\sin^2(p_\mu/2)}T+2\frac{\hat{k}_\mu\hat{k}_\nu}{\hat{k}^2}\frac{\sin(p_\nu T/2)}{\sin(p_\nu/2)}\\
&\cdot\sin^2(p_\mu R/2)\frac{\sin^2(k_\mu R/2)}{\sin(k_\mu/2)}\sin(k_\nu T/2)\frac{\sin((p_\nu+k_\nu)T/2)}{\sin((p_\nu+k_\nu)/2)}\Bigg] \qquad (3.36)
\end{aligned}
$$

and finally

$$\Delta<\omega^{(4F)}>=0, \qquad (3.37)$$

again because of symmetry properties in the colour indices. The functions Σ_1, Σ_2 and Σ_R can be found in section 2.2.2.

Putting everything together, the result is:

$$
\begin{aligned}
&\Delta < \omega^{(4)} > \\
= \quad &\left\{ \frac{C_2(G)C_2(F)}{6}\Delta_0 \int\limits_{BZ} \frac{d^4p}{(2\pi)^4}\frac{1}{\hat{p}^2}\sin^2(p_\nu T/2)\frac{\sin(p_\mu R/2)}{\sin(p_\mu/2)}\left(\frac{\sin(p_\mu R/2)}{\sin(p_\mu/2)}\right.\right. \\
&\left.\left. +\frac{1}{2}\frac{\sin(p_\mu(R-2)/2)}{\sin(p_\mu/2)}\right)\right. \\
&+C_2(G)C_2(F)\int\limits_{BZ}\frac{d^4p}{(2\pi)^4}\int\limits_{BZ}\frac{d^4k}{(2\pi)^4}\frac{1}{\hat{p}^2\hat{k}^2}\frac{\sin^2(p_\mu R/2)\sin^2(p_\nu T/2)}{\sin^2(p_\mu/2)} \\
&\cdot\left(\frac{\hat{k}_\nu^2}{\hat{k}^2}\frac{\sin^2(k_\nu T/2)}{\sin^2(k_\nu/2)}+\frac{1}{6}\frac{\hat{k}_\mu^2}{\hat{k}^2}\frac{\sin^2(k_\mu R/2)}{\sin^2(k_\mu/2)}\right) \\
&-\frac{2C_2(G)C_2(F)}{3}\int\limits_{BZ}\frac{d^4p}{(2\pi)^4}\int\limits_{BZ}\frac{d^4k}{(2\pi)^4}\frac{1}{\hat{p}^2\hat{k}^4}\frac{\sin^2(p_\mu R/2)\sin^2(p_\nu T/2)}{\sin^2(p_\mu/2)} \\
&\cdot\sin^2(k_\mu R/2)\sin^2(k_\nu T/2)\left(\frac{\hat{k}_\nu^2}{\sin^2(k_\nu/2)}-\frac{1}{2}\frac{\hat{k}_\mu^2}{\sin^2(k_\mu/2)}\right) \\
&-\frac{C_2(G)C_2(F)}{2}\int\limits_{BZ}\frac{d^4p}{(2\pi)^4)}\int\limits_{BZ}\frac{d^4k}{(2\pi)^4)}\frac{1}{\hat{p}^2\hat{k}^2}\frac{\hat{k}_\mu^2}{\hat{k}^2}\frac{\sin^2(p_\mu R/2)\sin^2(k_\mu R/2)}{\sin^2(p_\mu/2)\sin^2(k_\mu/2)} \\
&\cdot\sin^2(k_\nu T/2) \\
&-\frac{C_2(G)C_2(F)}{9}\int\limits_{BZ}\frac{d^4p}{(2\pi)^4}\int\limits_{BZ}\frac{d^4k}{(2\pi)^4}\frac{1}{\hat{p}^2\hat{k}^2}\frac{\hat{k}_\mu^2}{\hat{k}^2}\frac{\sin^2((p_\mu-k_\mu)/2)}{\sin^2(p_\mu/2)\sin^2(k_\mu/2)} \\
&\cdot\sin^2((p_\nu+k_\nu)T/2)\left(\frac{\sin((p_\mu+k_\mu)R/2)}{\sin((p_\mu+k_\mu)/2)}-\frac{\sin((p_\mu-k_\mu)R/2)}{\sin((p_\mu-k_\mu)/2)}\right)^2 \\
&-\frac{C_2(G)C_2(F)}{2}\int\limits_{BZ}\frac{d^4p}{(2\pi)^4}\int\limits_{BZ}\frac{d^4k}{(2\pi)^4}\frac{1}{\hat{p}^2\hat{k}^2}\frac{\hat{k}_\mu^2}{\hat{k}^2}\frac{\sin^2(p_\nu T/2)}{\sin^2(p_\nu/2)}\frac{\sin^2(k_\mu R/2)}{\sin^2(k_\mu/2)} \\
&-\frac{C_2(G)C_2(F)}{3}\int\limits_{BZ}\frac{d^4p}{(2\pi)^4)}\int\limits_{BZ}\frac{d^4k}{(2\pi)^4)}\frac{1}{\hat{p}^2\hat{k}^2}\frac{\hat{k}_\mu^2}{\hat{k}^2}\sin^2(p_\nu T/2)\frac{\sin(p_\mu R/2)}{\sin(p_\mu/2)} \\
&\cdot\frac{\sin(k_\mu R/2)}{\sin(k_\mu/2)}\frac{\sin((p_\mu+k_\mu)R/2)}{\sin((p_\mu+k_\mu)/2)} \\
&+\frac{C_2(G)C_2(F)}{3}\int\limits_{BZ}\frac{d^4p}{(2\pi)^4}\int\limits_{BZ}\frac{d^4k}{(2\pi)^4}\frac{1}{\hat{p}^2\hat{k}^2}\frac{\hat{k}_\mu^2}{\hat{k}^2}\sin^2(p_\nu T/2)\frac{\sin(p_\mu R/2)}{\sin(p_\mu/2)} \\
&\cdot\left(\frac{\sin(p_\mu(R-2)/2)\cos(p_\mu+k_\mu)}{\sin(p_\mu/2)\sin^2(k_\mu/2)}\right. \\
&-\frac{\sin((p_\mu+k_\mu)(R-2)/2)\cos(k_\mu(R+1)/2+p_\mu)}{\sin((p_\mu+k_\mu)/2)\sin^2(k_\mu/2)} \\
&\left.+\frac{\sin(p_\mu(R-2)/2)\cos(p_\mu/2-k_\mu)}{\sin(p_\mu/2)\sin(k_\mu/2)\sin((p_\mu+k_\mu)/2)}-\frac{\cos((p_\mu+k_\mu)R/2+k_\mu/2-p_\mu)}{\sin((p_\mu+k_\mu)/2)}\right)
\end{aligned}
$$

$$\cdot\frac{\sin(k_\mu(R-2)/2)}{\sin^2(k_\mu/2)}+\frac{\sin((p_\mu+k_\mu)(R-2)/2)\cos(k_\mu(R+2)/2+p_\mu/2)}{\sin(p_\mu/2)\sin(k_\mu/2)\sin((p_\mu+k_\mu)/2)}$$
$$-\frac{\sin(k_\mu(R-2)/2)\cos((p_\mu-k_\mu)R/2-k_\mu-p_\mu)}{\sin(p_\mu/2)\sin^2(k_\mu/2)}\Bigg)$$
$$+C_2(G)C_2(F)\int\limits_{BZ}\frac{d^4p}{(2\pi)^4}\int\limits_{BZ}\frac{d^4k}{(2\pi)^4}\frac{1}{\hat{p}^2\hat{k}^2}\frac{\hat{k}_\mu\hat{k}_\nu}{\hat{k}^2}\Bigg[\frac{\sin^2(p_\mu R/2)}{\sin^2(p_\mu/2)}\cos^2(p_\nu T/2)$$
$$\cdot\frac{\sin^2(k_\mu R/2)}{\sin(k_\mu/2)}\frac{\sin^2(k_\nu T/2)}{\sin(k_\nu/2)}-\frac{1}{2}\frac{\sin((p_\nu+k_\nu)T/2)\sin((p_\mu-k_\mu)/2)}{\sin(p_\mu/2)\sin(k_\mu/2)}$$
$$\cdot\left(\frac{\sin((p_\mu+k_\mu)R/2)}{\sin((p_\mu+k_\mu)/2)}-\frac{\sin((p_\mu-k_\mu)R/2)}{\sin((p_\mu-k_\mu)/2)}\right)$$
$$\cdot\frac{\sin(p_\mu R/2)}{\sin(p_\mu/2)}\frac{\sin(k_\nu T/2)}{\sin(k_\nu/2)}\cos(p_\nu T/2)\cos(k_\mu R/2)\Bigg]$$
$$+\frac{C_2(G)C_2(F)}{6}\int\limits_{BZ}\frac{d^4p}{(2\pi)^4}\int\limits_{BZ}\frac{d^4k}{(2\pi)^4}\frac{1}{\hat{p}^2\hat{k}^2}\frac{\hat{k}_\mu\hat{k}_\nu}{\hat{k}^2}\sin^2(p_\nu T/2)\frac{\sin(p_\mu R/2)}{\sin(p_\mu/2)}$$
$$\cdot\sin(k_\mu R/2)\frac{\sin^2(k_\nu T/2)}{\sin(k_\nu/2)}\left(\frac{\sin(p_\mu R/2)}{\sin(p_\mu/2)}\frac{\sin(k_\mu R/2)}{\sin(k_\mu/2)}+\frac{\sin((p_\mu+k_\mu)R/2)}{\sin((p_\mu+k_\mu)/2)}\right)$$
$$-\frac{C_2(G)C_2(F)}{12}\int\limits_{BZ}\frac{d^4p}{(2\pi)^4}\int\limits_{BZ}\frac{d^4k}{(2\pi)^4}\frac{1}{\hat{p}^2\hat{k}^2}\frac{\hat{k}_\mu\hat{k}_\nu}{\hat{k}^2}\sin^2(p_\nu T/2)\frac{\sin(p_\mu R/2)}{\sin(p_\mu/2)}$$
$$\cdot\frac{\sin^2(k_\nu T/2)}{\sin(k_\nu/2)}\Bigg(5\frac{\sin(p_\mu(R-1)/2)}{\sin(p_\mu/2)}\frac{\cos(p_\mu/2)}{\sin(k_\mu/2)}$$
$$-5\frac{\cos(k_\mu R/2+p_\mu/2)}{\sin(k_\mu/2)}\frac{\sin((p_\mu+k_\mu)(R-1)/2)}{\sin((p_\mu+k_\mu)/2)}$$
$$-7\frac{\sin(k_\mu(R-1)/2)\sin(k_\mu(R+1)/2)}{\sin(k_\mu/2)}\frac{\sin(p_\mu R/2)}{\sin(p_\mu/2)}$$
$$+7\frac{\cos(k_\mu(R+1)/2)}{\sin(p_\mu/2)}\frac{\sin((p_\mu+k_\mu)(R-1)/2)}{\sin((p_\mu+k_\mu)/2)}\Bigg)\Bigg\}+\Big\{(\mu,R)\leftrightarrow(\nu,T)\Big\}. \tag{3.38}$$

Looking again at (3.21), one sees now that

$$\Delta<S^{(2)}\omega^{(2)}>-\frac{1}{2}\Delta<\left(S^{(1)}\right)^2\omega^{(2)}>+\Delta<S^{(1)}\omega^{(3)}>-\Delta<\omega^{(4)}>=0. \tag{3.39}$$

has to be satisfied in order to show that (3.5) is true in next-to-leading order.

The only way to show this is to numerically evaluate the various eight-dimensional integrals in momentum space for arbitrary $\hat{R}$ and $\hat{T}$. Obviously this would take a lot of computer time; in the light of the fact that (3.5) is an identity and therefore in principle has not to be checked (as explained at the beginning of the chapter, these calculations are mainly done for illustrative purposes, and because the results will become useful later) this is not justifiable.

Therefore only a check for the very special case $\hat{R} = \hat{T} = 1$ was done. Most of the results above simplify significantly then (for example, the functions Σ_1, Σ_2, Σ_R and O_R vanish); most of the integrations can even be done almost exactly, with only the one numerical constant Δ_0 remaining.

But the contributions from $\Delta < \left(S^{(1)}\right)^2 \omega^{(2)} >$ and $\Delta < S^{(1)}\omega^{(3)} >$, which are now given by the following integrals

$$
\begin{aligned}
& \Delta < \left(S^{(1)}\right)^2 \omega^{(2)} > \Big|_{\hat{R}=\hat{T}=1} \\
= \; & -2 \int\limits_{BZ} \frac{d^4p}{(2\pi)^4} \int\limits_{BZ} \frac{d^4k}{(2\pi)^4} \frac{1}{\hat{p}^2 (\hat{k}^2)^2 (\widehat{p+k})^2} \\
& \Bigg[\Bigg((\widehat{p+2k})_\mu^2 \sum_{\rho=1}^{4} \hat{k}_\rho^2 \cos^2(p_\rho/2) + \cos^2(k_\mu/2) \left((\widehat{2p+k})\hat{k} \right)^2 \\
& + \hat{k}_\mu^2 \cos^2((p+k)_\mu/2) (\widehat{k-p})^2 \\
& - 2 (\widehat{p+2k})_\mu \hat{k}_\mu \cos((p+k)_\mu/2) \sum_{\rho=1}^{4} \hat{k}_\rho (\widehat{k-p})_\rho \cos(p_\rho/2) \\
& - 2 \Big[(\widehat{2p+k})\hat{k} ((\widehat{p+2k})_\mu \hat{k}_\mu \cos(k_\mu/2) \cos(p_\mu/2) \\
& - (\widehat{k-p})_\mu \cos(k_\mu/2) \hat{k}_\mu \cos((p+k)_\mu/2) \Big] \Bigg) \hat{p}_\nu^2 \\
& - \Bigg((\widehat{p+2k})_\mu (\widehat{p+2k})_\nu \sum_{\rho=1}^{4} \hat{k}_\rho^2 \cos^2(p_\rho/2) \\
& + \hat{k}_\mu \hat{k}_\nu \cos((p+k)_\mu/2) \cos((p+k)_\nu/2) (\widehat{k-p})^2 \\
& - \sum_{\rho=1}^{4} \hat{k}_\rho (\widehat{k-p})_\rho \cos(p_\rho/2) \\
& \cdot \Big[(\widehat{p+2k})_\mu \hat{k}_\nu \cos((p+k)_\nu/2) + (\widehat{p+2k})_\nu \hat{k}_\mu \cos((p+k)_\mu/2) \Big] \\
& - (2\widehat{p+k})\hat{k} \Big[(\widehat{p+2k})_\mu \hat{k}_\nu \cos(k_\nu/2) \cos(p_\nu/2) \\
& + (\widehat{p+2k})_\nu \hat{k}_\mu \cos(k_\mu/2) \cos(p_\mu/2) - (\widehat{k-p})_\mu \cos(k_\mu/2) \hat{k}_\nu \cos((p+k)_\nu/2) \\
& - (\widehat{k-p})_\nu \cos(k_\nu/2) \hat{k}_\nu \cos((p+k)_\mu/2) \Big] \Bigg) \hat{p}_\mu \hat{p}_\nu \qquad (3.40) \\
& \Delta < S^{(1)} \omega^{(3)} > \Big|_{\hat{R}=\hat{T}=1} \\
= \; & - \int\limits_{BZ} \frac{d^4p}{(2\pi)^4} \int\limits_{BZ} \frac{d^4k}{(2\pi)^4} \frac{1}{\hat{p}^2 (\hat{k}^2)^2 (\widehat{p+k})^2} \Bigg(\Bigg\{ \Big[\hat{p}_\nu \cos(k_\mu/2) \sum_{\rho \neq \mu} (\widehat{p+k})_\rho \hat{k}_\rho \\
& + \hat{p}_\mu \hat{k}_\mu (\widehat{p+k})_\nu \cos(k_\nu/2) \cos(p_\mu/2) + \hat{p}_\mu^2 \hat{k}_\nu \cos(k_\mu/2) \cos((p+k)_\nu/2) \Big] \\
& \cdot \hat{k}_\nu \cos((p+k)_\nu/2) \cos(k_\mu/2) \Bigg\} + \Big\{ \hat{\mu} \leftrightarrow \hat{\nu} \Big\} \Bigg), \qquad (3.41)
\end{aligned}
$$

still have to evaluated completely numerically. This was done using the standard routine *Vegas* from the Numerical Recipes [41]. On the other hand, the integrals

which can be done by hand give:

$$\Delta < S^{(2)}\omega^{(2)} >\Big|_{\hat{R}=\hat{T}=1} = \frac{5}{192}\Delta_0 - \frac{5}{36}\Delta_0^2 \tag{3.42}$$

$$\Delta < \omega^{(4)} >\Big|_{\hat{R}=\hat{T}=1} = \frac{5}{192}\Delta_0 - \frac{1}{6}\Delta_0^2 \tag{3.43}$$

Using the result of a numerical integration for Δ_0, one finally gets the following results:

$$\begin{aligned}
\Delta < S^{(2)}\omega^{(2)} > &= 0.00070077 + -0.00000005 \\
-\frac{1}{2}\Delta < \left(S^{(1)}\right)^2 \omega^{(2)} > &= 0.00187522 + -0.00000145 \\
\Delta < S^{(1)}\omega^{(3)} > &= -0.00254364 + -0.00000265 \\
-\Delta < \omega^{(4)} > &= -0.00003397 + -0.00000062
\end{aligned} \tag{3.44}$$

Add everything up:

$$\begin{aligned}
&\Delta < S^{(2)}\omega^{(2)} > -\frac{1}{2}\Delta < \left(S^{(1)}\right)^2 \omega^{(2)} > +\Delta < S^{(1)}\omega^{(3)} > -\Delta < \omega^{(4)} > \\
= \; & -0.00000162 + -0.00000478,
\end{aligned} \tag{3.45}$$

hence in the range of the numerical error, (3.39) is indeed satisfied—or, in other words, the action sum rule respectively the identity (3.5) is valid up to next-to-leading order (for $\hat{R} = \hat{T} = 1$).

3.3 Gauge invariance of the Wilson Loop

The gauge invariance of the expectation value of the Wilson loop in leading order has already been checked in section 3.2.1. For checking this in next-to-leading order, one makes use again of the relation (3.16) which connects the propagator in Feynman gauge with the propagator in an arbitrary gauge by using the insertion of the operator G.

If one applies this relation to an arbitrary graph with n gluon lines in an arbitrary gauge α, it follows that one can write this graph as a sum of the following contributions: the same graph with all propagators in Feynman gauge, n graphs with $n-1$ propagators in Feynman gauge and the insertion of G in the remaining line, $n(n-1)/2$ graphs with $n-2$ propagators in Feynman gauge and insertions of G into the two remaining lines, and so on; the last one is a graph with insertions of G into *all* lines. The coefficients of the terms in this sum are $(-1)^m \left(1 - \frac{1}{\alpha}\right)^m$, where m is the number of insertions of G.

Here is an example to illustrate this ($n = 3$); as usual a gluon line without an explicit index α represents a propagator in Feynman gauge, and a cross denotes the insertion of the operator G (3.15):

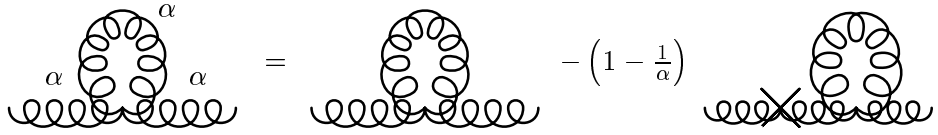

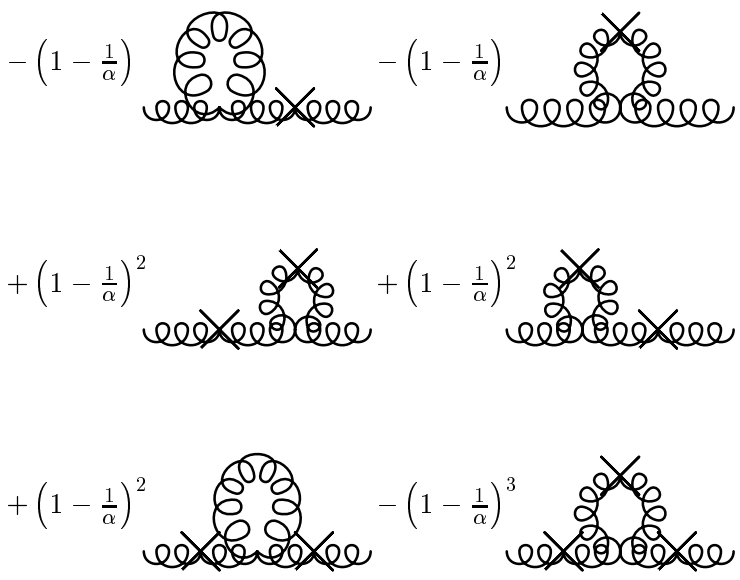

Now looking at the graphs contributing to $< W >$ in next-to-leading order (see figure 3.2), ones sees that there are up to four gluon lines in them. Hence one would expect that if one calculates $< W >$ in an arbitrary gauge, one gets a polynomial in $\left(1 - \frac{1}{\alpha}\right)$ of degree four. If one can show that all terms in this polynomial with the exception of one of order zero (which is independent of α) vanish, then the gauge invariance of the expectation value of the Wilson loop is proven.

Terms of order three and four

The only contributions with a power of $\left(1 - \frac{1}{\alpha}\right)$ greater than two come from the two vacuum polarization graphs (gluon tadpole and gluon loop) where G can be inserted into external as well as into internal lines, and from the spider graph. One can easily show that these contributions give zero. For this, use (3.23); introducing the operator G again, that formula is equivalent to:

$$\sum_l < A_l A_\mu^A(x) G >_{conn} = 0; \tag{3.46}$$

This means that even if only one end of the gluon line into which G is inserted is summed over the whole Wilson loop, while the other end is entirely arbitrary, the contribution of the graph will vanish. Diagrammatically:

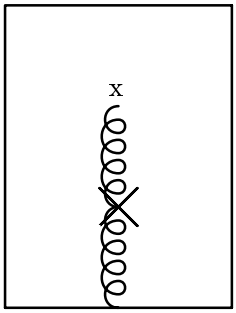

$= 0.$

So, obviously the contributions from the vacuum polarization graphs where G is inserted into an external line, and from the spider graph where G is inserted into the line whose endpoints is summed over the whole loop, vanish, and only terms up to $\left(1-\frac{1}{\alpha}\right)^2$ remain in the polynomial which results from $< W >$.

Terms of order one

The contributions of order $\left(1-\frac{1}{\alpha}\right)^1$ were already given in section 3.2.2 - the Δ terms were just the contributions to $< SW >_{conn}$ which resulted from exactly one insertion of G into a gluon line. It also has been shown in that section that the condition that all of these terms add up to zero (3.39) is equivalent to the validity of (3.5) in next-to-leading order. But as already stressed several times, (3.5) is an identity, hence one can conclude that the contributions of the graphs with exactly one G insertion indeed add up to zero.

Terms of order two

The only contributions which are left are the ones with two insertions of G. Using (3.46), one sees that such contributions can only come from $< \omega^{(3)} S^{(1)} >_0$, $< \omega^{(4B)} >_0$ and $< \omega^{(2)} \left(S^{(1)}\right)^2 >_{conn}$. Fortunately, the explicit calculation of these three contributions is not too hard; the end result is:

$$\begin{aligned} < \omega^{(3)} S^{(1)} >_0 &= < \omega^{(2)} \left(S^{(1)}\right)^2 >_{conn} = 2 < \omega^{(4B)} >_0 \\ &= 8\left(1-\frac{1}{\alpha}\right)^2 C_2(G)C_2(F) \int\limits_{BZ} \frac{d^4p}{(2\pi)^4} \int\limits_{BZ} \frac{d^4k}{(2\pi)^4} \frac{1}{(\hat{k}^2)^2 (\widehat{(p+k)^2})^2} \\ &\quad \cdot \sin^2(p_\mu \hat{R}/2) \sin^2(p_\nu \hat{T}/2) \\ &\quad \cdot \left(\frac{\hat{k}_\mu}{\hat{p}_\mu} \cos((p+k)_\mu/2) - \frac{\hat{k}_\nu}{\hat{p}_\nu} \cos((p+k)_\nu/2)\right)^2 . \end{aligned} \tag{3.47}$$

Considering now that $< W >$ is given by

$$< W > = -\frac{1}{2} g_0^3 < \omega^{(2)} \left(S^{(1)}\right)^2 >_{conn} - g_0^4 < \omega^{(4)} >_0 + g_0^4 < \omega^{(3)} S^{(1)} >_0 + \ldots , \tag{3.48}$$

one sees that the three contributions of order $\left(1-\frac{1}{\alpha}\right)^2$ indeed add up to zero.

Hence it has been shown that in the polynomial in $\left(1-\frac{1}{\alpha}\right)$ of degree 4 one gets from calculating $< W >$ in an arbitrary gauge, only the first term (of order $\left(1-\frac{1}{\alpha}\right)^0$ and hence independent of α) survives: The term of order 1 gives zero because of (3.39), which is equivalent to the identity (3.5); the term of order 2 has been shown to vanish exactly above, and the terms of order 3 and 4 vanish because of (3.46). Therefore the proof is complete: up to next-to-leading order, the expectation value of the Wilson loop is indeed gauge invariant.

3.4 Restriction to a fixed time slice

What remains to be checked is the restriction to one fixed time slice, expressed by the equation

$$\lim_{\hat{T}\to\infty} \frac{1}{\hat{T}} < S >_{q\bar{q}-0} = \lim_{\hat{T}\to\infty} < L(t) >_{q\bar{q}-0} . \tag{3.49}$$

Using (1.8), this is equivalent to:

$$\lim_{\hat{T}\to\infty} \frac{1}{\hat{T}} < SW >_{conn} = \lim_{\hat{T}\to\infty} < LW >_{conn} . \tag{3.50}$$

Alternatively, with (3.5), it can also be written as:

$$\lim_{\hat{T}\to\infty} < LW >_{conn} = g_0^2 \frac{\partial}{\partial g_0^2} \lim_{\hat{T}\to\infty} \frac{1}{\hat{T}} < W > \tag{3.51}$$

The expansion of $< LW >_{conn}$ is very similar to the one for $< SW >_{conn}$ (3.20):

$$\begin{aligned} & < LW > - < L >< W > \\ = \; & -g_0^2 < L^{(0)}\omega^{(2)} >_{conn} + g_0^4 < L^{(0)}S^{(2)}\omega^{(2)} >_{conn} \\ & -\frac{1}{2}g_0^4 < L^{(0)}(S^{(1)})^2\omega^{(2)} >_{conn} + g_0^4 < L^{(0)}S^{(2)}_{FP}\omega^{(2)} >_{conn} \\ & +g_0^4 < L^{(0)}S^{(2)}_{meas}\omega^{(2)} >_{conn} - g_0^4 < L^{(2)}\omega^{(2)} >_{conn} \\ & +g_0^4 < L^{(1)}S^{(1)}\omega^{(2)} >_{conn} - g_0^4 < L^{(1)}\omega^{(3)} >_{conn} \\ & +g_0^4 < L^{(0)}S^{(1)}\omega^{(3)} >_{conn} - g_0^4 < L^{(0)}\omega^{(4)} >_{conn} + O(g_0^6) \end{aligned} \tag{3.52}$$

For the right hand side of (3.51), one can again use (3.19).

3.4.1 Leading order

On the right hand side of (3.51), in leading order the only contribution comes from

$$\begin{aligned} < \omega^{(2)} >_0 \; = \; & 2C_2(F) \int\limits_{BZ} \frac{d^4p}{(2\pi)^4} \frac{\sin^2(p_3\hat{R}/2)\sin^2(p_4\hat{T}/2)}{\hat{p}^2} \\ & \cdot \left(\frac{1}{\sin^2(p_3/2)} + \frac{1}{\sin^2(p_4/2)} \right) . \end{aligned} \tag{3.53}$$

For convenience, the spatial direction of the Wilson loop, previously denoted simply by μ, has been chosen to be the x_3 direction here, and euclidean time, previously denoted by ν, has been identified with x_4.
Now the limit of large $\hat{T}$ has to be considered. Obviously

$$\lim_{\hat{T}\to\infty} \frac{1}{\hat{T}} \int\limits_{BZ} \frac{d^4p}{(2\pi)^4} \frac{\sin^2(p_4\hat{T}/2)}{\hat{p}^2} \frac{\sin^2(p_3\hat{R}/2)}{\sin^2(p_3/2)} = 0.$$

Only the second term can give a non-vanishing contribution; using

$$\lim_{\hat{T}\to\infty} \frac{1}{\hat{T}} \frac{\sin^2(p_4\hat{T}/2)}{\sin^2(p_4/2)} = 2\pi\delta(p_4)$$

(compare with section 2.2.1), what remains is:

$$\lim_{\hat{T}\to\infty} \frac{1}{\hat{T}} < \omega^{(2)} >_0 = 2C_2(F) \int\limits_{BZ} \frac{d^3p}{(2\pi)^3} \frac{\sin^2(p_3\hat{R}/2)}{\hat{\vec{p}}^2} \tag{3.54}$$

with

$$\hat{\vec{p}}^2 = \sum_{j=1}^{3} \hat{p}_j^2.$$

On the other hand, an insertion of $L^{(0)}$ leads to non-conservation of the fourth component of the momentum vector:

$$\begin{aligned} < A_\mu^A(p) A_\nu^B(q) L^{(0)} >_{conn} \;&=\; \delta^{AB} \frac{1}{2} \frac{(2\pi)^3 \delta^3(\vec{p}+\vec{q})}{\hat{p}^2\hat{q}^2} \Big[\left(\delta_{\mu\nu}\hat{p}^2 - \hat{p}_\mu\hat{p}_\nu\right) e^{-i(p+q)_\nu/2} \\ &\quad + \left(\delta_{\mu\nu}\hat{q}^2 - \hat{q}_\mu\hat{q}_\nu\right) e^{-i(p+q)_\mu/2} \Big]. \end{aligned} \tag{3.55}$$

Making use of this, an explicit calculation yields the following result:

$$\begin{aligned} &< L^{(0)}\omega^{(2)} >_{conn} \\ =\; & 2C_2(F) \int\limits_{BZ} \frac{d^4p}{(2\pi)^4} \int\limits_{-\pi}^{\pi} \frac{dq_4}{2\pi} \frac{\hat{\vec{p}}^2 + \frac{1}{2}\left(\hat{p}_4^2 + \hat{q}_4^2\right)}{\hat{p}^2\left(\hat{\vec{p}}^2 + \hat{q}_4^2\right)} \sin^2(p_3\hat{R}/2) \sin(p_4\hat{T}/2) \sin(q_4\hat{T}/2) \\ & \left(-\frac{\cos((p_4+q_4)(n_{c,4}-t))}{\sin^2(p_3/2)} + \frac{\cos((p_4+q_4)(n_{c,4}-t-1/2))}{\sin(p_4/2)\sin(q_4/2)} \right), \end{aligned} \tag{3.56}$$

where again n_c is the center of the Wilson loop and hence

$$n_{c,4} = n_{0,4} + \frac{1}{2}\hat{T}.$$

In the limit of large $\hat{T}$, the first term vanishes due to the fast oscillations of the two sines depending on $\hat{T}$; the second gives only a non-vanishing contribution for $p_4 = q_4 = 0$:

$$\lim_{\hat{T}\to\infty} < L^{(0)}\omega^{(2)} >_{conn} = 2C_2(F) \int\limits_{BZ} \frac{d^3p}{(2\pi)^3} \frac{\sin^2(p_3\hat{R}/2)}{\hat{\vec{p}}^2}, \tag{3.57}$$

which is identical to the result above. Hence in leading order the restriction to the fixed time slice t indeed works:

$$\lim_{\hat{T}\to\infty} \frac{1}{\hat{T}} < S >_{q\bar{q}-0} = \lim_{\hat{T}\to\infty} < L(t) >_{q\bar{q}-0} + O(g_0^4). \tag{3.58}$$

For the special case $n_{c,4} = t$ (the fixed time slice lying in the middle of the Wilson loop), the result above simplifies to

$$\begin{aligned} & < L^{(0)}\omega^{(2)} >_{conn} \\ = \; & 2C_2(F) \int\limits_{BZ} \frac{d^4p}{(2\pi)^4} \int\limits_{-\pi}^{\pi} \frac{dq_4}{2\pi} \frac{\hat{\vec{p}}^2 + \frac{1}{2}\left(\hat{p}_4^2 + \hat{q}_4^2\right)}{\hat{p}^2\left(\hat{\vec{p}}^2 + \hat{q}_4^2\right)} \sin^2(p_3\hat{R}/2)\sin(p_4\hat{T}/2)\sin(q_4\hat{T}/2) \\ & \left(-\frac{1}{\sin^2(p_3/2)} + \frac{\cos((p_4+q_4)/2))}{\sin(p_4/2)\sin(q_4/2)} \right), \end{aligned} \tag{3.59}$$

and it is obvious that the first term vanishes for all $\hat{T}$, because the integrand is odd in p_4 as well as in q_4. For the cosine in the numerator of the second term, use the trigonometric relation $\cos((p_4+q_4)/2)) = \cos(p_4/2)\cos(q_4/2) - \sin(p_4/2)\sin(q_4/2)$; the sines do not contribute because they would again give a function odd in p_4 as well as in q_4. Hence what remains is:

$$\begin{aligned} & < L^{(0)}\omega^{(2)} >_{conn} \\ = \; & 2C_2(F) \int\limits_{BZ} \frac{d^4p}{(2\pi)^4} \int\limits_{-\pi}^{\pi} \frac{dq_4}{2\pi} \frac{\hat{\vec{p}}^2 + \frac{1}{2}\left(\hat{p}_4^2 + \hat{q}_4^2\right)}{\hat{p}^2\left(\hat{\vec{p}}^2 + \hat{q}_4^2\right)} \sin^2(p_3\hat{R}/2) \frac{\sin(p_4\hat{T}/2)}{\tan(p_4/2)} \frac{\sin(q_4\hat{T}/2)}{\tan(q_4/2)}, \end{aligned} \tag{3.60}$$

an expression which in the limit $\hat{T} \to \infty$ again gives

$$\lim_{\hat{T}\to\infty} < L^{(0)}\omega^{(2)} >_{conn} = 2C_2(F) \int\limits_{BZ} \frac{d^3p}{(2\pi)^3} \frac{\sin^2(p_3\hat{R}/2)}{\hat{\vec{p}}^2}. \tag{3.61}$$

3.4.2 Next-to-leading order

The graphs corresponding to the next-to-leading order contributions were mostly given in the figures 3.1 and 3.2 already, but now the plaquettes are not summed over *all* possible positions, but only over the ones with a fixed time. Additionally, three extra graphs have to be considered now, corresponding to $< L^{(2)}\omega^{(2)} >_{conn}$, $< L^{(1)}S^{(1)}\omega^{(2)} >_{conn}$ and $< L^{(1)}\omega^{(3)} >_{conn}$ (see figure 3.3). There again the possible positions of the plaquette lie only on the fixed time slice.

By inspecting the calculation of $S^{(1)}$ and $S^{(2)}$ in [16] and modifying it to give explicit results for $L^{(1)}$ and $L^{(2)}$, one sees that essentially the contributions of the three graphs above can be obtained by using the usual four-gluon vertex in $< L^{(2)}\omega^{(2)} >_{conn}$ and the usual three-gluon vertex in the two other expectation values. The only crucial differences are that one has to replace the usual four momentum conservation at these vertices with conservation of only the spatial

components of the momentum, and that some additional phase factors appear. This will be studied in more detail below.

Now, as usual, consider the different types of graphs separately. There are:

- vacuum polarization graphs
- spider graphs
- graphs with two independent gluon lines

For simplicity, the Wilson loop will now be chosen to lie symmetrically to the fixed time slice, and only the special case $t = 0$ will be treated. Thus one has $n_{0,4} = -\frac{1}{2}\hat{T}$.

The vacuum polarization graphs

In contrast to the situation in section 3.2, there are now two additional vacuum polarization graphs (the first two displayed in figure 3.3); the other five are very similar to the ones already encountered in section 3.2, but now instead of calculating the effect of inserting the operator G, one has to use (3.55) in the gluon lines.

First, look at the cases where L is inserted into an external line (represented by the first, third, fifth, sixth and seventh graph in figure 3.1). Because of the non-conservation of the time component of the momentum, the relation (3.23) can not be used any more; one has to calculate the contributions explicitly. The result is:

$$4C_2(F)\sum_{\alpha,\beta,\gamma}\int_{BZ}\frac{d^4p}{(2\pi)^4}\int_{BZ}\frac{d^4q}{(2\pi)^4}\frac{\sin^2(p_3\hat{R}/2)\sin(p_4\hat{T}/2)\sin(q_4\hat{T}/2)}{(\hat{p}^2)^2\hat{q}^2}\Pi_{\alpha\beta}(p)$$
$$\frac{1}{2}\left[\left(\delta_{\beta\gamma}\hat{p}^2-\hat{p}_\beta\hat{p}_\gamma\right)e^{-i(p+q)_\gamma/2}+\left(\delta_{\beta\gamma}\hat{q}^2-\hat{q}_\beta\hat{q}_\gamma\right)e^{-i(p+q)_\beta/2}\right]$$
$$\frac{\delta_{3\alpha}-\delta_{4\alpha}}{\sin(p_\alpha/2)}\frac{\delta_{3\gamma}-\delta_{4\gamma}}{\sin(q_\gamma/2)}(2\pi)^3\delta(\vec{p}+\vec{q}). \qquad (3.62)$$

In the limit $\hat{T}\to\infty$, only the terms with $\alpha=\gamma=4$ give a non-vanishing contribution, and these only for $p_4 = q_4 = 0$. Hence the limit is, carrying out

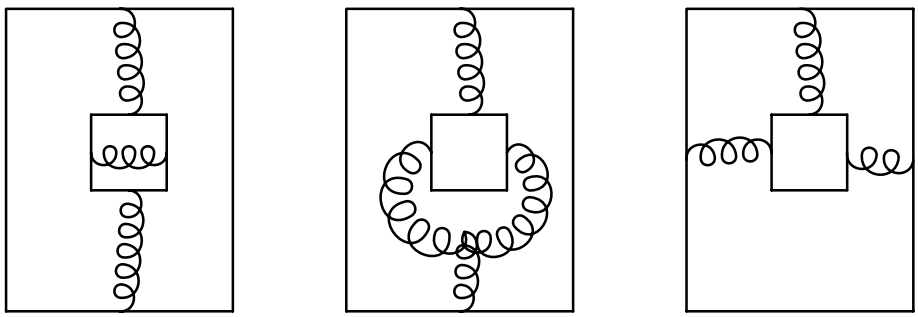

Figure 3.3: Additional contributions to $< LW >_{conn}$

the integration over q_1, q_2 and q_3 using the Delta-function:

$$4C_2(F)\sum_{\alpha,\beta,\gamma}\int_{BZ}\frac{d^3p}{(2\pi)^3}\frac{\sin^2(p_3\hat{R}/2)}{\left(\hat{\vec{p}}^2\right)^2}\Pi_{44}(\vec{p},0). \tag{3.63}$$

This is identical to

$$2\lim_{\hat{T}\to\infty}\frac{1}{\hat{T}}W_{VP},$$

where W_{VP} can be found in section 2.2.2, and, using (3.24), therefore also identical to

$$\lim_{\hat{T}\to\infty}\frac{1}{T}\Bigg(-<S^{(0)}\omega^{(2)}S^{(2)}>_{conn,ext}+<S^{(0)}\omega^{(2)}\frac{1}{2}\left(S^{(1)}\right)^2>_{conn,ext}$$
$$-<S^{(0)}\omega^{(2)}S^{(2)}_{FP}>_{conn,ext}-<S^{(0)}\omega^{(2)}S^{(2)}_{meas}>_{conn,ext}\Bigg), \tag{3.64}$$

where only the insertions of $S^{(0)}$ into the *external* gluon lines are considered.

Next, look at the graphs where the sum over the plaquettes on the time slice $t=0$ is inserted into an *internal* line, represented by the second and fourth graph in figure 3.1, and at the two graphs with insertions of $L^{(1)}$ respectively $L^{(2)}$ depicted in figure 3.3. They give the following contribution:

$$2C_2(F)\sum_{\alpha,\beta}\int_{BZ}\frac{d^4p}{(2\pi)^4}\int_{-\pi}^{\pi}\frac{dq_4}{2\pi}\frac{\sin^2(p_3\hat{R}/2)\sin(p_4\hat{T}/2)\sin(q_4\hat{T}/2)}{\hat{p}^2\left(\hat{\vec{p}}^2+\hat{q}_4^2\right)}$$
$$\frac{\delta_{3\alpha}-\delta_{4\alpha}}{\sin(p_\alpha/2)}\frac{\delta_{3\beta}-\delta_{4\beta}}{\sin(q_\beta/2)}\Pi^L_{\alpha\beta}(\vec{p},p_4,q_4), \tag{3.65}$$

where Π^L represents the vacuum polarization tensor with $L^{(0)}$ inserted into one of its internal lines respectively the two contributions with $L^{(1)}$ or $L^{(2)}$. In the limit $\hat{T}\to\infty$, this reduces to:

$$2C_2(F)\sum_{\alpha,\beta}\int_{BZ}\frac{d^3p}{(2\pi)^3}\frac{\sin^2(p_3\hat{R}/2)}{\left(\hat{\vec{p}}^2\right)^2}\Pi^L_{44}(\vec{p},0,0). \tag{3.66}$$

Now first consider the contribution from the second graph in figure 3.1, where $L^{(0)}$ is inserted into the internal line of the gluon tadpole. The four-gluon vertex appearing there is denoted by $\Gamma^{ABCD}_{\mu\nu\rho\lambda}(k,q,r,s)$. Its explicit form can be found in [16], for example; it is not important here. Then the contribution coming from this graph is proportional to:

$$\sum_{\rho,\lambda}\int_{BZ}\frac{d^4r}{(2\pi)^4}\int_{BZ}\frac{d^4s}{(2\pi)^4}(2\pi)^4\delta(p+q+r+s)\Gamma^{ABCD}_{\mu\nu\rho\lambda}(p,q,r,s)\frac{(2\pi)^3\delta(\vec{r}+\vec{s})}{\hat{r}^2\hat{s}^2}$$
$$\frac{1}{2}\left[\left(\delta_{\rho\lambda}\hat{r}^2-\hat{r}_\rho\hat{r}_\lambda\right)e^{-i(r+s)_\lambda/2}+\left(\delta_{\rho\lambda}\hat{s}^2-\hat{s}_\rho\hat{s}_\lambda\right)e^{-i(r+s)_\rho/2}\right], \tag{3.67}$$

where the Delta-function coming from the four-gluon vertex has been extraced explicitly from Γ. Splitting this four-dimensional Delta-function up into the

spatial and temporal components and looking now only at the relevant component where $p_4 = q_4 = 0$, this reduces to:

$$\int\limits_{BZ} \frac{d^4r}{(2\pi)^4} \int\limits_{BZ} \frac{d^4s}{(2\pi)^4} (2\pi)^3 \delta(\vec{p}+\vec{q}+\vec{r}+\vec{s})(2\pi)\delta(r_4+s_4) \frac{(2\pi)^3\delta(\vec{r}+\vec{s})}{\hat{r}^2\hat{s}^2}$$
$$\sum_{\rho,\lambda} \Gamma^{ABCD}_{\mu\nu\rho\lambda}((\vec{p},0),(\vec{q},0),r,s)$$
$$\frac{1}{2}\left[\left(\delta_{\rho\lambda}\hat{r}^2 - \hat{r}_\rho\hat{r}_\lambda\right) e^{-i(r+s)_\lambda/2} + \left(\delta_{\rho\lambda}\hat{s}^2 - \hat{s}_\rho\hat{s}_\lambda\right) e^{-i(r+s)_\rho/2} \right].$$

Carrying out the four s-integrations, using the second and third Delta-function, yields:

$$\sum_{\rho,\lambda} \int\limits_{BZ} \frac{d^4r}{(2\pi)^4} (2\pi)^3 (\vec{p}+\vec{q}) \Gamma^{ABCD}_{\mu\nu\rho\lambda}((\vec{p},0),(\vec{q},0),r,-r) \frac{\delta_{\rho\lambda}\hat{r}^2 - \hat{r}_\rho\hat{r}_\lambda}{\left(\hat{r}^2\right)^2}. \tag{3.68}$$

Using (3.10), one sees that this is the same result which one would have obtained if one would have inserted $S^{(0)}$ into the internal line of the gluon tadpole diagram and then looked only at the contribution for $p_4 = q_4 = 0$. Hence the result is:

$$\lim_{\hat{T}\to\infty} < L^{(0)}\omega^{(2)}S^{(2)} >_{conn} = \lim_{\hat{T}\to\infty} \frac{1}{\hat{T}} < S^{(0)}\omega^{(2)}S^{(2)} >_{conn}, \tag{3.69}$$

if only the insertion into the internal line is considered. But looking at the results for insertions into the external lines obtained above, one sees that this formula is true even if *all* possible insertions are considered.

Exactly the same arguments can be made for the fourth graph in 3.1, where $L^{(0)}$ is inserted into internal lines of the gluon loop. Here, too, one obtains

$$\lim_{\hat{T}\to\infty} < L^{(0)}\omega^{(2)} \left(S^{(1)}\right)^2 >_{conn} = \lim_{\hat{T}\to\infty} \frac{1}{\hat{T}} < S^{(0)}\omega^{(2)} \left(S^{(1)}\right)^2 >_{conn}, \tag{3.70}$$

using the Delta-functions from the two three-gluon vertices. Using the results obtained above for insertions into external lines, the end result is:

$$\begin{aligned} & \lim_{\hat{T}\to\infty} \Bigg(- < L^{(0)}\omega^{(2)}S^{(2)} >_{conn} + < L^{(0)}\omega^{(2)} \frac{1}{2} \left(S^{(1)}\right)^2 >_{conn} \\ & - < L^{(0)}\omega^{(2)}S^{(2)}_{FP} >_{conn} - < L^{(0)}\omega^{(2)}S^{(2)}_{meas} >_{conn} \Bigg) \\ = & \lim_{\hat{T}\to\infty} \frac{1}{\hat{T}} \Bigg(- < S^{(0)}\omega^{(2)}S^{(2)} >_{conn} + < S^{(0)}\omega^{(2)} \frac{1}{2} \left(S^{(1)}\right)^2 >_{conn} \\ & - < S^{(0)}\omega^{(2)}S^{(2)}_{FP} >_{conn} - < S^{(0)}\omega^{(2)}S^{(2)}_{meas} >_{conn} \Bigg), \end{aligned} \tag{3.71}$$

where now insertions into *all* gluon lines are allowed.

What remains are the two additional vacuum polarization graphs which were depicted in figure 3.3, incorporating $L^{(1)}$ and $L^{(2)}$. First look at the second of

these graphs, which involves a gluon loop where one of the two three-gluon vertices is replaced by $L^{(1)}$. As already mentioned above, the insertion of $L^{(1)}$ at this place amounts to using a slightly altered version of the three-gluon vertex $\Gamma^{ABC}_{\mu\nu\lambda}(p,k,q)$. The usual form can be found again in [16], for example; it comes from $S^{(1)}$. Doing the same derivation as outlined there, but for $L(0)$ instead for S, one gets:

$$\begin{aligned}\Gamma^{(L),ABC}_{\mu\nu\lambda}(p,q,k) &= ig_0(2\pi)^3\delta(\vec{p}+\vec{q}+\vec{k})f_{ABC}\\ &\Big[e^{i(p+q+k)(\hat{\mu}+\hat{\nu})/2}\delta_{\lambda\nu}\cos(p_\nu/2)(\widehat{q-k})_\mu\\ &+e^{i(p+q+k)(\hat{\nu}+\hat{\lambda})/2}\delta_{\mu\lambda}\cos(q_\lambda/2)(\widehat{k-p})_\nu\\ &+e^{i(p+q+k)(\hat{\lambda}+\hat{\mu})/2}\delta_{\nu\mu}\cos(k_\mu/2)(\widehat{p-q})_\lambda\Big]. \qquad (3.72)\end{aligned}$$

Using this, the graph

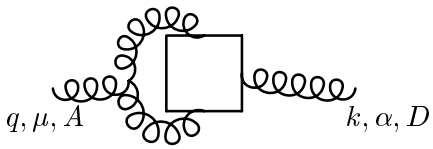

gives a contribution proportional to

$$\begin{aligned}&\int\limits_{BZ}\frac{d^4r}{(2\pi)^4}\int\limits_{BZ}\frac{d^4s}{(2\pi)^4}\frac{1}{\hat{r}^2\hat{s}^2}(2\pi)^4\delta(q-s-r)(2\pi)^3\delta(\vec{k}+\vec{r}+\vec{s})\\ &\sum_{\nu,\lambda}\Gamma^{ABC}_{\mu\nu\lambda}(q,-r,-s)\Gamma^{(L),DBC}_{\alpha\nu\lambda}(k,r,s), \qquad (3.73)\end{aligned}$$

where the Delta-functions have been extracted from the Γs and are displayed explicitly. Doing the integrations over the three spatial components of s using the first Delta-function, this gives:

$$\begin{aligned}&\int\limits_{BZ}\frac{d^4r}{(2\pi)^4}\int\limits_{-\pi}^{\pi}\frac{ds_4}{2\pi}\frac{1}{\hat{r}^2\left((\widehat{\vec{r}-\vec{q}})^2+\hat{s}_4^2\right)}(2\pi)\delta(q_4-s_4-r_4)(2\pi)^3\delta(\vec{k}+\vec{q})\\ &\sum_{\nu,\lambda}\Gamma^{ABC}_{\mu\nu\lambda}(q,-r,(\vec{r},-s_4))\Gamma^{(L),DBC}_{\alpha\nu\lambda}(k,r,(-\vec{r},s_4)).\end{aligned}$$

Now in the limit $\hat{T}\to\infty$, again only the contribution for $q_4=k_4=0$ is needed. Then the first Delta-function can be used to do the s_4-integration, and one gets:

$$\sum_{\nu,\lambda}\int\limits_{BZ}\frac{d^4r}{(2\pi)^4}\frac{(2\pi)^3\delta(\vec{k}+\vec{q})}{\hat{r}^2\left((\widehat{\vec{r}-\vec{q}})^2+\hat{r}_4^2\right)}\Gamma^{ABC}_{\mu\nu\lambda}((\vec{q},0),-r,r)\Gamma^{(L),DBC}_{\alpha\nu\lambda}((\vec{k},0),r,-r).$$

Looking now at (3.72), one sees that in this special case the phase factors give only factors of one, so that

$$\Gamma^{(L),DBC}_{\alpha\nu\lambda}((\vec{k},0),r,-r)=\Gamma^{DBC}_{\alpha\nu\lambda}((\vec{k},0),r,-r),$$

and the contribution from the graph is simply

$$\sum_{\nu,\lambda} \int\limits_{BZ} \frac{d^4r}{(2\pi)^4} \frac{(2\pi)^3 \delta(\vec{k}+\vec{q})}{\hat{r}^2 \left(\widehat{(\vec{r}-\vec{q})^2} + \hat{r}_4^2 \right)} \Gamma^{ABC}_{\mu\nu\lambda}((\vec{q},0),-r,r) \Gamma^{DBC}_{\alpha\nu\lambda}((\vec{k},0),r,-r). \quad (3.74)$$

But that is identical to the contribution which the general gluon loop graph would give if one would also consider only $q_4 = k_4 = 0$ there! Hence the final result is:

$$\lim_{\hat{T}\to\infty} < L^{(1)} S^{(1)} \omega^{(2)} >_{conn} = \lim_{\hat{T}\to\infty} \frac{1}{\hat{T}} < \left(S^{(1)} \right)^2 \omega^{(2)} >_{conn} . \quad (3.75)$$

Exactly the same type of argumentation can be used for the first graph, with the insertion of $L^{(2)}$, so that one gets also:

$$\lim_{\hat{T}\to\infty} < L^{(2)} \omega^{(2)} >_{conn} = \lim_{\hat{T}\to\infty} \frac{1}{\hat{T}} < S^{(2)} \omega^{(2)} >_{conn} . \quad (3.76)$$

Summarizing: in the limit $\hat{T} \to \infty$, all vacuum polarization graphs contributing to the correlator of $L(0)$ and W give the same contribution as the vacuum polarization graphs contributing to the correlator of S and W, divided by $\hat{T}$.

The spider graphs

There are two spider graphs here: the usual one with the three-gluon vertex, where $L^{(0)}$ is inserted into a gluon line (the eighth in figure 3.1), and the one where the three-gluon vertex is replaced by $L^{(1)}$ (the third in figure 3.3). For the normal spider graph, one has:

$$\lim_{\hat{T}\to\infty} \frac{1}{\hat{T}} < S^{(1)} \omega^{(3)} >_0 = 0, \quad (3.77)$$

hence in the limit of high $\hat{T}$, the contributions of these two spider graphs should also vanish.

Unfortunately there is no such elegant argument here as in the case of the vacuum polarization graphs; the contributions have to be calculated explicitly. The second one is simpler tban the first; one gets for it:

$$\begin{aligned}
& < \omega^{(3)} L^{(1)} >_{conn} \\
= \; & \frac{C_2(F) C_2(G)}{2} \int\limits_{BZ} \frac{d^4p}{(2\pi)^4} \int\limits_{BZ} \frac{d^4k}{(2\pi)^4} \int\limits_{-\pi}^{\pi} \frac{dq_4}{2\pi} \frac{\sin(p_3\hat{R}/2)\sin(p_4\hat{T}/2)}{\hat{p}^2 \hat{k}^2 \left(\widehat{(\vec{p}+\vec{k})^2} + \hat{q}_4^2 \right)} \\
& \left[4 \frac{\cos((k+p)_4/2)\cos((p+k)_3/2)(\widehat{k-p})_4}{\sin(p_3/2)} \cos(k_3\hat{R}/2) \frac{\sin((p+k)_3\hat{R}/2)}{\sin((p+k)_3/2)} \right. \\
& \cdot \frac{\sin(k_4\hat{T}/2)}{\sin(k_4/2)} \cos(q_4(\hat{T}-1)/2) \\
& \left. -2 \frac{\cos(p_4/2)(\widehat{2k+p})_3}{\sin(p_3/2)} \sin(p_4/2)\cos(q_4/2)\cos(k_4/2) \right.
\end{aligned}$$

$$
\begin{aligned}
&\cdot\frac{\sin(q_4\hat{T}/2)}{\sin(q_4/2)}\frac{\sin(k_4\hat{T}/2)}{\sin(k_4/2)}\sin((2k+p)_3\hat{R}/2)\\
&-4\frac{\cos(p_4/2)(\widehat{2k+p})_3}{\sin(p_3/2)}\sin(p_3\hat{R}/2)\sin(p_4/2)\cos((k+q)_4/2)O_T(q_4,k_4)\\
&-4\frac{\cos(p_4/2)\cos^2(k_4/2)(\widehat{2p+k})_3}{\sin(p_4/2)}\frac{\sin((p+k)_3\hat{R}/2)}{\sin((p+k)_3/2)}\frac{\sin(k_4\hat{T}/2)}{\sin(k_4/2)}\\
&\cdot\cos(k_3\hat{R}/2)\cos(q_4(\hat{T}-1)/2)\\
&+4\frac{\cos(p_3/2)(\widehat{q-k})_4}{\sin(p_4/2)}\cos(p_4/2)\cos((q+k)_4/2)\sin((q+k)_4\hat{T}/2)\\
&\cdot O_R(k_3,-p_3-k_3). \qquad (3.78)
\end{aligned}
$$

In the limit $\hat{T}\to\infty$, terms like

$$\frac{\sin(q_4\hat{T}/2)}{\sin(q_4/2)}$$

give constant contributions, whereas sines and cosines which depend on $\hat{T}$, but are not divided by the corresponding sines of the coordinates, give contributions proportional to $\hat{T}^{-1}$ because of the fast oscillations of these functions. Therefore all of the terms in the expression above go to zero in the limit:

$$\lim_{\hat{T}\to\infty} < \omega^{(3)}L^{(1)} >_{conn} = 0. \qquad (3.79)$$

The first spider graph is much more complicated:

$$
\begin{aligned}
&< L^{(0)}\omega^{(3)}S^{(1)} >_{conn} \sim \sum_{\gamma,\delta,\epsilon,\varphi}\int_{BZ}\frac{d^4p}{(2\pi)^4}\int_{BZ}\frac{d^4k}{(2\pi)^4}\int_{-\pi}^{\pi}\frac{dq_4}{2\pi}\Gamma_{\delta\epsilon\gamma}(p,k,-p-k)\\
&\frac{1}{2}\left(\frac{\left[\delta_{\gamma\varphi}\left(\left(\widehat{\vec{p}+\vec{k}}\right)^2+\hat{q}_4^2\right)-\hat{q}_\gamma\hat{q}_\varphi\right]\Big|_{\vec{q}=-\vec{p}-\vec{k}}\; e^{-i(p+k+q)\gamma/2}}{\hat{p}^2\hat{k}^2\left(\widehat{p+k}\right)^2\left(\left(\widehat{\vec{p}+\vec{k}}\right)^2+\hat{q}_4^2\right)}\right.\\
&\left.-\frac{\left[\delta_{\gamma\varphi}\left(\widehat{p+k}\right)^2-\left(\widehat{p+k}\right)_\gamma\left(\widehat{p+k}\right)_\varphi\right]e^{-i(p+k+q)_\varphi/2}}{\hat{p}^2\hat{k}^2\left(\widehat{p+k}\right)^2\left(\left(\widehat{\vec{p}+\vec{k}}\right)^2+\hat{q}_4^2\right)}\right)\\
&\cdot\left[\frac{\delta_{3\delta}-\delta_{4\delta}}{\sin(p_\delta/2)}\sin(p_3\hat{R}/2)\sin(p_4\hat{T}/2)\right.\\
&\cdot\left(2\delta_{3\epsilon}\delta_{4\varphi}\frac{\sin(k_3\hat{R}/2)}{\sin(k_3/2)}\frac{\sin(q_4\hat{T}/2)}{\sin(q_4/2)}\left(\cos((p+k)_3\hat{R}/2+k_4\hat{T}/2)\right.\right.\\
&\left.\left.-i\sin((p+k)_3\hat{R}/2+k_4\hat{T}/2)\right)\right.\\
&\left.+\delta_{3\epsilon}\delta_{3\varphi}\Big(-i\sin((q-k)_4\hat{T}/2)\frac{\sin(k_3\hat{R}/2)}{\sin(k_3/2)}\frac{\sin((p+k)_3\hat{R}/2)}{\sin((p+k)_3/2)}\right.
\end{aligned}
$$

$$
\begin{aligned}
&+2\sin((q+k)_4\hat{T}/2)O_R(k_3,-p_3-k_3)\Big)\\
&-2\delta_{4\epsilon}\delta_{3\varphi}\frac{\sin(k_4\hat{T}/2)}{\sin(k_4/2)}\frac{\sin((p+k)_3\hat{R}/2)}{\sin((p+k)_3/2)}\Big(\cos(q_4\hat{T}/2-k_3\hat{R}/2)\\
&+i\sin(q_4\hat{T}/2+k_3\hat{R}/2)\Big)\\
&-\delta_{4\epsilon}\delta_{4\varphi}\Big(i\sin((p+2k)_3\hat{R}/2)\frac{\sin(k_4\hat{T}/2)}{\sin(k_4/2)}\frac{\sin(q_4\hat{T}/2)}{\sin(q_4/2)}\\
&-2\sin(p_3\hat{R}/2)O_T(k_4,q_4)\Big)\Big)\\
&-\Big(\frac{\delta_{3\phi}}{\sin((p+k)_3/2)}+\frac{\delta_{4\phi}}{\sin(q_4/2)}\Big)\sin((p+k)_3\hat{R}/2)\sin(q_4\hat{T}/2)\\
&\cdot\Big(2\delta_{3\epsilon}\delta_{4\delta}\frac{\sin(k_3\hat{R}/2)}{\sin(k_3/2)}\frac{\sin(p_4\hat{T}/2)}{\sin(p_4/2)}\Big(\cos(p_3\hat{R}/2-k_4\hat{T}/2)\\
&+i\sin(p_3\hat{R}/2+k_4\hat{T}/2)\Big)\\
&+\delta_{3\epsilon}\delta_{3\delta}\Big(-i\sin((p-k)_4\hat{T}/2)\frac{\sin(k_3\hat{R}/2)}{\sin(k_3/2)}\frac{\sin(p_3\hat{R}/2)}{\sin(p_3/2)}\\
&+2\sin((p+k)_4\hat{T}/2)O_R(k_3,p_3)\Big)\\
&-2\delta_{4\epsilon}\delta_{3\delta}\frac{\sin(k_4\hat{T}/2)}{\sin(k_4/2)}\frac{\sin(p_3\hat{R}/2)}{\sin(p_3/2)}\Big(\cos(p_4\hat{T}/2-k_3\hat{R}/2)\\
&+i\sin(p_4\hat{T}/2+k_3\hat{R}/2)\Big)\\
&-\delta_{4\epsilon}\delta_{4\delta}\Big(i\sin((p-k)_3\hat{R}/2)\frac{\sin(k_4\hat{T}/2)}{\sin(k_4/2)}\frac{\sin(p_4\hat{T}/2)}{\sin(p_4/2)}\\
&-2\sin((p+k)_3\hat{R}/2)O_T(k_4,p_4)\Big)\Big)\Big].
\end{aligned}
\tag{3.80}
$$

Here the explicit expression for the three-gluon vertex $\Gamma_{\delta\epsilon\gamma}$ was not inserted and the sums were not carried out; this would only have given an even more complicated result. This is not necessary because even here one can already see that all of the terms which appear vanish in the limit (using the same arguments as above). Hence the result for this spider graph is also:

$$\lim_{\hat{T}\to\infty} < L^{(0)}\omega^{(3)}S^{(1)} >_{conn} = 0. \tag{3.81}$$

Thus indeed both spider graphs vanish in the limit of large $\hat{T}$.

The graphs with two independent gluon lines

As usual, $\omega^{(4)}$ is splitted up into its parts and every contribution is calculated separately. First one obtains, again using the symmetry properties of the colour indices:

$$< L^{(0)}\omega^{(4F)} >_{conn} = 0. \tag{3.82}$$

The contribution of $\omega^{(4)}$ which is proportional to $(C_2(F))^2$ only comes from $\omega^{(4A)}$ and can also be easily calculated:

$$< L^{(0)}\omega^{(4A)} >_{conn} = < \omega^{(2)} >< L^{(0)}\omega^{(2)} >_{conn} + C_2(G)C_2(F)\cdot(\ldots) \qquad (3.83)$$

In the limit of large $\hat{T}$, $< L^{(0)}\omega^{(2)} >_{conn}$ gives the same contribution as $< S^{(0)}\omega^{(2)} >_{conn} /\hat{T}$ and therefore $< L^{(0)}\omega^{(4A)} >_{conn}$ gives the same contribution as $< S^{(0)}\omega^{(4A)} >_{conn} /\hat{T}$.

The other parts are much more complicated. Because of the non-conservation of the momentum when $L^{(0)}$ is inserted, (3.23) no longer applies, so that the insertion into *both* lines has to be considered now. This leads to a doubling of the number of the graphs which have to be computed.

It is convenient to split the various contributions up again, classifying them according to the number of links in spatial and temporal direction. First look at the graphs where only spatial links appear; denote the relevant parts of $\omega^{(4)}$ by $\omega^{(4)}_{RR}$:

$$\begin{aligned}
& < L^{(0)}\omega^{(4A)}_{RR} >_{conn} \\
= \; & -2\frac{C_2(G)C_2(F)}{3}\int\limits_{BZ}\frac{d^4p}{(2\pi)^4}\int\limits_{BZ}\frac{d^4k}{(2\pi)^4}\int\limits_{-\pi}^{\pi}\frac{dq_4}{2\pi}\frac{1}{\hat{k}^2}\frac{\hat{\vec{p}}^2+\frac{1}{2}\hat{p}_4^2+\frac{1}{2}\hat{q}_4^2-\hat{p}_3^2}{\hat{p}^2\left(\hat{\vec{p}}^2+\hat{q}_4^2\right)} \\
& \frac{\sin^2(p_3\hat{R}/2)}{\sin^2(p_3/2)}\frac{\sin^2(k_3\hat{R}/2)}{\sin^2(k_3/2)}\sin^2(k_4\hat{T}/2)\sin(p_4\hat{T}/2)\sin(q_4\hat{T}/2) \qquad (3.84) \\
& < L^{(0)}\omega^{(4B)}_{RR} >_{conn} \\
= \; & -\frac{C_2(G)C_2(F)}{2}\int\limits_{BZ}\frac{d^4p}{(2\pi)^4}\int\limits_{BZ}\frac{d^4k}{(2\pi)^4}\int\limits_{-\pi}^{\pi}\frac{dq_4}{2\pi}\frac{1}{\hat{k}^2}\frac{\hat{\vec{p}}^2+\frac{1}{2}\hat{p}_4^2+\frac{1}{2}\hat{q}_4^2-\hat{p}_3^2}{\hat{p}^2\left(\hat{\vec{p}}^2+\hat{q}_4^2\right)} \\
& \cdot\Bigg[\sin((k-p)_4\hat{T}/2)\sin((k+q)_4\hat{T}/2)\frac{\sin^2(p_3\hat{R}/2)}{\sin^2(p_3/2)}\frac{\sin^2(k_3\hat{R}/2)}{\sin^2(k_3/2)} \\
& +4\sin((p+k)_4\hat{T}/2)\sin((q-k)_4\hat{T}/2)O_R^2(p_3,k_3)\Bigg] \qquad (3.85) \\
& < L^{(0)}\omega^{(4C)}_{RR} >_{conn} \\
= \; & \frac{C_2(F)C_2(G)}{2}\int\limits_{BZ}\frac{d^4p}{(2\pi)^4}\int\limits_{BZ}\frac{d^4k}{(2\pi)^4}\int\limits_{-\pi}^{\pi}\frac{dq_4}{2\pi}\frac{1}{\hat{k}^2}\frac{\hat{\vec{p}}^2+\frac{1}{2}\hat{p}_4^2+\frac{1}{2}\hat{q}_4^2-\hat{p}_3^2}{\hat{p}^2\left(\hat{\vec{p}}^2+\hat{q}_4^2\right)} \\
& \cdot\sin^2(k_4\hat{T}/2)\frac{\sin(k_3\hat{R}/2)}{\sin(k_3/2)}\cos(p_4\hat{T}/2)\cos(q_4\hat{T}/2) \qquad (3.86) \\
& \cdot\Bigg[2\;(\Sigma_1-\Sigma_2)|_{p_3\leftrightarrow k_3}+\frac{\sin(k_3\hat{R}/2)}{\sin(k_3/2)}\Sigma_R(p_3,-p_3)+\frac{\sin(p_3\hat{R}/2)}{\sin(p_3/2)}\Sigma_R(p_3,k_3)\Bigg] \\
& < L^{(0)}\omega^{(4D)}_{RR} >_{conn} \\
= \; & \frac{C_2(F)C_2(G)}{6}\int\limits_{BZ}\frac{d^4p}{(2\pi)^4}\int\limits_{BZ}\frac{d^4k}{(2\pi)^4}\int\limits_{-\pi}^{\pi}\frac{dq_4}{2\pi}\frac{1}{\hat{k}^2}\frac{\hat{\vec{p}}^2+\frac{1}{2}\hat{p}_4^2+\frac{1}{2}\hat{q}_4^2-\hat{p}_3^2}{\hat{p}^2\left(\hat{\vec{p}}^2+\hat{q}_4^2\right)}
\end{aligned}$$

$$
\begin{aligned}
&\cdot \sin^2(k_4\hat{T}/2)\frac{\sin(k_3\hat{R}/2)}{\sin(k_3/2)}\cos(p_4\hat{T}/2)\cos(q_4\hat{T}/2)\\
&\cdot\Bigg[2\,(\Sigma_1-\Sigma_2)|_{p_3\leftrightarrow k_3}+2\,\Sigma_R(0,-k_3)-2\,\Sigma_R(p_3-k_3,-p_3)\\
&+2\frac{\sin(k_3\hat{R}/2)}{\sin(k_3/2)}\frac{\sin^2(p_3\hat{R}/2)}{\sin^2(p_3/2)}-\frac{\sin(p_3\hat{R}/2)}{\sin(p_3/2)}\Sigma_R(p_3,k_3)\\
&+\frac{\sin(k_3\hat{R}/2)}{\sin(k_3/2)}\Sigma_R(p_3,-p_3)\Bigg] \qquad (3.87)\\
&<L^{(0)}\omega_{RR}^{(4E)}>_{conn}\\
=\;&\frac{C_2(F)C_2(G)}{6}\int\limits_{BZ}\frac{d^4p}{(2\pi)^4}\int\limits_{BZ}\frac{d^4k}{(2\pi)^4}\int\limits_{-\pi}^{\pi}\frac{dq_4}{2\pi}\frac{1}{\hat{k}^2}\frac{\hat{\vec{p}}^2+\frac{1}{2}\hat{p}_4^2+\frac{1}{2}\hat{q}_4^2-\hat{p}_3^2}{\hat{p}^2\left(\hat{\vec{p}}^2+\hat{q}_4^2\right)}\\
&\cdot\cos(p_4\hat{T}/2)\cos(q_4\hat{T}/2)\sin^2(k_4\hat{T}/2)\frac{\sin(k_3\hat{R}/2)}{\sin(k_3/2)}\Bigg[\frac{\sin(k_3\hat{R}/2)}{\sin(k_3/2)}\hat{R}\\
&+\frac{\sin(k_3\hat{R}/2)}{\sin(k_3/2)}\frac{\sin(p_3\hat{R}/2)}{\sin(p_3/2)}\frac{\sin((p+k)_3\hat{R}/2)}{\sin((p+k)_3/2)}\Bigg]. \qquad (3.88)
\end{aligned}
$$

Because of the fast oscillations of the two cosines for $\hat{T}\to\infty$, the contributions of these integrals vanish in the limit of large $\hat{T}$.

The next group consists of the graphs with two spatial and two temporal links, where $L^{(0)}$ is inserted into the line connecting the two spatial links. The corresponding parts of $\omega^{(4)}$ are denoted by $\omega_{RT1}^{(4)}$:

$$
\begin{aligned}
&<L^{(0)}\omega_{RT1}^{(4A)}>_{conn}\\
=\;&-2\frac{C_2(G)C_2(F)}{3}\int\limits_{BZ}\frac{d^4p}{(2\pi)^4}\int\limits_{BZ}\frac{d^4k}{(2\pi)^4}\int\limits_{-\pi}^{\pi}\frac{dq_4}{2\pi}\frac{1}{\hat{k}^2}\frac{\hat{\vec{p}}^2+\frac{1}{2}\hat{p}_4^2+\frac{1}{2}\hat{q}_4^2-\hat{p}_3^2}{\hat{p}^2\left(\hat{\vec{p}}^2+\hat{q}_4^2\right)}\\
&\frac{\sin^2(p_3\hat{R}/2)}{\sin^2(p_3/2)}\frac{\sin^2(k_4\hat{T}/2)}{\sin^2(k_4/2)}\sin^2(k_3\hat{R}/2)\sin(p_4\hat{T}/2)\sin(q_4\hat{T}/2) \qquad (3.89)\\
=\;&0\\
&<L^{(0)}\omega_{RT1}^{(4B)}>_{conn}\\
=\;&-\frac{C_2(G)C_2(F)}{2}\int\limits_{BZ}\frac{d^4p}{(2\pi)^4}\int\limits_{BZ}\frac{d^4k}{(2\pi)^4}\int\limits_{-\pi}^{\pi}\frac{dq_4}{2\pi}\frac{1}{\hat{k}^2}\frac{\hat{\vec{p}}^2+\frac{1}{2}\hat{p}_4^2+\frac{1}{2}\hat{q}_4^2-\hat{p}_3^2}{\hat{p}^2\left(\hat{\vec{p}}^2+\hat{q}_4^2\right)}\\
&\cdot\frac{\sin^2(p_3\hat{R}/2)}{\sin^2(p_3/2)}\frac{\sin^2(k_4\hat{T}/2)}{\sin^2(k_4/2)}\cos(p_4\hat{T}/2)\cos(q_4\hat{T}/2) \qquad (3.90)\\
&<L^{(0)}\omega_{RT1}^{(4C)}>_{conn}\\
=\;&\frac{C_2(G)C_2(F)}{2}\int\limits_{BZ}\frac{d^4p}{(2\pi)^4}\int\limits_{BZ}\frac{d^4k}{(2\pi)^4}\int\limits_{-\pi}^{\pi}\frac{dq_4}{2\pi}\frac{1}{\hat{k}^2}\frac{\hat{\vec{p}}^2+\frac{1}{2}\hat{p}_4^2+\frac{1}{2}\hat{q}_4^2-\hat{p}_3^2}{\hat{p}^2\left(\hat{\vec{p}}^2+\hat{q}_4^2\right)}\\
&\cdot\Bigg[\frac{\sin^2(k_4\hat{T}/2)}{\sin^2(k_4/2)}\sin^2(k_3\hat{R}/2)\cos(p_4\hat{T}/2)\cos(q_4\hat{T}/2)\Sigma_R(p_3,-p_3)
\end{aligned}
$$

$$+\frac{\sin^2(k_4\hat{T}/2)}{\sin^2(k_4/2)}\sin^2(k_3\hat{R}/2)\cos(p_4\hat{T}/2)\cos(q_4\hat{T}/2)\frac{\sin^2(p_3\hat{R}/2)}{\sin^2(p_3/2)}\Bigg] \quad (3.91)$$

$$< L^{(0)}\omega_{RT1}^{(4D)} >_{conn}$$

$$= \frac{C_2(G)C_2(F)}{6}\int\limits_{BZ}\frac{d^4p}{(2\pi)^4}\int\limits_{BZ}\frac{d^4k}{(2\pi)^4}\int\limits_{-\pi}^{\pi}\frac{dq_4}{2\pi}\frac{1}{\hat{k}^2}\frac{\hat{\vec{p}}^2+\frac{1}{2}\hat{p}_4^2+\frac{1}{2}\hat{q}_4^2-\hat{p}_3^2}{\hat{p}^2\left(\hat{\vec{p}}^2+\hat{q}_4^2\right)}$$

$$\cdot\Bigg[-\frac{\sin^2(k_4\hat{T}/2)}{\sin^2(k_4/2)}\sin^2(k_3\hat{R}/2)\cos(p_4\hat{T}/2)\cos(q_4\hat{T}/2)\Sigma_R(p_3,-p_3)$$

$$+2\frac{\sin^2(k_4\hat{T}/2)}{\sin^2(k_4/2)}\sin^2(k_3\hat{R}/2)\cos(p_4\hat{T}/2)\cos(q_4\hat{T}/2)\frac{\sin^2(p_3\hat{R}/2)}{\sin^2(p_3/2)}\Bigg] \quad (3.92)$$

$$< L^{(0)}\omega_{RT1}^{(4E)} >_{conn}$$

$$= \frac{C_2(G)C_2(F)}{6}\int\limits_{BZ}\frac{d^4p}{(2\pi)^4}\int\limits_{BZ}\frac{d^4k}{(2\pi)^4}\int\limits_{-\pi}^{\pi}\frac{dq_4}{2\pi}\frac{1}{\hat{k}^2}\frac{\hat{\vec{p}}^2+\frac{1}{2}\hat{p}_4^2+\frac{1}{2}\hat{q}_4^2-\hat{p}_3^2}{\hat{p}^2\left(\hat{\vec{p}}^2+\hat{q}_4^2\right)}$$

$$\cdot\frac{\sin^2(k_4\hat{T}/2)}{\sin^2(k_4/2)}\sin^2(k_3\hat{R}/2)\cos(p_4\hat{T}/2)\cos(q_4\hat{T}/2)\hat{R}. \quad (3.93)$$

For $\hat{T}\to\infty$, the factor $\frac{\sin^2(k_4\hat{T}/2)}{\sin^2(k_4/2)}$ gives a linear dependence on $\hat{T}$, but the two cosines both give factors of $\hat{T}^{-1}$, so that in total all of these integrals go with $\hat{T}^{-1}$ in the limit and hence vanish.

Then there are the graphs with two spatial and two temporal links where $L^{(0)}$ is inserted into the line connecting the two temporal links. The corresponding parts of $\omega^{(4)}$ are denoted by $\omega_{RT2}^{(4)}$:

$$< L^{(0)}\omega_{RT2}^{(4A)} >_{conn}$$

$$= -2\frac{C_2(G)C_2(F)}{3}\int\limits_{BZ}\frac{d^4p}{(2\pi)^4}\int\limits_{BZ}\frac{d^4k}{(2\pi)^4}\int\limits_{-\pi}^{\pi}\frac{dq_4}{2\pi}\frac{1}{\hat{k}^2}\frac{\hat{\vec{p}}^2}{\hat{p}^2\left(\hat{\vec{p}}^2+\hat{q}_4^2\right)}$$

$$\cdot\frac{\sin^2(k_3\hat{R}/2)}{\sin^2(k_3/2)}\sin^2(k_4\hat{T}/2)\frac{\sin(p_4\hat{T}/2)}{\tan(p_4/2)}\frac{\sin(q_4\hat{T}/2)}{\tan(q_4/2)}\sin^2(p_3\hat{R}/2) \quad (3.94)$$

$$< L^{(0)}\omega_{RT2}^{(4B)} >_{conn}$$

$$= -\frac{C_2(G)C_2(F)}{2}\int\limits_{BZ}\frac{d^4p}{(2\pi)^4}\int\limits_{BZ}\frac{d^4k}{(2\pi)^4}\int\limits_{-\pi}^{\pi}\frac{dq_4}{2\pi}\frac{1}{\hat{k}^2}\frac{\hat{\vec{p}}^2}{\hat{p}^2\left(\hat{\vec{p}}^2+\hat{q}_4^2\right)}$$

$$\cdot\frac{\sin^2(k_3\hat{R}/2)}{\sin^2(k_3/2)}\frac{\sin(p_4\hat{T}/2)}{\tan(p_4/2)}\frac{\sin(q_4\hat{T}/2)}{\tan(q_4/2)} \quad (3.95)$$

$$< L^{(0)}\omega_{RT2}^{(4C)} >_{conn}$$

$$= \frac{C_2(G)C_2(F)}{2}\int\limits_{BZ}\frac{d^4p}{(2\pi)^4}\int\limits_{BZ}\frac{d^4k}{(2\pi)^4}\int\limits_{-\pi}^{\pi}\frac{dq_4}{2\pi}\frac{1}{\hat{k}^2}\frac{\hat{\vec{p}}^2}{\hat{p}^2\left(\hat{\vec{p}}^2+\hat{q}_4^2\right)}$$

$$\cdot\Bigg[3\sin^2(k_4\hat{T}/2)\frac{\sin^2(k_3\hat{R}/2)}{\sin^2(k_3/2)}\cos((p+q)_4/2)\Sigma_T(p_4,q_4)$$

$$
\begin{aligned}
&+\cos(k_4\hat{T})\frac{\sin^2(k_3\hat{R}/2)}{\sin^2(k_3/2)}\sin^2(p_3\hat{R}/2)\frac{\sin(p_4\hat{T}/2)}{\tan(p_4/2)}\frac{\sin(k_4\hat{T}/2)}{\tan(q_4/2)}\\
&+\sin^2(p_3\hat{R}/2)\Sigma_R(k_3,-k_3)\frac{\sin(p_4\hat{T}/2)}{\tan(p_4/2)}\frac{\sin(q_4\hat{T}/2)}{\tan(q_4/2)}\Big] \qquad (3.96)\\
&< L^{(0)}\omega^{(4D)}_{RT2} >_{conn}\\
= \;& \frac{C_2(G)C_2(F)}{6}\int\limits_{BZ}\frac{d^4p}{(2\pi)^4}\int\limits_{BZ}\frac{d^4k}{(2\pi)^4}\int\limits_{-\pi}^{\pi}\frac{dq_4}{2\pi}\frac{1}{\hat{k}^2}\frac{\hat{\vec{p}}^2}{\hat{p}^2\left(\hat{\vec{p}}^2+\hat{q}_4^2\right)}\\
&\cdot\Big[\left(3-\cos(k_4\hat{T})\right)\sin^2(p_3\hat{R}/2)\frac{\sin^2(k_3\hat{R}/2)}{\sin^2(k_3/2)}\frac{\sin(p_4\hat{T}/2)}{\tan(p_4/2)}\frac{\sin(q_4\hat{T}/2)}{\tan(q_4/2)}\\
&+\left(1+2\cos(p_3\hat{R})\right)\sin^2(k_4\hat{T}/2)\frac{\sin^2(k_3\hat{R}/2)}{\sin^2(k_3/2)}\frac{\sin(p_4\hat{T}/2)}{\tan(p_4/2)}\frac{\sin(q_4\hat{T}/2)}{\tan(q_4/2)}\\
&-3\sin^2(k_4\hat{T}/2)\frac{\sin^2(k_3\hat{R}/2)}{\sin^2(k_3/2)}\cos((p+q)_4/2)\Sigma_T(p_4,q_4)\\
&-\sin^2(p_3\hat{R}/2)\Sigma_R(k_3,-k_3)\frac{\sin(p_4\hat{T}/2)}{\tan(p_4/2)}\frac{\sin(q_4\hat{T}/2)}{\tan(q_4/2)}\Big] \qquad (3.97)\\
&< L^{(0)}\omega^{(4E)}_{RT2} >_{conn}\\
= \;& \frac{C_2(G)C_2(F)}{6}\int\limits_{BZ}\frac{d^4p}{(2\pi)^4}\int\limits_{BZ}\frac{d^4k}{(2\pi)^4}\int\limits_{-\pi}^{\pi}\frac{dq_4}{2\pi}\frac{1}{\hat{k}^2}\frac{\hat{\vec{p}}^2}{\hat{p}^2\left(\hat{\vec{p}}^2+\hat{q}_4^2\right)}\\
&\cdot\Big[3\sin^2(k_4\hat{T}/2)\frac{\sin^2(k_3\hat{R}/2)}{\sin^2(k_3/2)}\frac{\sin((p+q)_4\hat{T}/2)}{\tan((p+q)_4/2)}\\
&+\hat{R}\sin^2(p_3\hat{R})\frac{\sin(p_4\hat{T}/2)}{\tan(p_4/2)}\frac{\sin(q_4\hat{T}/2)}{\tan(q_4/2)}\Big]. \qquad (3.98)
\end{aligned}
$$

Not all of these terms vanish seperately, but their sum gives:

$$
\begin{aligned}
< L^{(0)}\omega^{(4)}_{RT2} >_{conn} \;=\; & \frac{C_2(G)C_2(F)}{2}\int\limits_{BZ}\frac{d^4p}{(2\pi)^4}\int\limits_{BZ}\frac{d^4k}{(2\pi)^4}\int\limits_{-\pi}^{\pi}\frac{dq_4}{2\pi}\frac{1}{\hat{k}^2}\frac{\hat{\vec{p}}^2}{\hat{p}^2\left(\hat{\vec{p}}^2+\hat{q}_4^2\right)}\\
&\cdot\frac{\sin^2(k_3\hat{R}/2)}{\sin^2(k_3/2)}\frac{\sin(p_4\hat{T}/2)}{\tan(p_4/2)}\frac{\sin(q_4\hat{T}/2)}{\tan(q_4/2)}\cos(k_4\hat{T})\cos(p_3\hat{R}). \qquad (3.99)
\end{aligned}
$$

This expression vanishes in the limit of large $\hat{T}$, again because of the fast oscillations of the cosine.

The next large group consists of the graphs with three spatial links and one temporal link. Denoting the corresponding part with $\omega^{(4)}_{RRRT}$, they give:

$$
\begin{aligned}
&< L^{(0)}\omega^{(4A)}_{RRRT} >_{conn}\\
= \;& -\frac{C_2(G)C_2(F)}{3}\int\limits_{BZ}\frac{d^4p}{(2\pi)^4}\int\limits_{BZ}\frac{d^4k}{(2\pi)^4}\int\limits_{-\pi}^{\pi}\frac{dq_4}{2\pi}\frac{1}{\hat{k}^2}\frac{\hat{p}_4^2+\hat{q}_4^2}{\hat{p}^2\left(\hat{\vec{p}}^2+\hat{q}_4^2\right)}
\end{aligned}
$$

$$\cdot\frac{\sin^2(k_3\hat{R}/2)}{\sin^2(k_3/2)}\sin^2(k_4\hat{T}/2)\frac{\sin(p_4\hat{T}/2)}{\tan(p_4/2)}\frac{\sin(q_4\hat{T}/2)}{\tan(q_4/2)}\sin^2(p_3\hat{R}/2) \tag{3.100}$$

$$< L^{(0)}\omega^{(4B)}_{RRRT} >_{conn}$$

$$\begin{aligned}
= & -\frac{C_2(G)C_2(F)}{2}\int\limits_{BZ}\frac{d^4p}{(2\pi)^4}\int\limits_{BZ}\frac{d^4k}{(2\pi)^4}\int\limits_{-\pi}^{\pi}\frac{dq_4}{2\pi}\frac{1}{\hat{k}^2}\frac{\hat{p}_3\hat{p}_4}{\hat{p}^2\left(\hat{\vec{p}}^2+\hat{q}_4^2\right)}\frac{\sin(q_4\hat{T}/2)}{\tan(q_4/2)} \\
& \cdot\frac{\sin(k_3\hat{R}/2)}{\sin(k_3/2)}\left[\frac{\sin^2(p_3\hat{R}/2)}{\sin(p_3/2)}\frac{\sin(k_3\hat{R}/2)}{\sin(k_3/2)}-2\cos(p_3\hat{R}/2)O_R(p_3,q_3)\right] \\
& \cdot\left(\cos^2(k_4\hat{T}/2)\sin(p_4\hat{T}/2)\cos(p_4/2)-\sin^2(k_4\hat{T}/2)\cos(p_4\hat{T}/2)\sin(p_4/2)\right)
\end{aligned} \tag{3.101}$$

$$< L^{(0)}\omega^{(4C)}_{RRRT} >_{conn}$$

$$\begin{aligned}
= & \frac{C_2(G)C_2(F)}{2}\int\limits_{BZ}\frac{d^4p}{(2\pi)^4}\int\limits_{BZ}\frac{d^4k}{(2\pi)^4}\int\limits_{-\pi}^{\pi}\frac{dq_4}{2\pi}\frac{1}{\hat{k}^2}\frac{\hat{p}_4}{\hat{p}^2\left(\hat{\vec{p}}^2+\hat{q}_4^2\right)}\frac{\sin(q_4\hat{T}/2)}{\tan(q_4/2)} \\
& \cdot\Bigg[\left(\sin(p_4(\hat{T}+1)/2)+\sin(p_4(\hat{T}-1)/2)\right)\sin(p_3/2)\sin(p_3\hat{R}/2)\left(\Sigma_{1R}-\Sigma_{2R}\right) \\
& +\sin^2(p_3\hat{R}/2)\sin(p_4(\hat{T}+1)/2)\Sigma_R(k_3,-k_3) \\
& +\frac{\sin(k_3\hat{R}/2)}{\sin(k_3/2)}\sin(p_3\hat{R}/2)\sin(p_3/2)\sin(p_4(\hat{T}-1)/2)\cos(k_4\hat{T})\Sigma_R(p_3,k_3) \\
& +\sin(p_4\hat{T}/2)\sin^2(p_3\hat{R}/2)\cos(p_4/2)\Sigma_R(k_3,-k_3) \\
& -\sin(p_4(\hat{T}-1)/2)\frac{\sin(k_3\hat{R}/2)}{\sin(k_3/2)}\sin(p_3/2)\sin(p_3\hat{R}/2)\Sigma_R(k_3,p_3) \\
& -\sin(p_4(\hat{T}-1)/2)\frac{\sin(k_3\hat{R}/2)}{\sin(k_3/2)}\sin(p_3/2)\cos(p_3\hat{R}/2)O_R(k_3,p_3) \\
& +\sin^2(p_3\hat{R}/2)\left(\sin^2(k_4\hat{T}/2)\sin(p_4(\hat{T}-1)/2)+\sin(p_4\hat{T}/2)\cos(k_4\hat{T})\right) \\
& +2\sin(p_4(\hat{T}-1)/2)\sin^2(k_4\hat{T}/2)\frac{\sin(k_3\hat{R}/2)}{\sin(k_3/2)}\cos(p_3\hat{R}/2)\sin(p_3/2)O_R(k_3,p_3) \\
& -2\cos(p_4\hat{T}/2)\sin(p_4/2)\sin^2(k_4\hat{T}/2)\frac{\sin^2(k_3\hat{R}/2)}{\sin^2(k_3/2)}\sin^2(p_3\hat{R}/2)\Bigg]
\end{aligned} \tag{3.102}$$

$$< L^{(0)}\omega^{(4D)}_{RRRT} >_{conn}$$

$$\begin{aligned}
= & \frac{C_2(G)C_2(F)}{12}\int\limits_{BZ}\frac{d^4p}{(2\pi)^4}\int\limits_{BZ}\frac{d^4k}{(2\pi)^4}\int\limits_{-\pi}^{\pi}\frac{dq_4}{2\pi}\frac{1}{\hat{k}^2}\frac{\hat{p}_4}{\hat{p}^2\left(\hat{\vec{p}}^2+\hat{q}_4^2\right)}\frac{\sin(q_4\hat{T}/2)}{\tan(q_4/2)} \\
& \cdot\Bigg[\left(\sin(p_4(\hat{T}+1)/2)+\sin(p_4(\hat{T}-1)/2)\right)\sin(p_3/2)\sin(p_3\hat{R}/2) \\
& \cdot\left(\Sigma_{1R}-\Sigma_{2R}+\Sigma_R(0,k_3)-\Sigma_R(p_3+k_3,-p_3)\right) \\
& +\frac{\sin^2(k_3\hat{R}/2)}{\sin^2(k_3/2)}\sin^2(p_3\hat{R}/2)\left(\sin(p_4(\hat{T}-1)/2)+\sin(p_4(\hat{T}+1)/2)\cos(k_4\hat{T})\right)
\end{aligned}$$

$$
\begin{aligned}
&- \sin(p_3/2)\sin(p_3\hat{R}/2)\sin(p_4(\hat{T}-1)/2)\cos(k_4\hat{T})\frac{\sin(k_3\hat{R}/2)}{\sin(k_3/2)}\Sigma_R(k_3,p_3)\\
&- \sin^2(p_3\hat{R}/2)\sin(p_4(\hat{T}+1)/2)\Sigma_R(k_3,-k_3)\\
&+2\sin^2(p_3\hat{R}/2)\frac{\sin^2(k_3\hat{R}/2)}{\sin^2(k_3/2)}\Big(\sin(p_4\hat{T}/2)\cos(p_4/2)\\
&\quad - \sin^2(k_4\hat{T}/2)\sin(p_4(\hat{T}+1)/2)\Big)\\
&+\sin^2(p_3\hat{R}/2)\frac{\sin^2(k_3\hat{R}/2)}{\sin^2(k_3/2)}\Big(\sin(p_4\hat{T}/2)\cos(p_4/2)\\
&\quad - \sin^2(k_4\hat{T}/2)\sin(p_4(\hat{T}-1)/2)\Big)\\
&+\sin^2(k_4\hat{T}/2)\frac{\sin(k_3\hat{R}/2)}{\sin(k_3/2)}\sin(p_4(\hat{T}-1)/2)\sin(p_3/2)\\
&\cdot\Big(\sin(p_3\hat{R}/2)\Sigma_R(p_3,k_3)+\cos(p_3\hat{R}/2)O_R(p_3,k_3)\Big)\\
&- \sin^2(p_3\hat{R}/2)\sin(p_4\hat{T}/2)\cos(p_4/2)\Sigma_R(k_3,-k_3)\\
&+\frac{\sin^2(k_3\hat{R}/2)}{\sin^2(k_3/2)}\sin^2(p_3\hat{R}/2)\\
&\cdot\Big(\sin^2(k_4\hat{T}/2)\sin(p_4(\hat{T}-1)/2)+\cos(k_4\hat{T})\sin(p_4\hat{T}/2)\cos(p_4/2)\Big)\Big] \qquad (3.103)\\
&< L^{(0)}\omega^{(4E)}_{RRRT} >_{conn}\\
= \;& \frac{C_2(G)C_2(F)}{12}\int\limits_{BZ}\frac{d^4p}{(2\pi)^4}\int\limits_{BZ}\frac{d^4k}{(2\pi)^4}\int\limits_{-\pi}^{\pi}\frac{dq_4}{2\pi}\frac{1}{\hat{k}^2}\frac{\hat{p}_4}{\hat{p}^2\left(\hat{\vec{p}}^2+\hat{q}_4^2\right)}\frac{\sin(q_4\hat{T}/2)}{\tan(q_4/2)}\\
&\cdot\Big[\sin^2(k_3\hat{R}/2)\sin(p_4\hat{T}/2)\cos(p_4/2)\hat{R}\\
&+\frac{\sin(k_3\hat{R}/2)}{\sin(k_3/2)}\frac{\sin((p+k)_3\hat{R}/2)}{\sin((p+k)_3/2)}\sin(p_3\hat{R}/2)\sin(p_3/2)\\
&\cdot\Big(\sin^2(k_4\hat{T}/2)+\cos(k_4\hat{T})\Big)\sin(p_4(\hat{T}-1)/2)\\
&+\Big(\sin(p_4(\hat{T}+1)/2)+\sin(p_4(\hat{T}+1)/2)\Big)\sin(p_3\hat{R}/2)\sin(p_3/2)\\
&\cdot(\Sigma_R(p_3,0)-\Sigma_R(k_3,p_3-k_3))\\
&+\sin(p_4(\hat{T}+1)/2)\sin^2(p_3\hat{R}/2)\hat{R}\Big]. \qquad (3.104)
\end{aligned}
$$

All of these contributions go to zero in the limit of large $\hat{T}$.

What remains are the graphs with four temporal links and the graphs with three temporal and one spatial link. Only these can give non-vanishing contributions in the limit of large $\hat{T}$; the first ones will be denoted by $\omega^{(4)}_{TT}$ and the others with $\omega^{(4)}_{RTTT}$. The explicit results are:

$$< L^{(0)}\omega^{(4A)}_{TT} >_{conn}$$

$$
\begin{aligned}
&= -2\frac{C_2(G)C_2(F)}{3}\int\limits_{BZ}\frac{d^4p}{(2\pi)^4}\int\limits_{BZ}\frac{d^4k}{(2\pi)^4}\int\limits_{-\pi}^{\pi}\frac{dq_4}{2\pi}\frac{1}{\hat{k}^2}\frac{\hat{\vec{p}}^2}{\hat{p}^2\left(\hat{\vec{p}}^2+\hat{q}_4^2\right)}\\
&\cdot\frac{\sin^2(k_4\hat{T}/2)}{\sin^2(k_4/2)}\sin^2(k_3\hat{R}/2)\frac{\sin(p_4\hat{T}/2)}{\tan(p_4/2)}\frac{\sin(q_4\hat{T}/2)}{\tan(q_4/2)}\sin^2(p_3\hat{R}/2) \qquad (3.105)\\
&< L^{(0)}\omega_{TT}^{(4B)} >_{conn}\\
&= -\frac{C_2(G)C_2(F)}{2}\int\limits_{BZ}\frac{d^4p}{(2\pi)^4}\int\limits_{BZ}\frac{d^4k}{(2\pi)^4}\int\limits_{-\pi}^{\pi}\frac{dq_4}{2\pi}\frac{1}{\hat{k}^2}\frac{\hat{\vec{p}}^2}{\hat{p}^2\left(\hat{\vec{p}}^2+\hat{q}_4^2\right)}\\
&\cdot\Bigg[\sin^2((k-p)_3\hat{R}/2)\frac{\sin(p_4\hat{T}/2)}{\tan(p_4/2)}\frac{\sin(q_4\hat{T}/2)}{\tan(q_4/2)}\frac{\sin^2(k_4\hat{T}/2)}{\sin^2(k_4/2)}\\
&+4\sin((k-p)_3\hat{R}/2)\sin((k+p)_3\hat{R}/2)\frac{\sin(q_4\hat{T}/2)}{\tan(q_4/2)}\frac{\sin^2(k_4\hat{T}/2)}{\sin^2(k_4/2)}O_T(p_4,k_4)\\
&-4\sin^2((k+p)_3\hat{R}/2)\cos((p+q)_4/2)O_T(p_4,k_4)O_T(q_4,-k_4)\Bigg] \qquad (3.106)\\
&< L^{(0)}\omega_{TT}^{(4C)} >_{conn}\\
&= \frac{C_2(G)C_2(F)}{2}\int\limits_{BZ}\frac{d^4p}{(2\pi)^4}\int\limits_{BZ}\frac{d^4k}{(2\pi)^4}\int\limits_{-\pi}^{\pi}\frac{dq_4}{2\pi}\frac{1}{\hat{k}^2}\frac{\hat{\vec{p}}^2}{\hat{p}^2\left(\hat{\vec{p}}^2+\hat{q}_4^2\right)}\\
&\cdot\Bigg[2\frac{\sin(p_4\hat{T}/2)}{\tan(p_4/2)}\sin^2(p_3\hat{R}/2)\ (\Sigma_{1T}-\Sigma_{2T})|_{p_4=-q_4}\cos(q_4/2)\\
&+2\frac{\sin(k_4\hat{T}/2)}{\sin(k_4/2)}\sin^2(k_3\hat{R}/2)\,(\Sigma_{3T}-\Sigma_{4T})\cos((p+q)_4/2)\\
&-2\frac{\sin(p_4\hat{T}/2)}{\tan(p_4/2)}\frac{\sin(k_4\hat{T}/2)}{\sin(k_4/2)}O_T(q_4,k_4)\sin(q_4/2)\\
&\cdot\left(\sin^2(k_3\hat{R}/2)\cos(p_3\hat{R})-\sin^2(p_3\hat{R}/2)\cos(k_3\hat{R})\right)\\
&+\frac{\sin(p_4\hat{T}/2)}{\tan(p_4/2)}\frac{\sin(q_4\hat{T}/2)}{\tan(q_4/2)}\sin^2(p_3\hat{R}/2)\Sigma_T(q_4,-q_4)\\
&+\frac{\sin^2(k_4\hat{T}/2)}{\sin^2(k_4/2)}\sin^2(k_3\hat{R}/2)\\
&\cdot(\Sigma_T(p_4,q_4)\cos((p+q)_4/2)-O_T(p_4,q_4)\sin((p+q)_4/2))\\
&+\sin^2(p_3\hat{R}/2)\cos(k_3\hat{T})\frac{\sin(p_4\hat{T}/2)}{\tan(p_4/2)}\frac{\sin(k_4\hat{T}/2)}{\sin(k_4/2)}\\
&\cdot(\Sigma_T(q_4,k_4)\cos(q_4/2)-O_T(q_4,k_4)\sin(q_4/2))\\
&+\sin^2(k_3\hat{R}/2)\cos(p_3\hat{T})\frac{\sin(p_4\hat{T}/2)}{\tan(p_4/2)}\frac{\sin(k_4\hat{T}/2)}{\sin(k_4/2)}\\
&\cdot(\Sigma_T(k_4,q_4)\cos(q_4/2)-O_T(k_4,q_4)\sin(q_4/2))\Bigg] \qquad (3.107)\\
&< L^{(0)}\omega_{TT}^{(4D)} >_{conn}
\end{aligned}
$$

$$
\begin{aligned}
= \quad & \frac{C_2(G)C_2(F)}{6} \int\limits_{BZ} \frac{d^4p}{(2\pi)^4} \int\limits_{BZ} \frac{d^4k}{(2\pi)^4} \int\limits_{-\pi}^{\pi} \frac{dq_4}{2\pi} \frac{1}{\hat{k}^2} \frac{\hat{\vec{p}}^2}{\hat{p}^2 \left(\hat{\vec{p}}^2 + \hat{q}_4^2\right)} \\
& \cdot \Bigg[2 \frac{\sin(p_4\hat{T}/2)}{\tan(p_4/2)} \sin^2(p_3\hat{R}/2) \cos(q_4/2) \\
& \cdot \Big[(\Sigma_{1T} - \Sigma_{2T})|_{p_4=q_4} + \Sigma_T(0,q_4) - \Sigma_T(q_4+k_4,-k_4) \Big] \\
& + 2 \frac{\sin(k_4\hat{T}/2)}{\sin(k_4/2)} \sin^2(k_3\hat{R}/2) \cos((p+q)_4/2) \\
& \cdot [(\Sigma_{3T} - \Sigma_{4T}) + \Sigma_T(p_4+q_4,-k_4) - \Sigma_T(p_4-k_4,q_4)] \\
& + 2 \frac{\sin(p_4\hat{T}/2)}{\tan(p_4/2)} \frac{\sin(q_4\hat{T}/2)}{\tan(q_4/2)} \frac{\sin^2(k_4\hat{T}/2)}{\sin^2(k_4/2)} \\
& \cdot \Big(\sin^2(p_3\hat{R}/2) \cos^2(k_3\hat{R}/2) + \sin^2(k_3\hat{R}/2) \cos^2(p_3\hat{R}/2) \Big) \\
& + 2 \frac{\sin(p_4\hat{T}/2)}{\tan(p_4/2)} \frac{\sin(k_4\hat{T}/2)}{\sin(k_4/2)} O_T(k_4,q_4) \sin(q_4/2) \\
& \cdot \Big(\sin^2(p_3\hat{R}/2) \cos(k_3\hat{R}) - \sin^2(k_3\hat{R}/2) \cos(p_3\hat{R}) \Big) \\
& - \sin^2(p_3\hat{R}/2) \cos(k_3\hat{R}) \frac{\sin(p_4\hat{T}/2)}{\tan(p_4/2)} \frac{\sin(k_4\hat{T}/2)}{\sin(k_4/2)} \\
& \cdot (\Sigma_T(k_4,q_4) \cos(q_4/2) - O_T(k_4,q_4) \sin(q_4/2)) \\
& - \sin^2(p_3\hat{R}/2) \frac{\sin(p_4\hat{T}/2)}{\tan(p_4/2)} \frac{\sin(q_4\hat{T}/2)}{\tan(q_4/2)} \Sigma_T(k_4,-k_4) \\
& - \sin^2(k_3\hat{R}/2) \frac{\sin(k_4\hat{T}/2)}{\sin(k_4/2)} \cos(p_3\hat{R}) \frac{\sin(p_4\hat{T}/2)}{\tan(p_4/2)} \\
& \cdot (\Sigma_T(k_4,q_4) \cos(q_4/2) + O_T(k_4,q_4) \sin(q_4/2)) \\
& - \sin^2(k_3\hat{R}/2) \frac{\sin^2(k_4\hat{T}/2)}{\sin^2(k_4/2)} \\
& \cdot (\Sigma_T(p_4,q_4) \cos((p+q)_4/2) - O_T(p_4,q_4) \sin((p+q)_4/2)) \Bigg] \qquad (3.108) \\
& < L^{(0)} \omega_{TT}^{(4E)} >_{conn} \\
= \quad & \frac{C_2(G)C_2(F)}{6} \int\limits_{BZ} \frac{d^4p}{(2\pi)^4} \int\limits_{BZ} \frac{d^4k}{(2\pi)^4} \int\limits_{-\pi}^{\pi} \frac{dq_4}{2\pi} \frac{1}{\hat{k}^2} \frac{\hat{\vec{p}}^2}{\hat{p}^2 \left(\hat{\vec{p}}^2 + \hat{q}_4^2\right)} \\
& \cdot \Bigg[\sin^2(p_3\hat{R}/2) \frac{\sin(q_4\hat{T}/2)}{\tan(q_4/2)} \left(\Sigma_T(p_4,0) - \Sigma_T(k_4,p_4-k_4)\right) \\
& + \sin^2(k_3\hat{R}/2) \frac{\sin(k_4\hat{T}/2)}{\sin(k_4/2)} \left(\Sigma_T(k_4,p_4+q_4) - \Sigma_T(p_4,q_4+k_4)\right) \\
& + \frac{\sin(p_4\hat{T}/2)}{\tan(p_4/2)} \frac{\sin(q_4\hat{T}/2)}{\tan(q_4/2)} \hat{T} \sin^2(p_3\hat{R}/2) \\
& + \frac{\sin^2(k_4\hat{T}/2)}{\sin^2(k_4/2)} \frac{\sin((p+q)_4\hat{T}/2)}{\tan((p+q)_4/2)} \sin^2(k_3\hat{R}/2)
\end{aligned}
$$

$$+\frac{\sin(p_4\hat{T}/2)}{\tan(p_4/2)}\frac{\sin(k_4\hat{T}/2)}{\sin(k_4/2)}\frac{\sin((k+q)_4\hat{T}/2)}{\sin((k+q)_4/2)}\cos(q_4/2)$$
$$\cdot\Big(\sin^2(p_3\hat{R}/2)\cos(k_3\hat{R})+\sin^2(k_3\hat{R}/2)\cos(p_3\hat{R})\Big)\Big]. \tag{3.109}$$

and

$$< L^{(0)}\omega^{(4A)}_{RTTT} >_{conn}$$
$$= -\frac{C_2(G)C_2(F)}{3}\int\limits_{BZ}\frac{d^4p}{(2\pi)^4}\int\limits_{BZ}\frac{d^4k}{(2\pi)^4}\int\limits_{-\pi}^{\pi}\frac{dq_4}{2\pi}\frac{1}{\hat{k}^2}\frac{\hat{p}_4^2+\hat{q}_4^2}{\hat{p}^2\left(\hat{\vec{p}}^2+\hat{q}_4^2\right)}$$
$$\cdot\frac{\sin^2(k_4\hat{T}/2)}{\sin^2(k_4/2)}\sin^2(k_4\hat{R}/2)\frac{\sin(p_4\hat{T}/2)}{\tan(p_4/2)}\frac{\sin(q_4\hat{T}/2)}{\tan(q_4/2)}\sin^2(p_3\hat{R}/2) \tag{3.110}$$
$$< L^{(0)}\omega^{(4B)}_{RTTT} >_{conn}$$
$$= -C_2(G)C_2(F)\int\limits_{BZ}\frac{d^4p}{(2\pi)^4}\int\limits_{BZ}\frac{d^4k}{(2\pi)^4}\int\limits_{-\pi}^{\pi}\frac{dq_4}{2\pi}\frac{1}{\hat{k}^2}\frac{1}{\hat{p}^2\left(\hat{\vec{p}}^2+\hat{q}_4^2\right)}$$
$$\cdot\Big[\hat{p}_4\sin(p_4(\hat{T}-1)/2)\frac{\sin(k_4\hat{T}/2)}{\sin(k_4/2)}\frac{\sin(q_4\hat{T}/2)}{\tan(q_4/2)}+2\hat{q}_4O_T(q_4,k_4)$$
$$\cdot\Big(\cos(p_4\hat{T}/2)\cos(p_4/2)\cos(q_4/2)-\sin(p_4(\hat{T}-1)/2)\sin(p_4/2)\Big)\Big] \tag{3.111}$$
$$< L^{(0)}\omega^{(4C)}_{RTTT} >_{conn}$$
$$= -\frac{C_2(G)C_2(F)}{2}\int\limits_{BZ}\frac{d^4p}{(2\pi)^4}\int\limits_{BZ}\frac{d^4k}{(2\pi)^4}\int\limits_{-\pi}^{\pi}\frac{dq_4}{2\pi}\frac{1}{\hat{k}^2}\frac{1}{\hat{p}^2\left(\hat{\vec{p}}^2+\hat{q}_4^2\right)}$$
$$\cdot\Big[2\hat{p}_4\cos(p_4/2)\sin(p_4\hat{T}/2)\cos(q_4/2)\sin^2(p_3\hat{R}/2)\ (\Sigma_{1T}-\Sigma_{2T})|_{p_4=q_4}$$
$$-2\hat{p}_4\cos(p_4/2)\sin(p_4\hat{T}/2)\sin^2(p_3\hat{R}/2)\cos(k_3\hat{R})\sin(q_4/2)O_T(q_4,k_4)$$
$$+\hat{p}_4\cos(p_4/2)\sin(p_4\hat{T}/2)\sin^2(p_3\hat{R}/2)\frac{\sin(q_4\hat{T}/2)}{\tan(q_4/2)}\Sigma_T(k_4,-k_4)$$
$$+\hat{p}_4\cos(p_4/2)\sin(p_4\hat{T}/2)\sin^2(p_3\hat{R}/2)\cos(k_3\hat{R})\frac{\sin(k_4\hat{T}/2)}{\sin(k_4/2)}$$
$$\cdot(\Sigma_T(q_4,k_4)\cos(q_4/2)-O_T(q_4,k_4)\sin(q_4/2))$$
$$+2\hat{p}_4\sin(p_4(\hat{T}+1)/2)\sin^2(p_3\hat{R}/2)\frac{\sin(q_4\hat{T}/2)}{\tan(q_4/2)}\Sigma_T(k_4,-k_4)$$
$$-2\sin^2(k_3\hat{R}/2)\frac{\sin(k_4\hat{T}/2)}{\sin(k_4/2)}\sin^2(p_3\hat{R}/2)\hat{p}_4\cos(p_4/2)\sin(p_4\hat{T}/2)\Sigma_T(k,q_4)$$
$$+\sin^2(p_3\hat{R}/2)\frac{\sin(q_4\hat{T}/2)}{\tan(q_4/2)}\hat{p}_4\sin(p_4(\hat{T}-1)/2)\Sigma_T(k_4,-k_4)$$
$$+\sin^2(k_3\hat{R}/2)\frac{\sin(k_4\hat{T}/2)}{\sin(k_4/2)}$$

$$
\begin{aligned}
&\cdot \Big(\hat{q}_4 \Big(\sin(p_4(\hat{T}-1)/2)\sin(p_4/2) - \cos(p_4\hat{T}/2)\Big) O_T(k_4,q_4) \\
&\quad -\hat{p}_4 \sin(p_4(\hat{T}-1)/2)\cos(q_4/2)\Sigma_T(k_4,q_4)\Big) \\
&+\hat{p}_4 \Big(\sin(p_4(\hat{T}-1)/2) - \sin(p_4(\hat{T}+1)/2)\Big)\sin^2(p_3\hat{R}/2) \\
&\cdot \frac{\sin^2(k_4\hat{T}/2)}{\sin^2(k_4/2)}\frac{\sin(q_4\hat{T}/2)}{\sin(q_4/2)}\Big(\cos(k_3\hat{R}+\sin^2(k_3\hat{R}/2)\Big) \\
&+2\sin^2(k_3\hat{R}/2)\frac{\sin(k_4\hat{T}/2)}{\sin(k_4/2)}\sin^2(p_3\hat{R}/2) \\
&\cdot \hat{q}_4 \Big(\sin(p_4(\hat{T}-1)\sin(p_4/2) - \cos(p_4\hat{T}/2)\Big) O_T(k_4,q_4)\Big] \qquad (3.112) \\
&< L^{(0)}\omega^{(4D)}_{RTTT} >_{conn} \\
= \; &-\frac{C_2(G)C_2(F)}{3}\int\limits_{BZ}\frac{d^4p}{(2\pi)^4}\int\limits_{BZ}\frac{d^4k}{(2\pi)^4}\int\limits_{-\pi}^{\pi}\frac{dq_4}{2\pi}\frac{1}{\hat{k}^2}\frac{1}{\hat{p}^2\left(\hat{\vec{p}}^2+\hat{q}_4^2\right)} \\
&\cdot\Big[2\hat{p}_4\cos(p_4/2)\sin(p_4\hat{T}/2)\cos(q_4/2)\sin^2(p_3\hat{R}/2) \\
&\cdot\Big[(\Sigma_{1T}-\Sigma_{2T})|_{p_4=q_4}+\Sigma_T(0,q_4)-\Sigma_T(k_4+q_4,-k_4)\Big] \\
&+2\hat{p}_4\cos(p_4/2)\sin(p_4\hat{T}/2)\sin^2(p_3\hat{R}/2)\frac{\sin^2(k_4\hat{T}/2)}{\sin^2(k_4/2)}\frac{\sin(q_4\hat{T}/2)}{\tan(q_4/2)} \\
&\cdot\cos^2(k_3\hat{R}/2) \\
&+2\hat{p}_4\cos(p_4/2)\sin(p_4\hat{T}/2)\sin^2(p_3\hat{R}/2)\frac{\sin(k_4\hat{T}/2)}{\sin(k_4/2)}\cos(k_3\hat{R}) \\
&\cdot\sin(q_4/2)O_T(k_4,q_4) \\
&-\hat{p}_4\cos(p_4/2)\sin(p_4\hat{T}/2)\sin^2(p_3\hat{R}/2)\frac{\sin(q_4\hat{T}/2)}{\tan(q_4/2)}\Sigma_T(k_4,-k_4) \\
&-\hat{p}_4\cos(p_4/2)\sin(p_4\hat{T}/2)\sin^2(p_3\hat{R}/2)\cos(k_3\hat{R})\frac{\sin(k_4\hat{T}/2)}{\sin(k_4/2)} \\
&\cdot(\Sigma_T(k_4,q_4)\cos(q_4/2)-O_T(k_4,q_4)\sin(q_4/2)) \\
&-2\sin^2(p_3\hat{R}/2)\sin^2(k_3\hat{R}/2)\frac{\sin(k_4\hat{T}/2)}{\sin(k_4/2)}\hat{q}_4 \\
&\cdot\Big(\cos(k_4\hat{T}/2)-\sin(p_4(\hat{T}-1)/2)\sin(p_4/2)\Big)O_T(k_4,q_4) \\
&+\hat{p}_4\sin(p_4(\hat{T}-1)/2)\sin^2(p_3\hat{R}/2)\cos^2(k_3\hat{R}/2)\frac{\sin^2(k_4\hat{T}/2)}{\sin^2(k_4/2)}\frac{\sin(q_4\hat{T}/2)}{\tan(q_4/2)} \\
&+2\sin^2(p_3\hat{R}/2)\sin^2(k_3\hat{R}/2)\frac{\sin(k_4\hat{T}/2)}{\sin(k_4/2)}\hat{p}_4\cos(p_4/2)\sin(p_4\hat{T}/2) \\
&\cdot\cos(q_4/2)\Sigma_T(q_4,k_4) \\
&-2\sin^2(p_3\hat{R}/2)\hat{p}_4\cos(p_4/2)\sin(p_4\hat{T}/2)\frac{\sin(q_4\hat{T}/2)}{\tan(q_4/2)}\Sigma_T(k_4,-k_4)
\end{aligned}
$$

$$
\begin{aligned}
&+\sin^2(p_3\hat{R}/2)\sin^2(q_3\hat{R}/2)\frac{\sin(k_4\hat{T}/2)}{\sin(k_4/2)}\\
&\cdot\hat{q}_4\left(\cos(p_4\hat{T}/2)-\sin(p_4(\hat{T}-1)/2)\sin(p_4/2)\right)O_T(q_4,k_4)\\
&+\sin^2(p_3\hat{R}/2)\sin^2(q_3\hat{R}/2)\frac{\sin(k_4\hat{T}/2)}{\sin(k_4/2)}\hat{p}_4\sin(p_4(\hat{T}-1)/2)\Sigma_T(q_4,k_4)\\
&-\sin^2(p_3\hat{R}/2)\hat{p}_4\cos(p_4/2)\sin(p_4\hat{T}/2)\frac{\sin(q_4\hat{T}/2)}{\tan(q_4/2)}\Sigma_T(k_4,-k_4)\\
&+\hat{p}_4\left(\sin(p_4(\hat{T}+1)/2)+\sin(p_4(\hat{T}-1)/2)\right)\frac{\sin^2(k_4\hat{T}/2)}{\sin^2(k_4/2)}\frac{\sin(q_4\hat{T}/2)}{\tan(q_4/2)}\\
&\cdot\sin^2(p_3\hat{R}/2)\left(\sin^2(k_3\hat{R}/2)+\cos(k_3\hat{R})\right)\Big] \qquad (3.113)\\
&<L^{(0)}\omega^{(4E)}_{RTTT}>_{conn}\\
=\;&-\frac{C_2(G)C_2(F)}{3}\int\limits_{BZ}\frac{d^4p}{(2\pi)^4}\int\limits_{BZ}\frac{d^4k}{(2\pi)^4}\int\limits_{-\pi}^{\pi}\frac{dq_4}{2\pi}\frac{1}{\hat{k}^2}\frac{1}{\hat{p}^2\left(\hat{\vec{p}}^2+\hat{q}_4^2\right)}\\
&\cdot\Big[2\sin(p_4(\hat{T}+1)/2)\sin^2(p_3\hat{R}/2)\frac{\sin(q_4\hat{T}/2)}{\tan(q_4/2)}\hat{T}\\
&-2\sin(p_4(\hat{T}+1)/2)\sin^2(p_3\hat{R}/2)\sin^2(k_3\hat{R}/2)\\
&\cdot\frac{\sin(k_4\hat{T}/2)}{\sin(k_4/2)}\frac{\sin((q+k)_4\hat{T}/2)}{\sin((q+k)_4/2)}\cos(q_4/2)\\
&+\sin(p_4(\hat{T}-1)/2)\sin^2(p_3\hat{R}/2)\frac{\sin(q_4\hat{T}/2)}{\tan(q_4/2)}\hat{T}\\
&-\sin(p_4(\hat{T}-1)/2)\sin^2(p_3\hat{R}/2)\sin^2(k_3\hat{R}/2)\\
&\cdot\frac{\sin(k_4\hat{T}/2)}{\sin(k_4/2)}\frac{\sin((q+k)_4\hat{T}/2)}{\sin((q+k)_4/2)}\cos(q_4/2)\\
&+2\sin^2(p_3\hat{R}/2)\sin(p_4\hat{T}/2)\cos(p_4/2)\cos(q_4/2)\\
&\cdot(\Sigma_T(q_4,0)-\Sigma_T(k_4,q_4-k_4))\\
&+\sin^2(p_3\hat{R}/2)\sin(p_4\hat{T}/2)\cos(p_4/2)\frac{\sin(q_4\hat{T}/2)}{\tan(q_4/2)}\hat{T}\\
&+\sin^2(p_3\hat{R}/2)\sin(p_4\hat{T}/2)\cos(p_4/2)\cos(p_3\hat{R})\\
&\cdot\frac{\sin(k_4\hat{T}/2)}{\sin(k_4/2)}\frac{\sin((q+k)_4\hat{T}/2)}{\sin((q+k)_4/2)}\cos(q_4/2)\Big]. \qquad (3.114)
\end{aligned}
$$

The functions Σ_{1T} and Σ_{2T} are obtained from Σ_1 and Σ_2 by replacing $\hat{R}$ with $\hat{T}$, p_μ with p_4 and k_μ by k_4 (see section 2.2.2). The new functions Σ_{3T} and Σ_{4T} are the even parts of the following sums:

$$
\tilde{\Sigma}_{3T} \;=\; e^{i(k_4-p_4-z)(\hat{T}-1)/2}\sum_{l_1=0}^{\hat{T}-3}\sum_{l_2=l_1+1}^{\hat{T}-2}\sum_{l_3=l_2+1}^{\hat{T}-1}e^{-ik_4l_1}e^{ip_4l_2}e^{iq_4l_3}
$$

$$\tilde{\Sigma}_{4T} = e^{i(k_4-p_4-z)(\hat{T}-1)/2} \sum_{l_1=0}^{\hat{T}-3} \sum_{l_2=l_1+1}^{\hat{T}-2} \sum_{l_3=l_2+1}^{\hat{T}-1} e^{ip_4 l_1} e^{-ik_4 l_2} e^{iq_4 l_3}$$

The explicit results are:

$$\begin{aligned}
\Sigma_{3T} &= \frac{1}{4}\frac{\sin(q_4\hat{T}/2)}{\sin(q_4/2)}\frac{\sin(p_4(\hat{T}-2)/2)}{\sin(p_4/2)}\frac{\sin(k_4(\hat{T}-2)/2)\cos(k_4)}{\sin(k_4/2)} \\
&+\frac{1}{4}\frac{\sin(q_4\hat{T}/2)}{\sin(q_4/2)}\frac{\sin(p_4/2-k_4)}{\sin(p_4/2)}\frac{\sin((p-k)_4(\hat{T}-2)/2)}{\sin((p-k)_4/2)} \\
&+\frac{1}{4}\frac{\cos((p+q)_4(\hat{T}-2)/2+q_4/2)}{\sin(q_4/2)\sin((p+q)_4/2)}\frac{\sin(k_4(\hat{T}-2)/2)\cos(k_4)}{\sin(k_4/2)} \\
&-\frac{1}{4}\frac{\cos(p_4/2-k_4)}{\sin(q_4/2)\sin((p+q)_4/2)}\frac{\sin(p+q-k)_4(\hat{T}-2)/2)}{\sin((p+q-k)_4/2))} \qquad (3.115) \\
\Sigma_{4T} &= \frac{1}{4}\frac{\sin(q_4\hat{T}/2)}{\sin(q_4/2)}\frac{\sin(k_4(\hat{T}-2)/2)}{\sin(k_4/2)}\frac{\sin(p_4(\hat{T}-2)/2)\cos(p_4)}{\sin(p_4/2)} \\
&-\frac{1}{4}\frac{\sin(q_4\hat{T}/2)}{\sin(q_4/2)}\frac{\sin(p_4-k_4/2)}{\sin(k_4/2)}\frac{\sin((p-k)_4(\hat{T}-2)/2)}{\sin((p-k)_4/2)} \\
&+\frac{1}{4}\frac{\cos((q-k)_4(\hat{T}-2)/2+q_4/2)}{\sin(q_4/2)\sin((q-k)_4/2)}\frac{\sin(p_4(\hat{T}-2)/2)\cos(p_4)}{\sin(p_4/2)} \\
&-\frac{1}{4}\frac{\cos(p_4-k_4/2)}{\sin(q_4/2)\sin((q-k)_4/2)}\frac{\sin(p+q-k)_4(\hat{T}-2)/2)}{\sin((p+q-k)_4/2))} \qquad (3.116)
\end{aligned}$$

These results with $L^{(0)}$ above have to be compared to the expressions one gets by inserting $S^{(0)}$ into the graphs with $\omega^{(4)}$ in the limit of large $\hat{T}$. The graphs contributing to $< S^{(0)}\omega^{(4)} >_0$ can be split in the same way as outlined above, and with similar arguments as before, it can be shown that the contributions coming from $\omega^{(4)}_{RR}$, $\omega^{(4)}_{RT}$, and $\omega^{(4)}_{RRRT}$ vanish in the limit of large $\hat{T}$. Hence only the results for the graphs with $\omega^{(4)}_{TT}$ and $\omega^{(4)}_{RTTT}$, which can be obtained from the sections 2.2.2 and 3.2.2, are given here:

$$\begin{aligned}
&< S^{(0)}\omega^{(4A)}_{TT} >_{conn} \\
= &-2\frac{C_2(G)C_2(F)}{3}\int_{BZ}\frac{d^4p}{(2\pi)^4}\int_{BZ}\frac{d^4k}{(2\pi)^4}\frac{1}{\hat{p}^2}\frac{\hat{k}^2+\hat{\vec{k}}^2}{\left(\hat{k}^2\right)^2}\frac{\sin^2(p_4T/2)}{\sin^2(p_4/2)}\frac{\sin^2(k_4T/2)}{\sin^2(k_4/2)} \\
&\sin^2(p_3\hat{R}/2)\sin^2(k_3\hat{R}/2) \qquad (3.117) \\
&< S^{(0)}\omega^{(4B)}_{TT} >_{conn} \\
= &-\frac{C_2(G)C_2(F)}{2}\int_{BZ}\frac{d^4p}{(2\pi)^4}\int_{BZ}\frac{d^4k}{(2\pi)^4}\frac{1}{\hat{p}^2}\frac{\hat{k}^2+\hat{\vec{k}}^2}{\left(\hat{k}^2\right)^2}\left[\frac{\sin^2(p_4T/2)}{\sin^2(p_4/2)}\frac{\sin^2(k_4T/2)}{\sin^2(k_4/2)}\right. \\
&\left.+4O_T^2(p_4,k_4)\right]\cdot\left[\sin^2(p_3\hat{R}/2)\cos^2(k_3\hat{R}/2)+\sin^2(k_3\hat{R}/2)\cos^2(p_3\hat{R}/2)\right] \\
&\qquad (3.118)
\end{aligned}$$

$$
\begin{aligned}
&< S^{(0)}\omega_{TT}^{(4C)} >_{conn} \\
= \;& \frac{C_2(G)C_2(F)}{4}\int\limits_{BZ}\frac{d^4p}{(2\pi)^4}\int\limits_{BZ}\frac{d^4k}{(2\pi)^4}\frac{1}{\hat{p}^2}\frac{\hat{k}^2+\hat{\vec{k}}^2}{\left(\hat{k}^2\right)^2}\left[4\frac{\sin(p_4T/2)}{\sin(p_4/2)}(\Sigma_{1T}-\Sigma_{2T})\right. \\
&+\frac{\sin^2(p_4T/2)}{\sin^2(p_4/2)}\left(\frac{\sin^2(k_4T/2)}{\sin^2(k_4/2)}-T\right)+\frac{\sin(p_4T/2)}{\sin(p_4/2)}\frac{\sin(k_4T/2)}{\sin(k_4/2)}\cos(k_3R) \\
&\left.\left(\frac{\sin(p_4T/2)}{\sin(p_4/2)}\frac{\sin(k_4T/2)}{\sin(k_4/2)}-\frac{\sin((p+k)_3T/2)}{\sin((p+k)_3/2)}\right)\right]\cdot\sin^2(p_3\hat{R}/2) \qquad (3.119)\\
&< S^{(0)}\omega_{TT}^{(4D)} >_{conn} \\
= \;& \frac{C_2(G)C_2(F)}{12}\int\limits_{BZ}\frac{d^4p}{(2\pi)^4}\int\limits_{BZ}\frac{d^4k}{(2\pi)^4}\frac{1}{\hat{p}^2}\frac{\hat{k}^2+\hat{\vec{k}}^2}{\left(\hat{k}^2\right)^2}\left[3\frac{\sin^2(p_4T/2)}{\sin^2(p_4/2)}T\right. \\
&+2\frac{\sin^2(p_4T/2)}{\sin^2(p_4/2)}\frac{\sin^2(k_4T/2)}{\sin^2(k_4/2)}\cos^2(k_3\hat{R}/2)+4\frac{\sin(p_4T/2)}{\sin(p_4/2)}(\Sigma_{1T}-\Sigma_{2T}) \\
&\left.-(2-\cos(k_3R))\,\frac{\sin(p_\nu T/2)}{\sin(p_\nu/2)}\frac{\sin(k_\nu T/2)}{\sin(k_\nu/2)}\frac{\sin((p_\nu+k_\nu)T/2)}{\sin((p_\nu+k_\nu)/2)}\right]\cdot\sin^2(p_3\hat{R}/2) \\
& \qquad (3.120)\\
&< S^{(0)}\omega_{TT}^{(4E)} >_{conn} \\
= \;& \frac{C_2(G)C_2(F)}{3}\int\limits_{BZ}\frac{d^4p}{(2\pi)^4}\int\limits_{BZ}\frac{d^4k}{(2\pi)^4}\frac{1}{\hat{p}^2}\frac{\hat{k}^2+\hat{\vec{k}}^2}{\left(\hat{k}^2\right)^2}\left[\frac{\sin^2(p_4T/2)}{\sin^2(p_4/2)}T\sin^2(p_3\hat{R}/2)\right. \\
&\left.-\sin^2(p_3\hat{R}/2)\sin^2(k_3\hat{R}/2)\,\frac{\sin(p_4T/2)}{\sin(p_4/2)}\frac{\sin(k_4T/2)}{\sin(k_4/2)}\frac{\sin((p+k)_4T/2)}{\sin((p+k)_4/2)}\right]. \\
& \qquad (3.121)
\end{aligned}
$$

and

$$
\begin{aligned}
&< S^{(0)}\omega_{RTTT}^{(4A)} >_{conn} \\
= \;& 0 \qquad (3.122)\\
&< S^{(0)}\omega_{RTTT}^{(4B)} >_{conn} \\
= \;& -C_2(G)C_2(F)\int\limits_{BZ}\frac{d^4p}{(2\pi)^4}\int\limits_{BZ}\frac{d^4k}{(2\pi)^4}\frac{1}{\hat{p}^2}\frac{\hat{k}_3\hat{k}_4}{\left(\hat{k}^2\right)^2}\frac{\sin^2(k_3\hat{R}/2)}{\sin(k_3/2)}\frac{\sin(p_4\hat{T}/2)}{\sin(p_4/2)} \\
&\cdot\cos^2(p_3\hat{R}/2)\left[\frac{\sin^2(k_4\hat{T}/2)}{\sin(k_4/2)}\frac{\sin(p_4\hat{T}/2)}{\sin(p_4/2)}+2\cos(k_4\hat{T}/2)O_T(k_4,p_4)\right] \\
& \qquad (3.123)\\
&< S^{(0)}\omega_{RTTT}^{(4C)} >_{conn} \\
= \;& -\frac{C_2(G)C_2(F)}{2}\int\limits_{BZ}\frac{d^4p}{(2\pi)^4}\int\limits_{BZ}\frac{d^4k}{(2\pi)^4}\frac{1}{\hat{p}^2}\frac{\hat{k}_3\hat{k}_4}{\left(\hat{k}^2\right)^2} \\
&\cdot\left[2\sin^2(p_3\hat{R})\frac{\sin(p_4\hat{T}/2)}{\sin(p_4/2)}\frac{\sin^2(k_3\hat{R}/2)}{\sin(k_3/2)}\sin(k_4\hat{R}/2)\Sigma_T(k_4,p_4)\right.
\end{aligned}
$$

$$
\begin{aligned}
&+2\sin^2(p_3\hat{R}/2)\frac{\sin(p_4\hat{T}/2)}{\sin(p_4/2)}\frac{\sin^2(k_3\hat{R}/2)}{\sin(k_3/2)}\cos(k_4\hat{T}/2)O_T(p_4,k_4)\\
&+\sin^2(p_3\hat{R}/2)\frac{\sin(p_4\hat{T}/2)}{\sin(p_4/2)}\frac{\sin^2(k_3\hat{R}/2)}{\sin(k_3/2)}\\
&\cdot\Big(\sin(k_4\hat{T}/2)\Sigma_T(p_4,k_4)+\cos(k_4\hat{T}/2)O_T(p_4,k_4)\Big)\Big] \qquad (3.124)\\
&<S^{(0)}\omega^{(4D)}_{RTTT}>_{conn}\\
=\;&\frac{C_2(G)C_2(F)}{12}\int\limits_{BZ}\frac{d^4p}{(2\pi)^4}\int\limits_{BZ}\frac{d^4k}{(2\pi)^4}\frac{1}{\hat{p}^2}\frac{\hat{k}_3\hat{k}_4}{\left(\hat{k}^2\right)^2}\\
&\cdot\Big[\sin^2(p_4\hat{T}/2)\frac{\sin(p_3\hat{R}/2)}{\sin^2(p_3/2)}\frac{\sin^2(k_3\hat{R}/2)}{\sin(k_3/2)}\sin(k_4\hat{T}/2)\Sigma_T(p_4,k_4)\\
&+2\sin^2(p_3\hat{R}/2)\frac{\sin^2(p_4\hat{T}/2)}{\sin^2(p_4/2)}\frac{\sin^2(k_3\hat{R}/2)}{\sin(k_3/2)}\frac{\sin^2(k_4\hat{T}/2)}{\sin(k_4/2)}\\
&-4\sin^2(p_3\hat{R}/2)\frac{\sin^2(p_4\hat{T}/2)}{\sin^2(p_4/2)}\frac{\sin^2(k_3\hat{R}/2)}{\sin(k_3/2)}\cos(k_4\hat{T}/2)O_T(p_4,k_4)\\
&+2\sin^2(p_3\hat{R}/2)\frac{\sin^2(p_4\hat{T}/2)}{\sin^2(p_4/2)}\frac{\sin^2(k_3\hat{R}/2)}{\sin(k_3/2)}\\
&\cdot\Big(\sin(k_4\hat{T}/2)\Sigma_T(p_4,k_4)-\cos(k_4\hat{T}/2)O_T(p_4,k_4)\Big)\Big] \qquad (3.125)\\
&<S^{(0)}\omega^{(4E)}_{RTTT}>_{conn}\\
=\;&-\frac{C_2(G)C_2(F)}{2}\int\limits_{BZ}\frac{d^4p}{(2\pi)^4}\int\limits_{BZ}\frac{d^4k}{(2\pi)^4}\frac{1}{\hat{p}^2}\frac{\hat{k}_3\hat{k}_4}{\left(\hat{k}^2\right)^2}\frac{\sin(p_4\hat{T}/2)}{\sin(p_4/2)}\sin^2(p_3\hat{R}/2)\\
&\cdot\frac{\sin^2(k_3\hat{R}/2)}{\sin(k_3/2)}\sin(k_4\hat{T}/2)\frac{\sin((p+k)_4\hat{T}/2)}{\sin((p+k)_4/2)}. \qquad (3.126)
\end{aligned}
$$

Now using the expressions (3.105) to (3.126), it has to be shown that

$$\lim_{\hat{T}\to\infty}<L^{(0)}\omega^{(4)}>_{conn}=\lim_{\hat{T}\to\infty}\frac{1}{\hat{T}}<S^{(0)}\omega^{(4)}>_{conn}. \qquad (3.127)$$

For the parts with $\omega^{(4A)}$, this is easy to show; using

$$\lim_{\hat{T}\to\infty}<L^{(0)}\omega^{(2)}>_{conn}=\lim_{\hat{T}\to\infty}\frac{1}{\hat{T}}<S^{(0)}\omega^{(2)}>_{conn}.$$

one indeed gets:

$$\lim_{\hat{T}\to\infty}<L^{(0)}\omega^{(4A)}_{TT}>_{conn}=\lim_{\hat{T}\to\infty}\frac{1}{\hat{T}}<S^{(0)}\omega^{(4A)}_{TT}>_{conn} \qquad (3.128)$$

and

$$\lim_{\hat{T}\to\infty}<L^{(0)}\omega^{(4A)}_{RTTT}>_{conn}=\lim_{\hat{T}\to\infty}\frac{1}{\hat{T}}<S^{(0)}\omega^{(4A)}_{RTTT}>_{conn}=0. \qquad (3.129)$$

All the other contributions have to be checked explicitly by evaluating the eight- respectively nine-dimensional integrals using a numerical integration routine like *Vegas* [41]. This work, which requires lots of computer time, is still in progress.

Chapter 4

Energy Sum Rule

In deriving the energy sum rule in the form

$$\hat{V}(\hat{R},\hat{\beta}) = \lim_{\hat{T}\to\infty}\left[\eta_- < -\mathcal{P}'_t + \mathcal{P}'_s >_{q\bar{q}-0} + \frac{1}{4}\sum_{\vec{x}} < T_{\mu\mu}(\vec{x},t) >_{q\bar{q}-0}\right], \qquad (4.1)$$

essentially three steps were necessary:

1. Taking the derivative (1.19) of the potential, calculated on an anisotropic lattice, with respect to the anisotropy parameter ξ, and then returning to the isotropic lattice $\xi = 1$; this led to (1.20).

2. Introducing the abbreviations $\eta_\pm$ and using the formula derived in [42] for η_+; the result was (1.23).

3. Taking the limit of large $\hat{T}$ and thereby restricting the sum over all plaquettes to one fixed time slice.

There is no problem with the second step; the formula for η_+ used there was proven in [42] analytically, as well as checked numerically. But the first and third step are questionable; its not entirely clear if in the continuum limit, the potential really becomes completely independent of ξ (hence it is not clear if the derivative (1.19) really is zero), and the behaviour for large $\hat{T}$ is not clear, too.

In the first section of this chapter, some basic calculations will be done, and the energy sum rule will be cast into an equivalent form which is easier to check. The second section deals then with the explicit perturbative check. This will lead to a better understanding of the various terms which contribute to the potential energy (the energy in the electric and in the magnetic fields and the trace anomaly). The various contributions will be classified and their magnitudes will be compared in the third section. Finally, the limit of large $\hat{T}$ will be examined.

4.1 Preliminaries

It will turn out that it will be helpful to write the difference between the spatial and temporal plaquettes in the first term of (1.23) in the following way:

$$-\mathcal{P}_t + \mathcal{P}_s = -\mathcal{P}_t - \mathcal{P}_s + 2\mathcal{P}_s. \tag{4.2}$$

Then the potential is given by:

$$\begin{aligned}
\hat{V} &= \lim_{\hat{T}\to\infty} \frac{1}{\hat{T}} \left[\eta_- < -\mathcal{P}_t - \mathcal{P}_s + 2\mathcal{P}_s >_{q\bar{q}-0} + \frac{\beta_L(g_0)}{2g_0} < S >_{q\bar{q}-0} \right] \\
&= \lim_{\hat{T}\to\infty} \frac{1}{\hat{T}} \left[\frac{\eta_-}{\hat{\beta}} < -S + 2S_s >_{q\bar{q}-0} + \frac{\beta_L(g_0)}{2g_0} < S >_{q\bar{q}-0} \right] \\
&= \lim_{\hat{T}\to\infty} \frac{1}{\hat{T}} \left[-\frac{g_0^2}{2d(F)}\eta_- < S >_{q\bar{q}-0} + \frac{g_0^2}{d(F)}\eta_- < S_s >_{q\bar{q}-0} + \frac{\beta_L(g_0)}{2g_0} < S >_{q\bar{q}-0} \right],
\end{aligned} \tag{4.3}$$

where S_s denotes the part of the action which comes from summing only over the *spatial* plaquettes.

Because the expectation value of the action appears in two places in the formula above, the identity (3.5)

$$\lim_{T\to\infty} \frac{1}{T} < S >_{q\bar{q}-0,subtr} = -g_0^2 \frac{\partial}{\partial g_0^2} \hat{V} \tag{4.4}$$

becomes very useful now. When using it, one has to pay attention that the self-energy contributions have to be subtracted. Inserting this identity above, one gets:

$$\hat{V} = \frac{g_0^4}{2d(F)}\eta_- \frac{\partial}{\partial g_0^2}\hat{V} - \frac{\beta_L(g_0)}{2} g_0 \frac{\partial}{\partial g_0^2}\hat{V} + \lim_{\hat{T}\to\infty} \frac{1}{\hat{T}} \frac{g_0^2}{d(F)} \eta_- < S_s >_{q\bar{q}-0} \tag{4.5}$$

Until this point, everything had been exact. Now the following expansions will be used, where the explicit expressions for $\hat{\beta}_t$ and $\hat{\beta}_t$ were taken from [42]:

$$\begin{aligned}
\eta_\pm &= \frac{1}{2}\left(\frac{\partial \hat{\beta}_t}{\partial \xi} \pm \frac{\partial \hat{\beta}_s}{\partial \xi} \right)_{\xi=1} \\
&= \frac{1}{2}\left(\frac{\partial}{\partial \xi} \left(\xi\hat{\beta} + 2d(F)\xi c_t(\xi) \pm \frac{1}{\xi}\hat{\beta} \pm \frac{2d(F)}{\xi} c_s(\xi) \right) \right)_{\xi=1} + O(g_0^2) \\
&= \frac{1}{2}\left(\hat{\beta} + 2d(F)c_t(\xi) + 2d(F)\xi\frac{\partial c_t}{\partial \xi} \mp \frac{1}{\xi^2}\hat{\beta} \mp \frac{2d(F)}{\xi^2} c_s(\xi) \pm \frac{2d(F)}{\xi}\frac{\partial c_s}{\partial \xi} \right)_{\xi=1} + O(g_0^2) \\
&= \frac{1}{2}\left(\hat{\beta} + 2d(F)\frac{\partial c_t}{\partial \xi} \mp \hat{\beta} \pm 2d(F)\frac{\partial c_s}{\partial \xi} \right)_{\xi=1} + O(g_0^2) \\
&= \left\{ \begin{array}{c} d(F)\left(\frac{\partial c_t}{\partial \xi} + \frac{\partial c_s}{\partial \xi} \right)_{\xi=1} \\ \hat{\beta} + d(F)\left(\frac{\partial c_t}{\partial \xi} - \frac{\partial c_s}{\partial \xi} \right)_{\xi=1} \end{array} \right\} + O(g_0^2) = \left\{ \begin{array}{c} \beta_0 d(F) \\ \frac{2d(F)}{g_0^2} + cd(F) \end{array} \right\} + O(g_0^2)
\end{aligned} \tag{4.6}$$

Additionally one needs the leading order of the expansion of the lattice beta function:

$$\beta_L(g_0) \equiv -a\frac{\partial g_0}{\partial a} = -\beta_0 g_0^3 + O(g_0^5) \tag{4.7}$$

with

$$\beta_0 = \frac{11C_2(G)}{48\pi^2}.$$

Then one arrives at:

$$\begin{aligned}
\hat{V} &= g_0^2\frac{\partial}{\partial g_0^2}\hat{V} + \frac{1}{2}cg_0^4\frac{\partial}{\partial g_0^2}\hat{V} + \frac{1}{2}\beta_0 g_0^4\frac{\partial}{\partial g_0^2}\hat{V} \\
&\quad + \lim_{\hat{T}\to\infty}\frac{1}{\hat{T}}\left[2 < S_s >_{q\bar{q}-0} + g_0^2 c < S_s >_{q\bar{q}-0}\right] + O(g_0^6) \\
&= g_0^2\frac{\partial}{\partial g_0^2}\hat{V} + \left.\frac{\partial c_t}{\partial\xi}\right|_{\xi=1} g_0^4\frac{\partial}{\partial g_0^2}\hat{V} \\
&\quad + \lim_{\hat{T}\to\infty}\frac{1}{\hat{T}}\left[2 < S_s >_{q\bar{q}-0} + g_0^2 c < S_s >_{q\bar{q}-0}\right] + O(g_0^6),
\end{aligned} \tag{4.8}$$

where

$$c + \beta_0 = 2\left.\frac{\partial c_t}{\partial\xi}\right|_{\xi=1}$$

has been used. The formula (4.8) is equivalent to the energy sum rule up to next-to-leading order; it will be checked now in the following section.

All that is needed in order to do this are the expansions of the potential and of $< S_s >_{q\bar{q}-0}$. The explicit form of the potential up to next-to-leading order can be taken from chapter 2; for the other term, one gets the following expansion up to next-to-leading order, which is similar to the ones for $< SW >_{conn}$ (3.20) and $< LW >_{conn}$ (3.52):

$$\begin{aligned}
< S_s >_{q\bar{q}-0} &= -g_0^2 < S_s^{(0)}\omega^{(2)} >_{conn} + g_0^4 < S_s^{(0)}S^{(2)}\omega^{(2)} >_{conn} \\
&\quad - g_0^4 < S_s^{(0)}\frac{1}{2}(S^{(1)})^2\omega^{(2)} >_{conn} + g_0^4 < S_s^{(0)}S_{FP}^{(2)}\omega^{(2)} >_{conn} \\
&\quad + g_0^4 < S_s^{(0)}S_{meas}^{(2)}\omega^{(2)} >_{conn} + g_0^4 < S_s^{(1)}S^{(1)}\omega^{(2)} >_{conn} \\
&\quad - g_0^4 < S_s^{(2)}\omega^{(2)} >_{conn} + g_0^4 < S_s^{(0)}S^{(1)}\omega^{(3)} >_{conn} \\
&\quad - g_0^4 < S_s^{(0)}\omega^{(4)} >_{conn} - g_0^4 < S_s^{(1)}\omega^{(3)} >_{conn} \\
&\quad - g_0^4 < S_s^{(0)}\omega^{(2)} >_{conn} < \omega^{(2)} >_0 + O(g_0^6).
\end{aligned} \tag{4.9}$$

In contrast to (3.20) and (3.52), here a disconnected term (the last one) appears, because of the definition (1.8) of $< O >_{q\bar{q}-0}$.

For simplicity, but without loss of generality (because of the symmetry of the lattice), in the following the Wilson loop will be chosen to lie in the 3-4-plane.

4.2 Perturbative check

4.2.1 Leading order

In leading order, (4.8) reduces to the following simple formula:

$$\hat{V} = g_0^2\frac{\partial}{\partial g_0^2}\hat{V} - 2g_0^2\lim_{\hat{T}\to\infty}\frac{1}{\hat{T}} < S_s^{(0)}\omega^{(2)} >_{conn} \tag{4.10}$$

where use has been made of the fact that both the expansion for $< S_s >_{q\bar{q}-0}$ and the expansion for the potential start with g_0^2. But the latter one leads also to the following identity:

$$\hat{V} = g_0^2 \frac{\partial}{\partial g_0^2} \hat{V} + O(g_0^4), \tag{4.11}$$

hence in leading order, the energy sum rule is equivalent to the requirement

$$\lim_{\hat{T}\to\infty} \frac{1}{\hat{T}} < S_s^{(0)} \omega^{(2)} >_{conn} = 0, \tag{4.12}$$

i. e., in leading order, the expectation value of the spatial plaquettes has to vanish in the limit of large temporal extent of the Wilson loop.

An explicit calculation for this correlator can be done by first looking at the insertion of $S_s^{(0)}$ into an arbitrary gluon line:

$$< A_\mu^A(p) A_\nu^B(q) S_s^{(0)} >_{conn} = \delta^{AB} (2\pi)^4 \delta(p+q) \delta_\mu^s \frac{\delta_{\mu\nu} \hat{\vec{p}}^2 - \hat{p}_\mu \hat{p}_\nu}{(\hat{p}^2)} \delta_\nu^s \tag{4.13}$$

with

$$\delta_\mu^s := 1 - \delta_{\mu 4} = \begin{cases} 1 & \mu < 4 \\ 0 & \mu = 4 \end{cases} \tag{4.14}$$

Then the result for the correlator with the Wilson loop is:

$$< S_s^{(0)} \omega^{(2)} >_{conn,subtr} = -C_2(F) \int\limits_{BZ} \frac{d^4p}{(2\pi)^4} \frac{\cos(p_4 \hat{T})}{(\hat{p}^2)^2} \frac{\sin^2(p_3 \hat{R}/2)}{\sin^2(p_3/2)} \left(\hat{\vec{p}}^2 - \hat{p}_3^2 \right) \tag{4.15}$$

Taking the limit, one obviously obtains:

$$\lim_{\hat{T}\to\infty} \frac{1}{\hat{T}} < S_s^{(0)} \omega^{(2)} >_{conn,subtr} = 0; \tag{4.16}$$

the expectation value of the spatial plaquettes (the energy in the magnetic fields) does indeed vanish in leading order, and therefore the energy sum rule is true in leading order.

Looking at the relevant Feynman diagrams makes this a bit clearer. On the one hand, there are the possibilities where both gluon lines end on spatial lines of the Wilson loop:

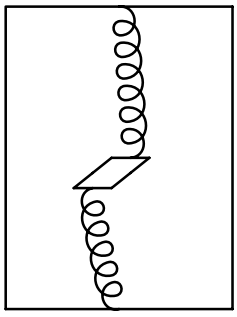

Here a sum over all spatial plaquettes is to be understood (which is denoted by

the perspective view of the plaquette), and, as usual, the end points of the gluon lines can be attached to all four links of the plaquette. Obviously, such diagrams can give no contribution proportional to $\hat{T}$; therefore their contributions to $< S_s^{(0)}\omega^{(2)} >_{conn,subtr}$ vanish when dividing by $\hat{T}$ and then taking the limit. On the other hand, the sum over all of the diagrams of the following form:

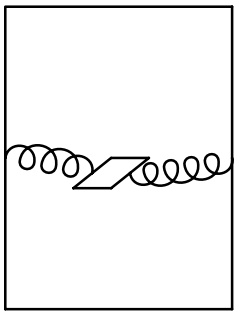

would give a contribution proportional to $\hat{T}$. But such diagrams can not appear, because the propagator in Feynman gauge connects only links which are parallel to each other. Only spatial plaquettes appear here, hence no gluon line can connect the plaquettes to temporal line of the Wilson loop.

4.2.2 Next-to-leading order

Using the result derived above

$$\lim_{\hat{T}\to\infty} \frac{1}{\hat{T}} < S_s^{(0)}\omega^{(2)} >_{conn,subtr} = 0, \tag{4.17}$$

one sees that only the higher terms in the expansion of $< S_s >_{q\bar{q}-0}$ can give non-vanishing contributions in the limit of large $\hat{T}$. Hence the term $g_0^2 < S_s >_{q\bar{q}-0}$ in (4.8) is of order g_0^6 and does not contribute in next-to-leading order:

$$\hat{V} = g_0^2 \frac{\partial}{\partial g_0^2}\hat{V} + \left.\frac{\partial c_t}{\partial \xi}\right|_{\xi=1} g_0^4 \frac{\partial}{\partial g_0^2}\hat{V} + 2 \lim_{\hat{T}\to\infty} \frac{1}{\hat{T}} < S_s >_{q\bar{q}-0} + O(g_0^6). \tag{4.18}$$

The remaining graphs which contribute to $< S_s >_{q\bar{q}-0}$ can, as usual, be divided into the three groups

- vacuum polarization graphs
- spider graphs
- graphs with two independent gluon lines

And again as usual, these three types of graphs will be examined separately.

The vacuum polarization graphs

The relevant graphs are shown in figure 4.1. Using the same argument as for the one diagram in leading order, one sees easily that most graphs do not contribute

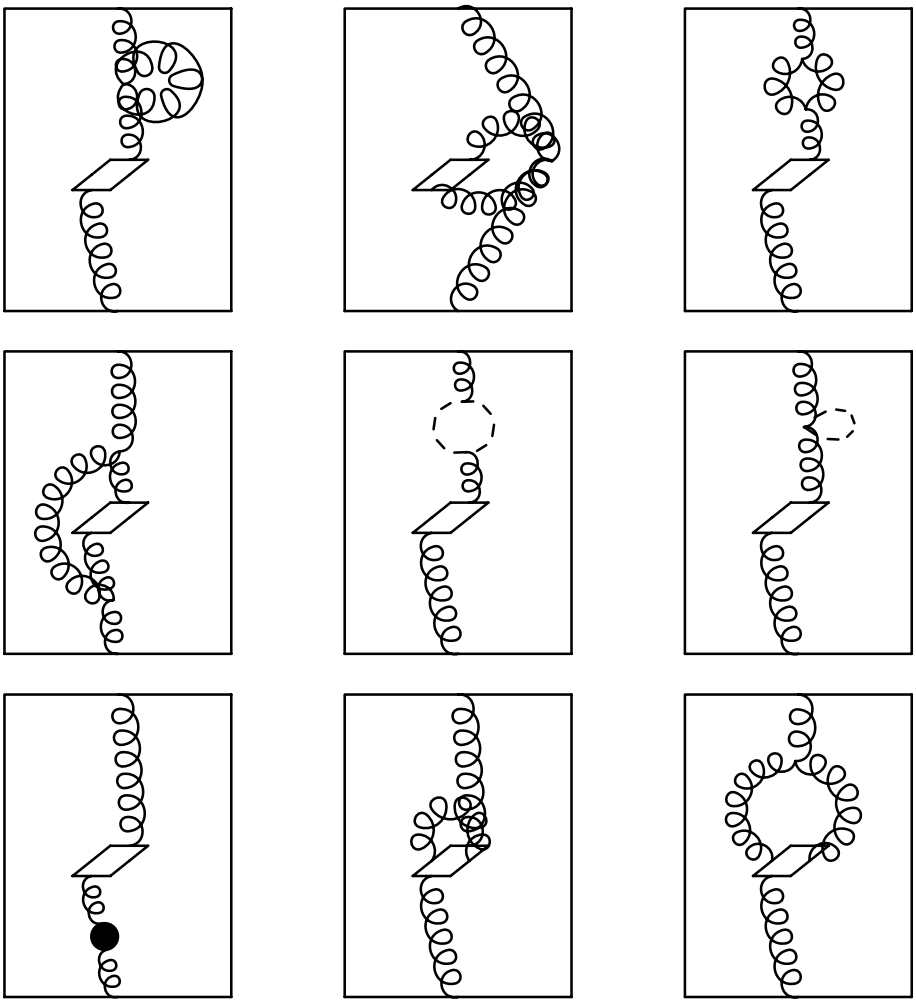

Figure 4.1: Vacuum polarization graphs contributing to the expectation value of the spatial plaquettes

for $\hat{T} \to \infty$; only the second and the fourth graph survive:

$$\begin{aligned} & \lim_{\hat{T}\to\infty} \frac{< S_s^{(0)} S^{(2)} \omega^{(2)} >_{conn,ext}}{\hat{T}} = \lim_{\hat{T}\to\infty} \frac{< S_s^{(0)} \frac{1}{2} (S^{(1)})^2 \omega^{(2)} >_{conn,ext}}{\hat{T}} \\ = & \lim_{\hat{T}\to\infty} \frac{< S_s^{(2)} \omega^{(2)} >_{conn}}{\hat{T}} = \lim_{\hat{T}\to\infty} \frac{< S_s^{(0)} S_{FP}^{(2)} \omega^{(2)} >_{conn}}{\hat{T}} \\ = & \lim_{\hat{T}\to\infty} \frac{< S_s^{(0)} S_{meas}^{(2)} \omega^{(2)} >_{conn}}{\hat{T}} = \lim_{\hat{T}\to\infty} \frac{< S_s^{(1)} S^{(1)} \omega^{(2)} >_{conn}}{\hat{T}} = 0 \end{aligned} \quad (4.19)$$

(because of the insertion of $S_s^{(0)}$, respectively $S_s^{(2)}$, only graphs can contribute in which at least one of the external gluon lines ends on a spatial line of the Wilson loop—but the sum over such graphs does not give a contribution proportional to $\hat{T}$ and hence vanishes in the limit). The subscript "ext" in the first two terms means that there, only the insertions of $S_s^{(0)}$ into *external* lines are considered.

The remaining graphs (number two and four) will be studied later in more detail.

The spider graphs

As in section 3.4.2, there are two spider graphs which have to be taken into account here:

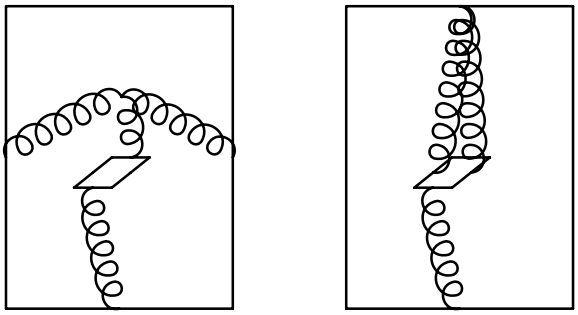

The first graph behaves for $\hat{T} \to \infty$ like $< S^{(1)}\omega^{(3)} >_{conn}$, the ordinary spider graph without plaquette insertions:

$$\lim_{\hat{T}\to\infty} \frac{1}{\hat{T}} < S_s^{(0)} S^{(1)}\omega^{(3)} >_{conn} = \lim_{\hat{T}\to\infty} \frac{1}{\hat{T}} < S^{(1)}\omega^{(3)} >_{conn} = 0 \tag{4.20}$$

Treating the second graph is even more simple; it does not contribute at all, even for finite $\hat{T}$:

$$< S_s^{(1)}\omega^{(3)} >_{conn} = 0. \tag{4.21}$$

The reason for this is that $S_s^{(1)}$ contains a three-gluon vertex. Because this vertex only incorporates spatial plaquettes and the gluon lines are in Feynman gauge, all three gluon lines can only be connected to the spatial lines in the Wilson loop. But then the polarizations of all three gluons which meet at the vertex are identical—and for this configuration, the vertex vanishes.

Therefore both spider graphs give no contributions. The only graphs which are left now, beside the two vacuum polarization graphs mentioned above, are

The graphs with two independent gluon lines

Here one has to consider two types of contributions. First, as usual, there are the contributions coming from $\omega^{(4)}$, but, as already mentioned, here additionally a disconnected contribution appears. This is depicted in the following two graphs:

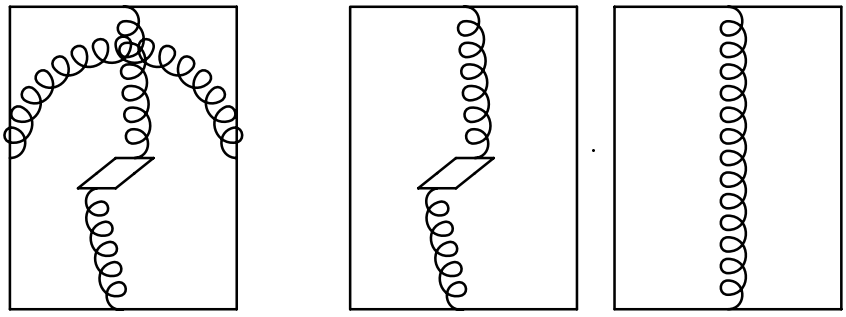

The first graph gives contributions proportional to $(C_2(F))^2$ and to $C_2(F) \cdot C_2(G)$; the product of the two loops in the second graph gives a color factor $(C_2(F))^2$. An explicit calculation yields:

$$\begin{aligned} & < S_s^{(0)} \omega^{(4A)} >_{conn} \\ = \; & 2\,(C_2(F))^2 \int\limits_{BZ} \frac{d^4p}{(2\pi)^4} \frac{\sin^2(p_3\hat{R}/2)\sin^2(p_4\hat{T}/2)}{\hat{p}^2} \left(\frac{1}{\sin^2(p_3/2)} + \frac{1}{\sin^2(p_4/2)} \right) \\ & \cdot \int\limits_{BZ} \frac{d^4p}{(2\pi)^4} \frac{\cos(p_4\hat{T}/2)}{(\hat{p}^2)^2} \frac{\sin^2(p_3\hat{R}/2)}{\sin^2(p_3/2)} \left(\hat{\vec{p}}^2 - \hat{p}_3^2 \right) \\ & + C_2(F)C_2(G) \cdot (\ldots) \end{aligned} \tag{4.22}$$

and

$$\begin{aligned} & < \omega^{(2)} >_0 < S_s^{(0)} \omega^{(2)} >_{conn} \\ = \; & -2\,(C_2(F))^2 \int\limits_{BZ} \frac{d^4p}{(2\pi)^4} \frac{\sin^2(p_3\hat{R}/2)\sin^2(p_4\hat{T}/2)}{\hat{p}^2} \left(\frac{1}{\sin^2(p_3/2)} + \frac{1}{\sin^2(p_4/2)} \right) \\ & \cdot \int\limits_{BZ} \frac{d^4p}{(2\pi)^4} \frac{\cos(p_4\hat{T}/2)}{(\hat{p}^2)^2} \frac{\sin^2(p_3\hat{R}/2)}{\sin^2(p_3/2)} \left(\hat{\vec{p}}^2 - \hat{p}_3^2 \right); \end{aligned} \tag{4.23}$$

hence the contributions proportional to $(C_2(F))^2$ cancel exactly, and the disconnected part vanishes.

But there are still contributions left from $\omega^{(4)}$ which are proportional to $C_2(F) \cdot C_2(G)$. These graphs can be classified into three categories:

1. Graphs in which only temporal links of the Wilson loop appear; these links can not be connected with the spatial plaquettes using the gluon propagators in Feynman gauge, and therefore their contributions vanish.

2. Graphs in which only spatial links of the Wilson loop appear; these do not give contributions proportional to $\hat{T}$ and therefore in the limit of large $\hat{T}$, they vanish.

3. Graphs in which temporal as well as spatial links appear - these have to be treated explicitly.

In order to examine the contributions of the graphs of the third category, split $\omega^{(4)}$ again into the parts A to F and then look only at the graphs with spatial as well as temporal links; write for these $\omega_{RT}^{(4A)}$ to $\omega_{RT}^{(4F)}$. The results for the various contributions are:

$$\begin{aligned} & < S_s^{(0)} \omega_{RT}^{(4A)} >_{conn} \\ = \; & -\frac{C_2(F)C_2(G)}{6} \int\limits_{BZ} \frac{d^4p}{(2\pi)^4} \int\limits_{BZ} \frac{d^4k}{(2\pi)^4} \frac{\hat{\vec{p}}^2 - \hat{p}_3^2}{(\hat{p}^2)^2} \frac{1}{\hat{k}^2} \frac{\sin^2(p_3R/2)}{\sin^2(p_3/2)} \frac{\sin^2(k_4T/2)}{\sin^2(k_4/2)} \\ & [1 - \cos(k_3R) - \cos(p_4T) + \cos(p_4T)\cos(k_3R)] \\ & + (C_2(F))^2 \cdot (\ldots) \end{aligned} \tag{4.24}$$

$$
\begin{aligned}
& < S_s^{(0)} \omega_{RT}^{(4B)} >_{conn} \\
= & -\frac{C_2(F)C_2(G)}{2} \int\limits_{BZ} \frac{d^4p}{(2\pi)^4} \int\limits_{BZ} \frac{d^4k}{(2\pi)^4} \frac{\hat{\vec{p}}^2 - \hat{p}_3^2}{\left(\hat{p}^2\right)^2} \frac{1}{\hat{k}^2} \frac{\sin^2(p_3R/2)}{\sin^2(p_3/2)} \frac{\sin^2(k_4T/2)}{\sin^2(k_4/2)}
\end{aligned} \tag{4.25}
$$

$$
\begin{aligned}
& < S_s^{(0)} \omega_{RT}^{(4C)} >_{conn} \\
= & \frac{C_2(F)C_2(G)}{8} \int\limits_{BZ} \frac{d^4p}{(2\pi)^4} \int\limits_{BZ} \frac{d^4k}{(2\pi)^4} \frac{\hat{\vec{p}}^2 - \hat{p}_3^2}{\left(\hat{p}^2\right)^2} \frac{1}{\hat{k}^2} \\
& \left[3 \frac{\sin^2(p_3R/2)}{\sin^2(p_3/2)} \left(\frac{\sin^2(k_4T/2)}{\sin^2(k_4/2)} - T \right) \right. \\
& - \frac{\sin^2(p_3R/2)}{\sin^2(p_3/2)} \cos(p_4T) \left(\frac{\sin^2(k_4T/2)}{\sin^2(k_4/2)} - 3T \right) \\
& + \frac{\sin^2(k_4T/2)}{\sin^2(k_4/2)} \left(\frac{\sin^2(p_3R/2)}{\sin^2(p_3/2)} - R \right) (1 - \cos(k_3R)) \\
& \left. - 2 \frac{\sin^2(p_3R/2)}{\sin^2(p_3/2)} \cos(p_4T) \frac{\sin^2(k_4T/2)}{\sin^2(k_4/2)} \cos(k_3R) \right]
\end{aligned} \tag{4.26}
$$

$$
\begin{aligned}
& < S_s^{(0)} \omega_{RT}^{(4D)} >_{conn} \\
= & \frac{C_2(F)C_2(G)}{24} \int\limits_{BZ} \frac{d^4p}{(2\pi)^4} \int\limits_{BZ} \frac{d^4k}{(2\pi)^4} \frac{\hat{\vec{p}}^2 - \hat{p}_3^2}{\left(\hat{p}^2\right)^2} \frac{1}{\hat{k}^2} \\
& \left[\frac{\sin^2(p_3R/2)}{\sin^2(p_3/2)} \frac{\sin^2(k_4T/2)}{\sin^2(k_4/2)} \left(8 - 2\cos(p_4T)\cos(k_3R)\right) \right. \\
& - 3 \frac{\sin^2(p_3R/2)}{\sin^2(p_3/2)} \left(\frac{\sin^2(k_4T/2)}{\sin^2(k_4/2)} - T \right) \\
& - \frac{\sin^2(k_4T/2)}{\sin^2(k_4/2)} \left(\frac{\sin^2(p_3R/2)}{\sin^2(p_3/2)} - R \right) \\
& - \frac{\sin^2(p_3R/2)}{\sin^2(p_3/2)} \cos(p_4T) \left(\frac{\sin^2(k_4T/2)}{\sin^2(k_4/2)} + 3T \right) \\
& \left. - \frac{\sin^2(k_4T/2)}{\sin^2(k_4/2)} \cos(k_3R) \left(\frac{\sin^2(p_3R/2)}{\sin^2(p_3/2)} + R \right) \right]
\end{aligned} \tag{4.27}
$$

$$
\begin{aligned}
& < S_s^{(0)} \omega_{RT}^{(4E)} >_{conn} \\
= & \frac{C_2(F)C_2(G)}{12} \int\limits_{BZ} \frac{d^4p}{(2\pi)^4} \int\limits_{BZ} \frac{d^4k}{(2\pi)^4} \frac{\hat{\vec{p}}^2 - \hat{p}_3^2}{\left(\hat{p}^2\right)^2} \frac{1}{\hat{k}^2} \\
& \left[3 \frac{\sin^2(p_3R/2)}{\sin^2(p_3/2)} T \left(1 - \cos(p_4T)\right) + \frac{\sin^2(k_4T/2)}{\sin^2(k_4/2)} R \left(1 - \cos(k_3R)\right) \right].
\end{aligned} \tag{4.28}
$$

And finally, because of the symmetry properties in the colour indices one gets as usual:

$$
< S_s^{(0)} \omega_{RT}^{(4F)} >_{conn} = 0. \tag{4.29}
$$

Adding everything, the result is:

$$\begin{aligned} < S_s^{(0)} \omega_{RT}^{(4)} >_{conn;C_2(F)C_2(G)} &= \frac{C_2(F)C_2(G)}{2} \int\limits_{BZ} \frac{d^4p}{(2\pi)^4} \int\limits_{BZ} \frac{d^4k}{(2\pi)^4} \frac{\hat{\vec{p}}^2 - \hat{p}_3^2}{\left(\hat{p}^2\right)^2} \frac{1}{\hat{k}^2} \\ & \frac{\sin^2(p_3 R/2)}{\sin^2(p_3/2)} \cos(p_4 T) \frac{\sin^2(k_4 T/2)}{\sin^2(k_4/2)} \cos(k_3 R) \end{aligned} \tag{4.30}$$

Divide by $\hat{T}$ and take the limit:

$$\lim_{\hat{T}\to\infty} \frac{< S_s^{(0)} \omega^{(4)} >_{conn;C_2(F)C_2(G)}}{\hat{T}} = \lim_{\hat{T}\to\infty} \frac{< S_s^{(0)} \omega_{RT}^{(4)} >_{conn;C_2(F)C_2(G)}}{\hat{T}} = 0. \tag{4.31}$$

Hence nearly all contributions vanish, and only the vacuum polarization graphs contribute to $< S_s >_{q\bar{q}-0}$ in next-to-leading order!

Check in next-to-leading order

Making use of the fact that only the vacuum polarization graphs contribute to the expectation value of the spatial plaquettes, the result is now simply:

$$\begin{aligned} < S_s >_{q\bar{q}-0} &= g_0^4 \lim_{\hat{T}\to\infty} \frac{1}{\hat{T}} \left(< S_s^{(0)} S^{(2)} \omega^{(2)} >_{conn} - < S_s^{(0)} \frac{1}{2} (S^{(1)})^2 \omega^{(2)} >_{conn} \right) \\ &= C_2(F) g_0^4 \int\limits_{BZ} \frac{d^3p}{(2\pi)^3} \frac{\cos(p_3 \hat{R})}{\left(\hat{\vec{p}}^2\right)^2} \Pi_{44}^{(s)}(\vec{p}, 0). \end{aligned} \tag{4.32}$$

As usual, the self energy contributions have been subtracted here. The vacuum polarization tensor $\Pi_{\mu\nu}^s$ (with the insertion of the sum over the spatial plaquettes) is given by the sum of the following two contributions (given for an arbitrary dimension d; see appendix C):

$$\begin{aligned} & \Pi_{\mu\nu}^{Loop,s} \\ = \; & C_2(G) \int\limits_{BZ} \frac{d^dk}{(2\pi)^d} \sum_{i,j=1}^{d-1} \frac{\hat{\vec{k}}^2 \delta_{ij} - \hat{k}_i \hat{k}_j}{\left(\hat{k}^2\right)^2 \widehat{(p+k)^2}} \\ & \Big[\delta_{ij} \widehat{(p+2k)}_\mu \widehat{(p+2k)}_\nu \cos(p_i/2) \cos(p_j/2) \\ & + \delta_{\mu\nu} \widehat{(2p+k)}_i \widehat{(2p+k)}_j \cos(k_\mu/2) \cos(k_\nu/2) \\ & + \delta_{\mu i} \delta_{\nu j} \widehat{(p-k)}^2 \cos((p+k)_i/2) \cos((p+k)_j/2) \\ & + \Big\{ \delta_{\mu i} \Big(\widehat{(2p+k)}_j \widehat{(2p+k)}_\nu \cos(k_i/2) \cos(p_i/2) \\ & + \widehat{(p-k)}_j \widehat{(p+2k)}_\nu \cos((p+k)_i/2) \cos(p_j/2) \end{aligned}$$

$$+(\widehat{p-k})_\nu(2\widehat{p+k})_j\cos((p+k)_i/2)\cos(k_\nu/2)\Big)\Big\}+\Big\{(\mu,i)\leftrightarrow(\nu,j)\Big\}\Big] \tag{4.33}$$

$$\begin{aligned}
&\Pi_{\mu\nu}^{Tadpole,s}\\
=\;&-\frac{1}{2}C_2(G)\Big\{\delta_{\mu\nu}\left[\frac{2(d-2)}{d}\Delta_0-\frac{(d+1)(d-2)}{3d(d-1)}\Delta_0\hat{\vec{p}}^2\right]\\
&+\delta^s_{\mu\nu}\left[\frac{(2d-5)(d-2)}{d-1}\Delta_0-\frac{7}{6d}+\left(\frac{(2d-1)(d-2)}{4d(d-1)}\Delta_0-\frac{1}{4d}\right)\hat{p}_\mu^2\right.\\
&\left.+\left(-\frac{(5d-2)(d-2)}{6d(d-1)}\Delta_0+\frac{1}{d}\right)\hat{\vec{p}}^2-\frac{d-2}{6d(d-1)}\Delta_0\hat{p}^2\right]\\
&+\frac{d-2}{6(d-1)}\Delta_0\hat{p}_\mu\hat{p}_\nu\left(\delta^s_\mu+\delta^s_\nu\right)+\frac{(4d-1)(d-2)}{12d(d-1)}\Delta_0\hat{p}_\mu\hat{p}_\nu\delta^s_\mu\delta^s_\nu\Big\}\\
&+\left(C_2(F)-\frac{1}{6}C_2(G)\right)\Big\{\delta_{\mu\nu}\frac{(d-2)^2}{d(d-1)}\Delta_0\hat{\vec{p}}^2\\
&+\delta^s_{\mu\nu}\left[\left(\frac{4-2d}{d}\Delta_0+\frac{1}{d}\right)\hat{\vec{p}}^2+\frac{(d-2)^2}{d(d-1)}\Delta_0\hat{p}^2\right]\\
&-\frac{(d-2)^2}{d(d-1)}\Delta_0\hat{p}_\mu\hat{p}_\nu\left(\delta^s_\mu+\delta^s_\nu\right)-\left(\frac{4-2d}{d}\Delta_0+\frac{1}{d}\right)\hat{p}_\mu\hat{p}_\nu\delta^s_\mu\delta^s_\nu\Big\}
\end{aligned} \tag{4.34}$$

with

$$\delta^s_{\mu\nu}:=\sum_{\mu,\nu}\delta^s_\mu\delta_{\mu\nu}\delta^s_\nu \tag{4.35}$$

and the usual abbreviation

$$\Delta_0\equiv\int\limits_{BZ}\frac{d^dk}{(2\pi)^d}\frac{1}{\hat{k}^2}$$

(see appendix C).

As already explained above, vacuum polarization graphs in which the sum over the spatial plaquettes is inserted into an external line can not contribute; therefore the ghost graphs and the graph with the insertion of the integration measure do not appear here, because they do not have internal gluon lines.

Only the $\mu=\nu=d=4$ components contribute in the limit of large $\hat{T}$, and from these, only the part with $p_4=0$. Then the formulas above reduce to:

$$\Pi_{44}^{Tadpole,s}(\vec{p},0)=C_2(G)\Delta_0\left(\frac{1}{12}\hat{\vec{p}}^2-\frac{1}{2}\right)+C_2(F)\frac{1}{3}\Delta_0\hat{\vec{p}}^2 \tag{4.36}$$

$$\begin{aligned}
\Pi_{44}^{Loop,s}(\vec{p},0)=\;&C_2(G)\int\limits_{BZ}\frac{d^4k}{(2\pi)^4}\frac{1}{\left(\hat{k}^2\right)\left((\widehat{\vec{p}+\vec{k}})^2+\hat{k}_4^2\right)}\\
&\Big[(\widehat{2k})_4^2\hat{\vec{k}}^2\left(3-\frac{1}{4}\hat{\vec{p}}^2\right)+\hat{\vec{k}}^2\left(1-\frac{1}{4}\hat{k}_4^2\right)\left(2\widehat{\vec{p}+\vec{k}}\right)^2\\
&-(\widehat{2k})_4^2\left(\hat{\vec{k}}^2-\frac{1}{4}\sum_i\hat{k}_i^2\hat{p}_i^2\right)
\end{aligned}$$

$$- \left(1 - \frac{1}{4}\hat{k}_4^2\right) \left(\sum_i \left(2\widehat{p+k}\right)_i \hat{k}_i \right)^2 \Bigg] . \tag{4.37}$$

There is a source for a potential infrared divergence in the p-integral in (4.32); one has to check that the vacuum polarization tensor goes to zero for $p \to 0$. Inserting $p = 0$ above, the results are:

$$\Pi_{44}^{Tadpole,s}(0) = -\frac{1}{2} C_2(G) \Delta_0 = -\Pi_{44}^{Loop,s}(0)$$

and therefore

$$\Pi_{44}^{(s)}(0) = \Pi_{44}^{Tadpole,s}(0) + \Pi_{44}^{Loop,s}(0) = 0. \tag{4.38}$$

Hence there is no infrared divergence, and the integral can be done without problems.

Inserting the formula (4.32) for the expectation value of the spatial plaquettes, (4.18) becomes:

$$\hat{V} = g_0^2 \frac{\partial}{\partial g_0^2} \hat{V} + \left.\frac{\partial c_t}{\partial \xi}\right|_{\xi=1} g_0^4 \frac{\partial}{\partial g_0^2} \hat{V} + 2C_2(F) g_0^4 \int\limits_{BZ} \frac{d^3p}{(2\pi)^3} \frac{\cos(p_3 \hat{R})}{\left(\hat{\vec{p}}^2\right)^2} \Pi_{44}^{(s)}(\vec{p}, 0) \tag{4.39}$$

Then the expansion for the potential

$$\hat{V} = g_0^2 V^{(2)} + g_0^4 V^{(4)} + O(g_0^6) \tag{4.40}$$

yields

$$V^{(4)} = 2V^{(4)} + \left.\frac{\partial c_t}{\partial \xi}\right|_{\xi=1} V^{(2)} + 2C_2(F) \int\limits_{BZ} \frac{d^3p}{(2\pi)^3} \frac{\cos(p_3 \hat{R})}{\left(\hat{\vec{p}}^2\right)^2} \Pi_{44}^{(s)}(\vec{p}, 0). \tag{4.41}$$

The explicit expression for the potential can be taken from chapter 2. Additionally, use

$$\left.\frac{\partial c_t}{\partial \xi}\right|_{\xi=1} = -\frac{1}{4} C_2(F) \cdot 0.586844 + 4C_2(G) \cdot 0.005306, \tag{4.42}$$

derived in [42], to obtain finally the following expression, which is equivalent to the energy sum rule in next-to-leading order:

$$\begin{aligned} & \int\limits_{BZ} \frac{d^3p}{(2\pi)^3} \frac{\cos(p_3 \hat{R})}{\left(\hat{\vec{p}}^2\right)^2} \Pi_{44}^{(s)}(\vec{p}, 0) \\ = \; & \frac{C_2(G)}{4\pi\hat{R}} \left(0.023220 \ln \hat{R} + 0.057400\right) + \frac{C_2(F)}{4\pi\hat{R}} 0.051644. \end{aligned} \tag{4.43}$$

Now it is convenient to split up $\Pi^{Tadpole}$ into two parts, corresponding to the group theoretical factors:

$$\Pi^{Tadpole} = C_2(G) \Pi^{Tadpole,1} + C_2(F) \Pi^{Tadpole,2}; \tag{4.44}$$

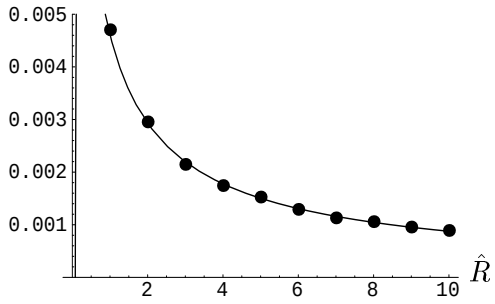

Figure 4.2: Comparison of the calculated values to the fitted curve; see text

then (4.43) splits also into two parts:

$$(I) \qquad \int_{BZ} \frac{d^3p}{(2\pi)^3} \frac{\cos(p_3\hat{R})}{\left(\hat{\vec{p}}^2\right)^2} \Pi_{44}^{Tadpole,s,2}(\vec{p},0) = \frac{1}{4\pi\hat{R}} 0.051644 \tag{4.45}$$

$$(II) \qquad \int_{BZ} \frac{d^3p}{(2\pi)^3} \frac{\cos(p_3\hat{R})}{\left(\hat{\vec{p}}^2\right)^2} \left(\Pi_{44}^{Tadpole,s,1}(\vec{p},0) + \Pi_{44}^{Loop,s,1}(\vec{p},0)\right)$$

$$= \frac{1}{4\pi\hat{R}} \left(0.023220 \ln \hat{R} + 0.057400\right) \tag{4.46}$$

In the first part (4.45), insert the explicit expression $\Pi_{44}^{Tadpole,2}(\vec{p},0) = \frac{1}{3}\Delta_0\,\hat{\vec{p}}^2$; the remaining integral gives in the continuum limit (see section 2.2.1):

$$\int_{BZ} \frac{d^3p}{(2\pi)^3} \frac{\cos(p_3\hat{R})}{\hat{\vec{p}}^2} = \frac{1}{4\pi\hat{R}}. \tag{4.47}$$

Hence the first part of (4.43) requires simply the following formula to hold:

$$\frac{1}{3}\Delta_0 = 0.051644. \tag{4.48}$$

Inserting for Δ_0 the numerically calculated value (see appendix C), one sees that this formula is indeed satisfied—to very good accuracy!

The second part (4.46) is a little bit more complicated. The integral on the left hand side can be only evaluated numerically; this has been done for $\hat{R}$ between 1 and 10 using again the routine *Vegas* from [41]. The resulting numbers can be compared to the function on the right hand side.
A fit of the calculated values to a function of the form

$$\frac{1}{4\pi\hat{R}} \left(a \ln \hat{R} + b\right),$$

using Mathematica, gives:

$$a = 0.02268 \pm 0.00078; \qquad b = 0.05792 \pm 0.00132 \tag{4.49}$$

If the energy sum rule is valid, the results should be $a = 0.2322$ and $b = 0.05740$. The numbers from the fit agree very well with this in the range of their numerical errors. Hence the second part of (4.43) is also valid.

For illustrative purposes, figure 4.2 gives a plot of the calculated values (left hand side of (4.46)), as well as of the curve on which they should lie if the energy sum rule is valid (right hand side of (4.46)). The very good agreement between the points and the curve is obvious.

Summarizing: Both parts, (4.45) and (4.46), of the formula (4.43), which is equivalent to the energy sum rule in next-to-leading order, are satisfied with good numerical accuracy, or in other words:

The energy sum rule is valid up to next-to-leading order with good numerical accuracy.

4.3 Contributions to the potential

Using the validity of the energy sum rule and the results obtained for the spatial plaquettes, one can now analyze the various contributions to the potential:

$$\begin{aligned} \hat{V} &= \text{electric field energy} + \text{magnetic field energy} \\ &\quad + \text{trace anomaly} \\ &= -\eta_- \lim_{\hat{T}\to\infty} \frac{1}{\hat{T}} < \mathcal{P}_t >_{q\bar{q}-0,subtr} + \eta_- \lim_{\hat{T}\to\infty} \frac{1}{\hat{T}} < \mathcal{P}_s >_{q\bar{q}-0,subtr} \\ &\quad + \frac{1}{4} \lim_{\hat{T}\to\infty} \frac{1}{\hat{T}} < \sum_{x,\mu} T_{\mu\mu}(x) >_{q\bar{q}-0,subtr} \end{aligned} \tag{4.50}$$

First, look at the contribution of the magnetic field energy.

$$\begin{aligned} \eta_- < \mathcal{P}_s >_{q\bar{q}-0,subtr} &= \frac{\eta_-}{\beta} < S_s >_{q\bar{q}-0,subtr} \\ &= < S_s >_{q\bar{q}-0,subtr} + \frac{1}{2} c g_0^2 < S_s >_{q\bar{q}-0,subtr}, \end{aligned}$$

where the constant c is again given by

$$c = \left(\frac{\partial c_t}{\partial \xi} - \frac{\partial c_s}{\partial \xi} \right)_{\xi=1};$$

the functions c_t and c_s can be found in [42].

As already pointed out in the last section, in the limit of large $\hat{T}$, the leading order of $< S_s >_{q\bar{q}-0,subtr}$ vanishes, and the lowest non-vanishing contribution is of order g_0^4; hence up to next-to-leading order, the second term does not contribute here. The first term is given by the two vacuum polarization graphs where the sum over the spatial plaquettes has been inserted into an internal line. According to the results obtained in the last section, one gets then for the contribution of the magnetic field energy:

magnetic field energy

$$
\begin{aligned}
&= \eta_- \lim_{\hat{T}\to\infty} \frac{1}{\hat{T}} < \mathcal{P}_s >_{q\bar{q}-0,subtr} \\
&= \frac{C_2(F)}{4\pi\hat{R}} \left(\frac{11C_2(G)}{48\pi^2} g_0^4 \ln\left(7.501\hat{R}\right) + \frac{1}{2} \left.\frac{\partial c_t}{\partial \xi}\right|_{\xi=1} g_0^4 + \frac{1}{8} C_2(F) g_0^4 \right) \\
&\approx \frac{C_2(F)}{4\pi\hat{R}} g_0^4 \left(C_2(G) \left(0.023 \ln \hat{R} + 0.058\right) + 0.052\, C_2(F) \right). \qquad (4.51)
\end{aligned}
$$

For the electric field energy, use

$$
< \mathcal{P}_t >_{q\bar{q}-0,subtr} \;=\; \frac{1}{\hat{\beta}} (< S >_{q\bar{q}-0,subtr} - < S_s >_{q\bar{q}-0,subtr})
$$

and

$$
\lim_{\hat{T}\to\infty} \frac{1}{\hat{T}} < S >_{q\bar{q}-0,subtr} = \hat{\beta} \frac{\partial \hat{V}}{\partial \hat{\beta}}.
$$

Inserting the explicit form of the potential and of $< S_s >_{q\bar{q}-0,subtr}$, one then obtains for the contribution of the electric field energy:

$$
\begin{aligned}
&\text{electric field energy} \\
&= -\eta_- \lim_{\hat{T}\to\infty} \frac{1}{\hat{T}} < \mathcal{P}_t >_{q\bar{q}-0,subtr} \\
&= -\frac{C_2(F)}{4\pi\hat{R}} \left(g_0^2 + \frac{11C_2(G)}{16\pi^2} g_0^4 \ln\left(7.501\hat{R}\right) - \frac{1}{2} \left.\frac{\partial c_s}{\partial \xi}\right|_{\xi=1} g_0^4 + \frac{3}{8} C_2(F) g_0^4 \right) \\
&\approx -\frac{C_2(F)}{4\pi\hat{R}} \left(g_0^2 + g_0^4 C_2(G) \left(0.070 \ln \hat{R} + 0.141\right) + 0.302\, g_0^4\, C_2(F) \right). \qquad (4.52)
\end{aligned}
$$

Finally, for the trace anomaly one can use

$$
\sum_{x,\mu} T_{\mu\mu}(x) = \frac{2\beta_L}{g_0} S
$$

and again

$$
\lim_{\hat{T}\to\infty} \frac{1}{\hat{T}} < S >_{q\bar{q}-0,subtr} = \hat{\beta} \frac{\partial \hat{V}}{\partial \hat{\beta}}.
$$

Then one sees that the contribution of the trace anomaly to the potential is given by:

$$
\begin{aligned}
&\text{trace anomaly} \\
&= \frac{1}{4} \lim_{\hat{T}\to\infty} \frac{1}{\hat{T}} < \sum_{x,\mu} T_{\mu\mu}(x) >_{q\bar{q}-0,subtr} \\
&= -\frac{11C_2(F)C_2(G)}{96\pi^2} \frac{g_0^4}{4\pi\hat{R}} \\
&\approx -0.011 C_2(F) C_2(G) \frac{g_0^4}{4\pi\hat{R}}. \qquad (4.53)
\end{aligned}
$$

Looking at the three contributions (4.52), (4.51) and (4.53), one notices several things:

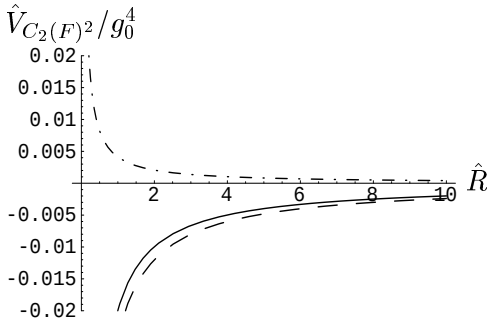

Figure 4.3: Contributions to the potential in NLO, proportional to $(C_2(F))^2$, divided by g_0^4: electric field energy (dashed), magnetic field energy (dot-dashed), potential(solid)

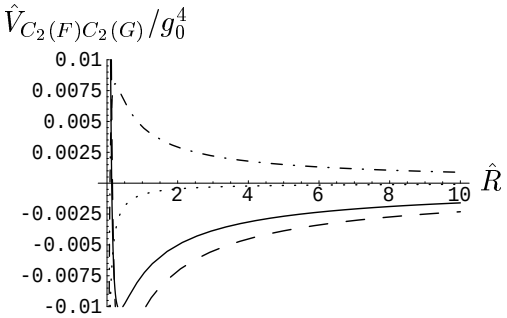

Figure 4.4: Contributions to the potential in NLO, proportional to $C_2(F)C_2(G)$, divided by g_0^4: electric field energy (dashed), magnetic field energy (dot-dashed), trace anomaly (dotted), potential (solid)

- The contribution from the electric field energy is negative and appears already in leading order. Both group theoretical factors contribute in next-to-leading order.
- The contribution from the magnetic field energy is positive and appears first in next-to-leading order; but even there, only the vacuum polarization graphs give a non-vanishing contribution. Again, both group theoretical factors contribute.
- The contribution from the trace anomaly is negative and appears first in next-to-leading order; it is proportional to $C_2(F) \cdot C_2(G)$.

Comparing the explicit numerical factors which appear in the three contributions, or even better, looking at the plots where the magnitudes of these terms are displayed (figures 4.3 and 4.4; for the special case of $SU(3)$, see figure 4.5), one additionally sees that the energy in the magnetic fields is smaller than the one in the electric fields, so that only a part of the electric field energy is cancelled and the overall contribution of the energy in the fields is negative. The trace anomaly gives an additional negative contribution, which for large $\hat{R}$ is small compared to the energy in the fields. This is in strong contrast with the situation for a confining potential, discussed in section 1.3.3, where the trace

anomaly and the energy in the fields both gave exactly equal contributions to the potential.

4.4 Restriction to a fixed time slice

What remains to be shown is that one can restrict the sum over the plaquettes to a fixed time slice:

$$\lim_{\hat{T}\to\infty} \frac{1}{\hat{T}} < \mathcal{P}_t >_{q\bar{q}-0} \;=\; \lim_{\hat{T}\to\infty} < \mathcal{P}'_t(t) >_{q\bar{q}-0} \tag{4.54}$$

$$\lim_{\hat{T}\to\infty} \frac{1}{\hat{T}} < \mathcal{P}_s >_{q\bar{q}-0} \;=\; \lim_{\hat{T}\to\infty} < \mathcal{P}'_s(t) >_{q\bar{q}-0}, \tag{4.55}$$

where $\mathcal{P}'_t(t)$ respectively $\mathcal{P}'_s(t)$ denotes the sum over all plaquettes on the time slice t. Using

$$\mathcal{P}_s + \mathcal{P}_t = \frac{1}{\hat{\beta}} S \tag{4.56}$$

and assuming that

$$\lim_{\hat{T}\to\infty} \frac{1}{\hat{T}} < S >_{q\bar{q}-0} = \lim_{\hat{T}\to\infty} < L(t) >_{q\bar{q}-0} \tag{4.57}$$

(see section 4.4), it suffices to show that the restriction to a fixed time slice works for the spatial plaquettes; this is equivalent to showing that

$$\lim_{\hat{T}\to\infty} \frac{1}{\hat{T}} < S_s >_{q\bar{q}-0} = \lim_{\hat{T}\to\infty} < L_s(t) >_{q\bar{q}-0} \; . \tag{4.58}$$

The left hand side of this equation has already been discussed in section 4.2; for the right hand side, one gets an analogous expansion:

$$\begin{aligned} < L_s >_{q\bar{q}-0} \;=\; & -g_0^2 < L_s^{(0)} \omega^{(2)} >_{conn} + g_0^4 < L_s^{(0)} S^{(2)} \omega^{(2)} >_{conn} \\ & - g_0^4 < L_s^{(0)} \frac{1}{2} (S^{(1)})^2 \omega^{(2)} >_{conn} + g_0^4 < L_s^{(0)} S^{(2)}_{FP} \omega^{(2)} >_{conn} \\ & + g_0^4 < L_s^{(0)} S^{(2)}_{meas} \omega^{(2)} >_{conn} + g_0^4 < L_s^{(1)} S^{(1)} \omega^{(2)} >_{conn} \end{aligned}$$

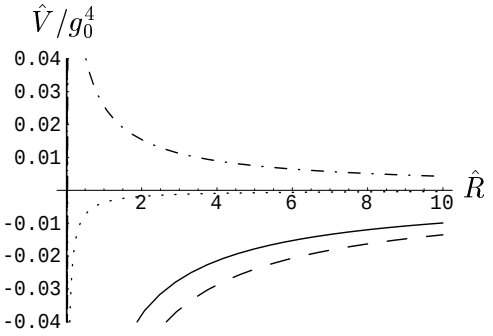

Figure 4.5: All contributions to the potential in NLO for SU(3), divided by g_0^4: electric field energy (dashed), magnetic field energy (dot-dashed), trace anomaly (dotted), potential (solid)

$$
\begin{aligned}
&-g_0^4 < L_s^{(2)}\omega^{(2)} >_{conn} + g_0^4 < L_s^{(0)} S^{(1)} \omega^{(3)} >_{conn} \\
&-g_0^4 < L_s^{(0)}\omega^{(4)} >_{conn} - g_0^4 < L_s^{(1)}\omega^{(3)} >_{conn} \\
&-g_0^4 < L_s^{(0)}\omega^{(2)} >_{conn} < \omega^{(2)} >_0 + O(g_0^6).
\end{aligned} \tag{4.59}
$$

4.4.1 Leading order

For calculating the correlator $< L_s^{(0)}\omega^{(2)} >_{conn}$, it is convenient, as usual, first to look at the insertion of $L_s^{(0)}$ into an arbitrary line. The result is very similar to the one obtained when inserting $S_s^{(0)}$ (4.13); the only difference is that the fourth component of the momentum is not conserved:

$$
< A_\mu^A(p) A_\nu^B(q) L_s^{(0)} >_{conn} = \delta^{AB}(2\pi)^3 \delta(\vec{p}+\vec{q}) \sum_{\mu,\nu} \delta_\mu^s \frac{\delta_{\mu\nu}\hat{\vec{p}}^2 - \hat{p}_\mu \hat{p}_\nu}{\hat{p}^2 \left(\hat{\vec{p}}^2 + \hat{q}_4^2\right)} \delta_\nu^s. \tag{4.60}
$$

With this, one gets the following simple result for the correlator with the Wilson loop in leading order:

$$
\begin{aligned}
& < L_s^{(0)}(t)\omega^{(2)} >_{conn} \\
= \; & -2C_2(F)C_2(G) \int\limits_{BZ} \frac{d^4p}{(2\pi)^4} \int\limits_{-\pi}^{\pi} \frac{dq_4}{2\pi} \frac{\hat{\vec{p}}^2 - \hat{p}_3^2}{\hat{p}^2 \left(\hat{\vec{p}}^2 + \hat{q}_4^2\right)} \frac{\sin^2(p_3 \hat{R}/2)}{\sin^2(p_3/2)} \\
& \cdot \sin(p_4 \hat{T}/2) \sin(q_4 \hat{T}/2) \cos((p+q)_4 (n_{c,4} - t)),
\end{aligned} \tag{4.61}
$$

where again a Wilson loop lying in the 3-4-plane has been used and $n_{c,4}$ is the fourth coordinate of the center of the loop. For $\hat{T} \to \infty$, this correlator vanishes; for the special choice $n_{c,4} = t$ the correlator vanishes even for every finite $\hat{T}$, because then the function under the integral is odd.

Thus one sees that in leading order, the restriction to one time slice indeed works:

$$
\lim_{\hat{T}\to\infty} \frac{1}{\hat{T}} < S_s >_{q\bar{q}-0} = \lim_{\hat{T}\to\infty} < L_s(t) >_{q\bar{q}-0} + O(g_0^4). \tag{4.62}
$$

4.4.2 Next-to-leading order

The relevant graphs for the next order can be found essentially already in section 4.2.2: the only crucial difference is that in that section, the plaquettes were summed over *all* space-time, whereas here they are summed only over the *fixed* time slice t. Now, as usual, it is convenient to look at the three different types of graphs seperately. For simplicity, again only the special case $n_{c,4} = t = 0$ will be treated.

The vacuum polarization graphs

Here one can use arguments very similar to the ones in the sections 4.2.2 and 3.4.2. First look again at the graphs where $L_s^{(0)}$ is inserted into an external line.

They give a contribution proportional to

$$\int\limits_{BZ} \frac{d^4p}{(2\pi)^4} \int\limits_{-\pi}^{\pi} \frac{dq_4}{2\pi} \frac{\sin^2(p_3\hat{R}/2)}{\sin(p_3/2)} \sin(p_4\hat{T}/2)\sin(q_4\hat{T}/2)$$
$$\sum_{j=1}^{3} \left(\frac{\Pi_{3j}(p)}{\sin(p_3)} - \frac{\Pi_{4j}(p)}{\sin(p_4)} \right) \frac{\delta_{j3}\hat{\vec{p}}^2 - \hat{p}_j\hat{p}_3}{\hat{p}^2\left(\hat{\vec{p}}^2 + \hat{q}_4^2\right)}. \tag{4.63}$$

Obviously the function under the integral is odd in q_4 and therefore the integral vanishes even for every finite $\hat{T}$. This is in accordance with the results of section 4.2.2, where it was shown that in the limit of large $\hat{T}$, the vacuum polarisation graphs with an insertion of $S_s^{(0)}$ into an external line do not contribute.

Next consider an insertion of $L_s^{(0)}$ into an internal line and the two graphs coming from the vertex insertions $L_s^{(1)}$ and $L_s^{(2)}$ (corresponding to the first two graphs in figure 3.3, but here only with spatial plaquettes). These give the following contribution:

$$2C_2(F) \sum_{\alpha,\beta} \int\limits_{BZ} \frac{d^4p}{(2\pi)^4} \int\limits_{-\pi}^{\pi} \frac{dq_4}{2\pi} \frac{\sin^2(p_3\hat{R}/2)\sin(p_4\hat{T}/2)\sin(q_4\hat{T}/2)}{\hat{p}^2\left(\hat{\vec{p}}^2 + \hat{q}_4^2\right)}$$
$$\frac{\delta_{3\alpha} - \delta_{4\alpha}}{\sin(p_\alpha/2)} \frac{\delta_{3\beta} - \delta_{4\beta}}{\sin(q_\beta/2)} \Pi_{\alpha\beta}^{L_s}(\vec{p}, p_4, q_4), \tag{4.64}$$

where Π^{L_s} represents the vacuum polarization tensor with $L_s^{(0)}$ inserted into one of its internal lines respectively the two contributions with the vertex insertions $L_s^{(1)}$ or $L_s^{(2)}$. In the limit $\hat{T} \to \infty$, this reduces to:

$$2C_2(F) \sum_{\alpha,\beta} \int\limits_{BZ} \frac{d^3p}{(2\pi)^3} \frac{\sin^2(p_3\hat{R}/2)}{\left(\hat{\vec{p}}^2\right)^2} \Pi_{44}^{L_s}(\vec{p}, 0, 0). \tag{4.65}$$

Now first look at the gluon tadpole graph. The contribution coming from this graph is proportional to:

$$\sum_{\rho,\lambda} \int\limits_{BZ} \frac{d^4r}{(2\pi)^4} \int\limits_{BZ} \frac{d^4s}{(2\pi)^4} (2\pi)^4 (p+q+r+s) \Gamma_{\mu\nu\rho\lambda}^{ABCD}(p,q,r,s) \frac{(2\pi)^3\delta(\vec{r}+\vec{s})}{\hat{r}^2\left(\hat{\vec{r}}^2 + \hat{s}_4^2\right)}$$
$$\delta_\rho^s \left(\delta_{\rho\lambda}\hat{r}^2 - \hat{r}_\rho\hat{r}_\lambda\right) \delta_\lambda^s, \tag{4.66}$$

where again the Delta-function coming from the four-gluon vertex has been extraced explicitly from Γ. Now split this four-dimensional Delta-function up into a three-dimensional spatial Delta-function and another for the temporal components. Additionally, as explained above, it suffices to look at the special case $p_4 = q_4 = 0$:

$$\int\limits_{BZ} \frac{d^4r}{(2\pi)^4} \int\limits_{BZ} \frac{d^4s}{(2\pi)^4} (2\pi)^3 (\vec{p}+\vec{q}+\vec{r}+\vec{s}) (2\pi)\delta(r_4+s_4) \frac{(2\pi)^3\delta(\vec{r}+\vec{s})}{\hat{r}^2\left(\hat{\vec{r}}^2 + \hat{s}_4^2\right)}$$
$$\sum_{\rho,\lambda} \Gamma_{\mu\nu\rho\lambda}^{ABCD}((\vec{p},0),(\vec{q},0),r,s) \delta_\rho^s \left(\delta_{\rho\lambda}\hat{r}^2 - \hat{r}_\rho\hat{r}_\lambda\right) \delta_\lambda^s.$$

Carrying out the four s-integrations, using the second and third Delta-function, gives:

$$\sum_{\rho,\lambda} \int_{BZ} \frac{d^4r}{(2\pi)^4}(2\pi)^3(\vec{p}+\vec{q})\Gamma^{ABCD}_{\mu\nu\rho\lambda}((\vec{p},0),(\vec{q},0),r,-r)\delta^s_\rho \frac{\delta_{\rho\lambda}\hat{r}^2 - \hat{r}_\rho\hat{r}_\lambda}{(\hat{r}^2)^2}\delta^s_\lambda. \quad (4.67)$$

If one compares this with the result one would have obtained if one would have inserted the sum over *all* spatial plaquettes $S_s^{(0)}$, using (4.13), and then looking again only at $p_4 = q_4 = 0$ (the only important part for $\hat{T} \to \infty$), one sees that one gets exactly the same result, and therefore:

$$\lim_{\hat{T}\to\infty} < L_s^{(0)}\omega^{(2)}S^{(2)} >_{conn} = \lim_{\hat{T}\to\infty} \frac{1}{\hat{T}} < S_s^{(0)}\omega^{(2)}S^{(2)} >_{conn} \quad (4.68)$$

holds, if only the insertion into the *internal* line is considered. But above it already had been shown that an insertion of $L_s^{(0}$ into an *external* line gives for $\hat{T} \to \infty$ the same result as an insertion of $S_s^{(0)}$—therefore the result is finally that an insertion of $L_s^{(0}$ into *any* line of the gluon tadpole graph is equivalent to an insertion of $S_s^{(0)}$ in the limit of large $\hat{T}$.

Exactly the same arguments can be made for the graph where $L_s^{(0)}$ is inserted into any line of the gluon loop graph. There one obtains:

$$\lim_{\hat{T}\to\infty} < L^{(0)}\omega^{(2)}\left(S^{(1)}\right)^2 >_{conn} = \lim_{\hat{T}\to\infty} \frac{1}{\hat{T}} < S^{(0)}\omega^{(2)}\left(S^{(1)}\right)^2 >_{conn} . \quad (4.69)$$

So, summarizing, for the vacuum polarization graphs with an insertion, the result is:

$$\begin{aligned} & \lim_{\hat{T}\to\infty} \Big(- < L_s^{(0)}\omega^{(2)}S^{(2)} >_{conn} + < L_s^{(0)}\omega^{(2)}\frac{1}{2}\left(S^{(1)}\right)^2 >_{conn} \\ & - < L_s^{(0)}\omega^{(2)}S^{(2)}_{FP} >_{conn} - < L_s^{(0)}\omega^{(2)}S^{(2)}_{meas} >_{conn} \Big) \\ = & \lim_{\hat{T}\to\infty} \frac{1}{\hat{T}} \Big(- < S_s^{(0)}\omega^{(2)}S^{(2)} >_{conn} + < S_s^{(0)}\omega^{(2)}\frac{1}{2}\left(S^{(1)}\right)^2 >_{conn} \\ & - < S_s^{(0)}\omega^{(2)}S^{(2)}_{FP} >_{conn} - < S_s^{(0)}\omega^{(2)}S^{(2)}_{meas} >_{conn} \Big), \end{aligned} \quad (4.70)$$

where now insertions into *all* gluon lines are allowed.

What remains are the two additional vacuum polarization graphs, incorporating $L_s^{(1)}$ and $L_s^{(2)}$, analogous to the first two graphs in figure 3.3, but with the sum over the plaquettes restricted to a *fixed* time slice. The operators $L_s^{(1)}$ and $L_s^{(2)}$ both only contain *spatial* links, but in the limit of large $\hat{T}$, only the $4-4-$component of the vacuum polarization tensor Π contributes - hence the contributions of these graphs vanish in the limit:

$$\lim_{\hat{T}\to\infty} < L_s^{(1)}S^{(1)}\omega^{(2)} >_{conn} = \lim_{\hat{T}\to\infty} < L_s^{(2)}\omega^{(2)} >_{conn} = 0. \quad (4.71)$$

Again that is identical to the results one obtains if one had inserted S_s instead of L_s, divided by $\hat{T}$ and taken the limit:

$$\lim_{\hat{T}\to\infty} \frac{< S_s^{(1)} S^{(1)} \omega^{(2)} >_{conn}}{\hat{T}} = \lim_{\hat{T}\to\infty} \frac{< S_s^{(2)} \omega^{(2)} >_{conn}}{\hat{T}} = 0. \tag{4.72}$$

Therefore one sees that for *all* vacuum polarization graphs, in the limit of large $\hat{T}$, the contributions coming from an insertion of S_s (and dividing by $\hat{T}$) are exactly the same as the contributions coming from an insertion of L_s, so for these graphs, the restriction to one fixed time slice works.

The spider graphs

In section 4.2.2, it was seen that the two spider graphs do not contribute in the limit of large $\hat{T}$. Therefore if one calculates them with L_s instead of S_s, their contributions should also go to zero.

For the first spider graph, corresponding to $< L_s^{(1)} \omega^{(3)} >_{conn}$, one can use the same argument as in section 4.2.2: $L_s^{(1)}$ contains a (slightly modified) three-gluon vertex, which connects only gluons with a spatial polarization with each other, and does not conserve the fourth component of the momentum. Using Feynman gauge, the polarizations of the gluons at the vertex are the same as the one on the Wilson loop; and because there is only one spatial direction available on the Wilson loop, all three gluons meeting at the vertex have the *same* polarization. But for three gluons with the same polarization, the three-gluon vertex vanishes - hence the result is simply:

$$< L_s^{(1)} \omega^{(3)} >_{conn} = 0 \tag{4.73}$$

- and that is equal to the result for $< S_s^{(1)} \omega^{(3)} >_{conn}$. Thus obviously one has

$$\lim_{\hat{T}\to\infty} \frac{1}{\hat{T}} < S_s^{(1)} \omega^{(3)} >_{conn} = \lim_{\hat{T}\to\infty} < L_s^{(1)} \omega^{(3)} >_{conn} . \tag{4.74}$$

The treatment of the second spider graph is more complicated; it has to be calculated explicitly. Fortunately one can use the results of section 3.4.2 for this; using that here only *spatial* plaquettes are inserted, the formula obtained there simplifies considerably, so that in the end one gets:

$$\begin{aligned} & < L_s^{(0)} S^{(1)} \omega^{(3)} > \\ \sim & \int_{BZ} \frac{d^4p}{(2\pi)^4} \int_{BZ} \frac{d^4k}{(2\pi)^4} \int_{-\pi}^{\pi} \frac{dq_4}{2\pi} \sin(p_3 \hat{R}/2) \sin(p_4 \hat{T}/2) \\ & \left[2i \frac{\widehat{(p+2k)}_4 \cos(p_3/2) \sum_{j\neq\mu} \widehat{(p+k)}_j^2}{\hat{p}^2 \hat{k}^2 \widehat{(p+k)}^2 \left(\left(\widehat{\vec{p}+\vec{k}} \right)^2 + \hat{q}_4^2 \right)} \sin((k+q)_4 \hat{T}/2) O_R(p_3+k_3, -k_3) \right. \end{aligned}$$

$$
\begin{aligned}
&+2i\left(\frac{(\widehat{p+q})_4\cos((p+k)_3/2)\left(\hat{\vec{k}}^2-\hat{k}_3^2\right)+(2\widehat{p+k})_3\cos(q_4/2)\hat{\vec{k}}^2}{\hat{p}^2\hat{k}^2\left(\hat{\vec{k}}^2+\hat{q}_4^2\right)\left(\left(\widehat{\vec{p}+\vec{k}}\right)^2+\left(\widehat{p-q}\right)_4^2\right)}\right.\\
&\left.-\frac{\sum_j(2\widehat{p+k})_j\hat{k}_j\hat{k}_3\cos(q_4/2)}{\hat{p}^2\hat{k}^2\left(\hat{\vec{k}}^2+\hat{q}_4^2\right)\left(\left(\widehat{\vec{p}+\vec{k}}\right)^2+\left(\widehat{p-q}\right)_4^2\right)}\right)\\
&\cdot\frac{\sin(k_3\hat{R}/2)}{\sin(k_3/2)}\frac{\sin((p-q)_4\hat{T}/2)}{\sin((p-q)_4/2)}\cos((p+k)_3\hat{R}/2)\cos(k_4\hat{T}/2)\\
&+2i\left(\frac{(2\widehat{p+k})_3\cos(k_3/2)\hat{k}_3^2-\sum_j(2\widehat{p+k})_j\hat{k}_j\hat{k}_3\cos(k_3/2)}{\hat{p}^2\hat{k}^2\left(\hat{\vec{k}}^2+\hat{q}_4^2\right)\left(\left(\widehat{\vec{p}+\vec{k}}\right)^2+\left(\widehat{p-q}\right)_4^2\right)}\right.\\
&\left.-\frac{(\widehat{p-2q})_4\cos(p_3/2)\left(\hat{\vec{k}}^2-\hat{k}_3^2\right)}{\hat{p}^2\hat{k}^2\left(\hat{\vec{k}}^2+\hat{q}_4^2\right)\left(\left(\widehat{\vec{p}+\vec{k}}\right)^2+\left(\widehat{p-q}\right)_4^2\right)}\right)\\
&\cdot\sin((k+q-p)_4\hat{T}/2)O_R(p_3+k_3,-k_3)\\
&-2i\frac{(\widehat{k+q})_4\cos((p+k)_3/2)\left(\hat{\vec{p}}^2-\hat{p}_3^2\right)}{\hat{p}^2\hat{k}^2\left(\hat{\vec{p}}^2+\hat{q}_4^2\right)\left(\left(\widehat{\vec{p}+\vec{k}}\right)^2+\left(\widehat{k-q}\right)_4^2\right)}\frac{\sin(k_3\hat{R}/2)}{\sin(k_3/2)}\frac{\sin((k-q)_4\hat{T}/2)}{\sin((k-q)_4/2)}\\
&\cdot\cos((p+k)_3\hat{R}/2)\cos(k_4\hat{T}/2)\Big].
\end{aligned}
\tag{4.75}
$$

A careful analysis of the individual terms reveals that for large $\hat{T}$, all of them go to zero, so that one indeed gets:

$$
\lim_{\hat{T}\to\infty}\frac{1}{\hat{T}}<S_s^{(0)}S^{(1)}\omega^{(3)}>_{conn}=\lim_{\hat{T}\to\infty}<L_s^{(0)}S^{(1)}\omega^{(3)}>_{conn}=0. \tag{4.76}
$$

The graphs with two independent gluon lines

There are again two graphs to consider here: first, the disconnected one, corresponding to $<L_s^{(0)}\omega^{(2)}>_{conn}<\omega^{(2)}>_0$, and second the one containing $\omega^{(4)}$. But using the results obtained in leading order, where it was shown that $<L_s^{(0)}\omega^{(2)}>_{conn}=0$, the disconnected contribution vanishes. In the same way, one can show that

$$
<L_s^{(0)}\omega^{(4A)}>_{conn}=0.
$$

For the remaining graphs, it is convenient to distinguish between the following three classes again, as already in section 4.2.2. The argumentation is also very similar:

1. Graphs in which only temporal links of the Wilson loop appear; these links can not be connected with the spatial plaquettes using the gluon propagators in Feynman gauge, and therefore their contributions vanish.

2. Graphs in which only spatial links of the Wilson loop appear; these will be discussed below. The relevant parts of $\omega^{(4)}$ will be denoted by $\omega^{(4)}_{RR}$.

3. Graphs in which temporal as well as spatial links appear - these are the most complicated ones and will be also discussed below. The relevant parts of $\omega^{(4)}$ will be denoted by $\omega^{(4)}_{RT}$.

As usual, $\omega^{(4)}$ is split into the parts B to F (part A has already been treated above), and as usual, $\omega^{(4F)}$ gives no contribution at all.

Here again the results from section 3.4.2 can be used, but because only spatial plaquettes are inserted, the formulas simplify considerably. The graphs of the second category give the following result:

$$
\begin{aligned}
& < L_s^{(0)} \omega_{RR}^{(4B)} > \\
= \; & -\frac{C_2(G)C_2(F)}{2} \int\limits_{BZ} \frac{d^4p}{(2\pi)^4} \int\limits_{BZ} \frac{d^4k}{(2\pi)^4} \int\limits_{-\pi}^{\pi} \frac{dq_4}{2\pi} \frac{1}{\hat{k}^2} \frac{\hat{\vec{p}}^2 - \hat{p}_3^2}{\hat{p}^2 \left(\hat{\vec{p}}^2 + \hat{q}_4^2\right)} \\
& \cdot \Bigg[\sin((k-p)_4\hat{T}/2) \sin((k+q)_4\hat{T}/2) \frac{\sin^2(p_3\hat{R}/2)}{\sin^2(p_3/2)} \frac{\sin^2(k_3\hat{R}/2)}{\sin^2(k_3/2)} \\
& + 4 \sin((p+k)_4\hat{T}/2) \sin((q-k)_4\hat{T}/2) O_R^2(p_3,k_3) \Bigg] \qquad (4.77) \\
& < L_s^{(0)} \omega_{RR}^{(4C)} > \\
= \; & \frac{C_2(F)C_2(G)}{2} \int\limits_{BZ} \frac{d^4p}{(2\pi)^4} \int\limits_{BZ} \frac{d^4k}{(2\pi)^4} \int\limits_{-\pi}^{\pi} \frac{dq_4}{2\pi} \frac{1}{\hat{k}^2} \frac{\hat{\vec{p}}^2 - \hat{p}_3^2}{\hat{p}^2 \left(\hat{\vec{p}}^2 + \hat{q}_4^2\right)} \\
& \cdot \sin^2(k_4\hat{T}/2) \frac{\sin(k_3\hat{R}/2)}{\sin(k_3/2)} \cos(p_4\hat{T}/2) \cos(q_4\hat{T}/2) \qquad (4.78) \\
& \cdot \Bigg[2 \left(\Sigma_1 - \Sigma_2\right)|_{p_3 \leftrightarrow k_3} + \frac{\sin(k_3\hat{R}/2)}{\sin(k_3/2)} \Sigma_R(p_3,-p_3) + \frac{\sin(p_3\hat{R}/2)}{\sin(p_3/2)} \Sigma_R(p_3,k_3) \Bigg] \\
& < L_s^{(0)} \omega_{RR}^{(4D)} > \\
= \; & \frac{C_2(F)C_2(G)}{6} \int\limits_{BZ} \frac{d^4p}{(2\pi)^4} \int\limits_{BZ} \frac{d^4k}{(2\pi)^4} \int\limits_{-\pi}^{\pi} \frac{dq_4}{2\pi} \frac{1}{\hat{k}^2} \frac{\hat{\vec{p}}^2 - \hat{p}_3^2}{\hat{p}^2 \left(\hat{\vec{p}}^2 + \hat{q}_4^2\right)} \\
& \cdot \sin^2(k_4\hat{T}/2) \frac{\sin(k_3\hat{R}/2)}{\sin(k_3/2)} \cos(p_4\hat{T}/2) \cos(q_4\hat{T}/2) \\
& \cdot \Bigg[2 \left(\Sigma_1 - \Sigma_2\right)|_{p_3 \leftrightarrow k_3} + 2\,\Sigma_R(0,-k_3) - 2\,\Sigma_R(p_3-k_3,-p_3) \\
& + 2 \frac{\sin(k_3\hat{R}/2)}{\sin(k_3/2)} \frac{\sin^2(p_3\hat{R}/2)}{\sin^2(p_3/2)} - \frac{\sin(p_3\hat{R}/2)}{\sin(p_3/2)} \Sigma_R(p_3,k_3)
\end{aligned}
$$

$$+\frac{\sin(k_3\hat{R}/2)}{\sin(k_3/2)}\Sigma_R(p_3,-p_3)\Big] \tag{4.79}$$

$$< L_s^{(0)}\omega_{RR}^{(4E)} >$$

$$= \frac{C_2(F)C_2(G)}{6}\int\limits_{BZ}\frac{d^4p}{(2\pi)^4}\int\limits_{BZ}\frac{d^4k}{(2\pi)^4}\int\limits_{-\pi}^{\pi}\frac{dq_4}{2\pi}\frac{1}{\hat{k}^2}\frac{\hat{\vec{p}}^2-\hat{p}_3^2}{\hat{p}^2\left(\hat{\vec{p}}^2+\hat{q}_4^2\right)}$$

$$\cdot\cos(p_4\hat{T}/2)\cos(q_4\hat{T}/2)\sin^2(k_4\hat{T}/2)\frac{\sin(k_3\hat{R}/2)}{\sin(k_3/2)}\Big[\frac{\sin(k_3\hat{R}/2)}{\sin(k_3/2)}\hat{R}$$

$$+\frac{\sin(k_3\hat{R}/2)}{\sin(k_3/2)}\frac{\sin(p_3\hat{R}/2)}{\sin(p_3/2)}\frac{\sin((p+k)_3\hat{R}/2)}{\sin((p+k)_3/2)}\Big]. \tag{4.80}$$

Because of the fast oscillations of the two cosines for $\hat{T}\to\infty$, the contributions of these integrals vanish in the limit of large $\hat{T}$. On the other hand, the graphs of the third category give:

$$< L_s^{(0)}\omega_{RT}^{(4B)} >$$

$$= -\frac{C_2(G)C_2(F)}{2}\int\limits_{BZ}\frac{d^4p}{(2\pi)^4}\int\limits_{BZ}\frac{d^4k}{(2\pi)^4}\int\limits_{-\pi}^{\pi}\frac{dq_4}{2\pi}\frac{1}{\hat{k}^2}\frac{\hat{\vec{p}}^2-\hat{p}_3^2}{\hat{p}^2\left(\hat{\vec{p}}^2+\hat{q}_4^2\right)}$$

$$\cdot\frac{\sin^2(p_3\hat{R}/2)}{\sin^2(p_3/2)}\frac{\sin^2(k_4\hat{T}/2)}{\sin^2(k_4/2)}\cos(p_4\hat{T}/2)\cos(q_4\hat{T}/2) \tag{4.81}$$

$$< L_s^{(0)}\omega_{RT}^{(4C)} >$$

$$= \frac{C_2(G)C_2(F)}{2}\int\limits_{BZ}\frac{d^4p}{(2\pi)^4}\int\limits_{BZ}\frac{d^4k}{(2\pi)^4}\int\limits_{-\pi}^{\pi}\frac{dq_4}{2\pi}\frac{1}{\hat{k}^2}\frac{\hat{\vec{p}}^2-\hat{p}_3^2}{\hat{p}^2\left(\hat{\vec{p}}^2+\hat{q}_4^2\right)}$$

$$\cdot\Big[\frac{\sin^2(k_4\hat{T}/2)}{\sin^2(k_4/2)}\sin^2(k_3\hat{R}/2)\cos(p_4\hat{T}/2)\cos(q_4\hat{T}/2)\Sigma_R(p_3,-p_3)$$

$$+\frac{\sin^2(k_4\hat{T}/2)}{\sin^2(k_4/2)}\sin^2(k_3\hat{R}/2)\cos(p_4\hat{T}/2)\cos(q_4\hat{T}/2)\frac{\sin^2(p_3\hat{R}/2)}{\sin^2(p_3/2)}\Big] \tag{4.82}$$

$$< L_s^{(0)}\omega_{RT}^{(4D)} >$$

$$= \frac{C_2(G)C_2(F)}{6}\int\limits_{BZ}\frac{d^4p}{(2\pi)^4}\int\limits_{BZ}\frac{d^4k}{(2\pi)^4}\int\limits_{-\pi}^{\pi}\frac{dq_4}{2\pi}\frac{1}{\hat{k}^2}\frac{\hat{\vec{p}}^2-\hat{p}_3^2}{\hat{p}^2\left(\hat{\vec{p}}^2+\hat{q}_4^2\right)}$$

$$\cdot\Big[-\frac{\sin^2(k_4\hat{T}/2)}{\sin^2(k_4/2)}\sin^2(k_3\hat{R}/2)\cos(p_4\hat{T}/2)\cos(q_4\hat{T}/2)\Sigma_R(p_3,-p_3)$$

$$+2\frac{\sin^2(k_4\hat{T}/2)}{\sin^2(k_4/2)}\sin^2(k_3\hat{R}/2)\cos(p_4\hat{T}/2)\cos(q_4\hat{T}/2)\frac{\sin^2(p_3\hat{R}/2)}{\sin^2(p_3/2)}\Big] \tag{4.83}$$

$$< L_s^{(0)}\omega_{RT}^{(4E)} >$$

$$= \frac{C_2(G)C_2(F)}{6}\int\limits_{BZ}\frac{d^4p}{(2\pi)^4}\int\limits_{BZ}\frac{d^4k}{(2\pi)^4}\int\limits_{-\pi}^{\pi}\frac{dq_4}{2\pi}\frac{1}{\hat{k}^2}\frac{\hat{\vec{p}}^2-\hat{p}_3^2}{\hat{p}^2\left(\hat{\vec{p}}^2+\hat{q}_4^2\right)}$$

$$\cdot \frac{\sin^2(k_4\hat{T}/2)}{\sin^2(k_4/2)} \sin^2(k_3\hat{R}/2)\cos(p_4\hat{T}/2)\cos(q_4\hat{T}/2)\hat{R}. \tag{4.84}$$

As already pointed out in section 3.4.2, for $\hat{T} \to \infty$, the factor $\frac{\sin^2(k_4\hat{T}/2)}{\sin^2(k_4/2)}$ gives a linear dependence on $\hat{T}$, but the two cosines both give factors of $\hat{T}^{-1}$, so that in total all of these integrals go with $\hat{T}^{-1}$ in the limit and hence vanish. Thus one gets:

$$\lim_{\hat{T}\to\infty} < L_s^{(0)}\omega^{(4)} > = \lim_{\hat{T}\to\infty} \frac{< S_s^{(0)}\omega^{(4)} >}{\hat{T}} = 0. \tag{4.85}$$

Taking together all of the results obtained in the last subsections, one sees that indeed

$$\lim_{\hat{T}\to\infty} < L_s >_{q\bar{q}-0} = \lim_{\hat{T}\to\infty} \frac{< S_s >_{q\bar{q}-0}}{\hat{T}} \tag{4.86}$$

is satisfied up to next-to-leading order—up to that order, the restriction to one fixed time slice works for the spatial plaquettes. Thus the check of the energy sum rule is now completed.

Chapter 5

Summary

In this work, it was shown that in lattice perturbation theory, both sum rules, (1.12) and (1.23), hold up to next-to-leading order in the coupling constant. Additionally, the possibility to restrict the expectation value of the action and the expectation value of the magnetic field energy to the sum of the plaquettes on a fixed time slice has been investigated. Two spin-offs of the check were a proof of the transversality of the gluonic vacuum polarization on the lattice in leading order and a proof of the gauge invariance of the expectation value of the Wilson loop up to next-to-leading order. This is not completely obvious, since gauge transformations on the lattice are implemented via unitary transformations of the link variables.

The scaling behaviour of the potential which is used in the derivation of the action sum rule was checked explicitly by using known results for the potential [30, 39, 34]. The crucial part of this sum rule is the identity (1.7) respectively (3.5). The perturbative examination of this identity yielded methods and valuable results which could be used in the examination of the energy sum rule.

Additionally, it opened up a way to proof the gauge invariance of the expectation value of the Wilson loop perturbatively up to next-to-leading order. By expressing this expectation value as a polynomial with respect to the gauge parameter, it was possible to show that its dependance on the gauge parameter vanishes in all orders of the gauge parameter and up to next-to-leading order of the coupling constant. For eliminating the dependance on the gauge parameter in first order, the action sum rule could be used.

The examination of the restriction of the expectation value of the action to one fixed time slice (the possibility to replace this expectation value by $\hat{T}$ times the expectation value of the Lagrangian, the sum of all plaquettes on a fixed time slice) turned out to be much more difficult. It was first shown that this is possible in leading order. For the graphs in next-to-leading order, this was accomplished for the vacuum polarization graphs, the spider graphs and some of the graphs with two independent gluon lines; work on the rest is still in progress. The eight- and nine-dimensional integrals have to be evaluated numerically, and that requires lots of computer time.

On the other hand, all parts of the energy sum rule were shown to be true up

to next-to-leading order: first it was checked without the restriction to a fixed time slice. It was shown that both the expectation value of the magnetic field energy and the contribution from the trace anomaly vanish in leading order, so that the only contribution to the potential in that order stems from the energy in the electric fields.

In next-to-leading order it turned out that the expectation value of the (euclidean) energy in the magnetic fields receives its only contributions from the graphs in which the sum over the spatial plaquettes is inserted into internal lines of the gluonic vacuum polarization. By computing the contributions of these graphs numerically and examining the two parts of the potential with different group theoretical factors separately, the validity of the energy sum rule was confirmed with good numerical accuracy.

For the expectation value of the magnetic energy it was possible to show that it can be restricted to one fixed time slice. The leading order was again relatively easy and could be demonstrated and explained explicitly. In the next-to-leading order, similar arguments as before concerning the expectation value of the action could be used to take care of the vacuum polarization graphs. The contributions from the spider graphs and from the graphs with two independent gluon lines were calculated explicitly and shown to vanish, as expected.

Now the questions which were posed in the introduction can be addressed using the results obtained in the checks. Unfortunately the conclusions which were obtained here are not very helpful because they apply only if the coupling constant is small enough to allow perturbation theory to give sensible results. In contrast, in real physical systems like mesons, the coupling constant is large and perturbation theory breaks down. But the proven validity of the sum rules in the small coupling regime suggests that they are true also in the non-perturbative region, hence it it still possible to draw some sensible conclusions from the results.

The first interesting point to notice is that there are cancellations between the expectation values of the energy in the electric and in the magnetic fields: the (euclidean) electric field energy is always negative, the magnetic field energy is positive. This is true for both contributions (with different group theoretical factors) to the potential. But here the magnitude of the magnetic field energy is much smaller than the magnitude of the electric field energy, in contrast to Monte Carlo simulations in the non-perturbative regime where they both have comparable sizes. Hence the problem of large cancellations between these two contributions which appears in these simulations does not appear in the weak coupling limit.

Another result is that the trace anomaly contributes only a very small part to the potential for large quark-antiquark separations; this is in strong contrast to the case of a confining potential, where it contributes exactly one half of the potential energy!

To close, I will give an outlook to the open problems, possible extensions and future projects. Now that the sum rules have been checked perturbatively in

the regime of a small coupling constant, one should use Monte Carlo simulations in order to perform a check in the physical regime of large coupling constant. There the same questions will be interesting as investigated here: the problem of cancellations between the contributions from the magnetic and electric field energies and the contribution of the trace anomaly, which is expected to have the same magnitude as the energy in the fields in the confining region. Additionally, a look at the sum rule for the glueball mass would be interesting.

Another promising approach is using a nonperturbative model like the stochastic vacuum model of Dosch and Sominov [43]. A recent calculation of the quark-antiquark potential in this model and subsequent comparison with the predictions of the lattice sum rules gave good consistency [44].

On the other hand, one could use the sum rules to check the consistency of the results obtained in Monte Carlo simulations. One first step in this direction was done already in [29], where a (corrected) version of Michael's action sum rule was used.

A possible extension is the incorporation of dynamical fermions into the sum rules, so that one could study the effects of string breaking more closely. Alternatively the sum rules could be investigated for finite temperature, which should shed some light on the phase transition to the quark-gluon plasma.

Hence there is much potential for future work on the lattice sum rules, and lots of additional interesting results can be expected.

Appendix A

General SU(N) formulas

A.1 Basics

The Lie group $G = SU(N)$ has $N^2 - 1$ generators. In the fundamental representation of the group $SU(N)$, these generators, denoted by T^A, are given by hermitian, traceless, complex $N \times N$ matrices. They obey the following basic commutation and anticommutation relations:

$$[T^A, T^B] = i \sum_C f_{ABC} T^C \tag{A.1}$$

$$\{T^A, T^B\} = \frac{1}{d(F)} \delta^{AB} i d_{d(R)} + \sum_C d_{ABC} T^C, \tag{A.2}$$

where $d(F) = N$ is the dimension of the fundamental representation F and $id_{d(F)}$ denotes the $d(F)$-dimensional identity matrix. The real numbers f_{ABC} are called *structure constants*.

In the adjoint representation, the generators are denoted by t^A and are given by complex $(N^2 - 1) \times (N^2 - 1)$ matrices, whose elements are:

$$\left(t^A\right)_{BC} = -i f_{ABC}. \tag{A.3}$$

A.2 Traces

For the generators T^A in any representation R, one always has:

$$\mathrm{Tr}(T^A T^B) = T(R) \delta^{AB} \tag{A.4}$$

with a constant $T(R)$ depending on the representation. For the fundamental representation, $T(R)$ is simply $\frac{1}{2}$; for the adjoint representation, it is N. Using this and the commutators and anticommutators given above, one gets:

$$\mathrm{Tr}(T^A T^B) = \frac{1}{2} \delta^{AB} \tag{A.5}$$

$$\mathrm{Tr}(T^A T^B T^C) = \frac{1}{4}(d_{ABC} + i f_{ABC}) \tag{A.6}$$

$$\mathrm{Tr}(T^A T^B T^C T^D) = \frac{1}{4d(F)} \delta_{AB} \delta_{CD} - \frac{1}{8} \sum_E (f_{ABE} f_{CDE} - d_{ABE} d_{CDE})$$

$$+\frac{i}{8}\sum_E (f_{ABE}d_{CDE} + d_{ABE}f_{CDE}) \tag{A.7}$$

$$\mathrm{Tr}(t^A t^B) = N\delta_{AB}. \tag{A.8}$$

A.3 Sums

For any representation R, the quadratic Casimir operator $C_2(R)$ is defined by

$$\sum_A T^A T^A =: C_2(R) i d_{d(R)}. \tag{A.9}$$

In the special case of the fundamental representation F, one gets

$$C_2(F) = \frac{N^2-1}{2N}, \tag{A.10}$$

and for the adjoint representation G:

$$C_2(G) = N. \tag{A.11}$$

Additionally, the following relation holds for every representation R:

$$T(R) = \frac{C_2(R)d(R)}{d(G)}, \tag{A.12}$$

where $d(G)$ is the dimension of the adjoint representation, which is equal to the order of the group, i. e. the number of its generators. Hence for $SU(N)$, the formula gives:

$$T(R) = \frac{C_2(R)d(R)}{N^2-1}. \tag{A.13}$$

This agrees with the results for $T(R)$ given above for the fundamental as well as the adjoint representation.

Using the formulas given above and the symmetry respectively anti-symmetry of the structure constants and the d_{ABC}, the following sums can be evaluated:

$$\sum_A d_{AAB} = 0 \tag{A.14}$$

$$\sum_{D,E} f_{ADE}f_{CDE} = C_2(G)\delta_{AC} = N\delta_{AC} \tag{A.15}$$

$$\sum_{D,E} d_{ADE}f_{CDE} = 0 \tag{A.16}$$

$$\sum_{D,E} d_{ADE}d_{CDE} = \left(4C_2(F) - \frac{2}{d(F)} - C_2(G)\right)\delta_{AC} = \frac{N^2-4}{N}\delta_{AC} \tag{A.17}$$

$$\sum_{A,B,C} f_{ABC}f_{ABC} = C_2(G)d(G) = N(N^2-1) \tag{A.18}$$

$$\sum_{A,B,C} d_{ABC}f_{ABC} = 0 \tag{A.19}$$

$$\sum_{A,B,C} d_{ABC}d_{ABC} = d(G)\left(4C_2(F) - \frac{2}{d()} - C_2(G)\right) = \frac{(N^2-1)(N^2-4)}{N}. \tag{A.20}$$

Appendix B

Sums along the Wilson Loop

Some sums along the Wilson loop appear so often that it is convenient to summarize them here.

B.1 Unrestricted sums

The easiest sum is the one which contains only one vector potential:

$$\begin{aligned}
&\sum_l A_l \\
= &\sum_{l=0}^{\hat{R}-1} A_\mu(n_0 + l\hat{\mu}) + \sum_{l=0}^{\hat{T}-1} A_\nu(n_0 + \hat{R}\hat{\mu} + l\hat{\nu}) - \sum_{l=0}^{\hat{R}-1} A_\mu(n_0 + \hat{R}\hat{\mu} + \hat{T}\hat{\nu} - l\hat{\mu}) \\
&- \sum_{l=0}^{\hat{T}-1} A_\nu(n_0 + \hat{T}\hat{\nu} - l\hat{\nu})
\end{aligned} \tag{B.1}$$

Insert the Fourier representation for A:

$$A_\alpha(x) = \int_{BZ} \frac{d^4p}{(2\pi)^4} A_\alpha(p) e^{ipx + ip_{\alpha/2}}. \tag{B.2}$$

This yields:

$$\begin{aligned}
&\sum_l A_l \\
= &\sum_\alpha \int_{BZ} \frac{d^4p}{(2\pi)^4} A_\alpha(p) e^{ipn_0} \left(\delta_{\alpha\mu} \sum_{l=0}^{\hat{R}-1} e^{ip_\mu l + ip_\mu/2} + \delta_{\alpha\nu} \sum_{l=0}^{\hat{T}-1} e^{ip_\mu \hat{R} + ip_\nu l + ip_\nu/2} \right. \\
&\left. -\delta_{\alpha\mu} \sum_{l=0}^{\hat{R}-1} e^{ip_\mu \hat{R} + ip_\nu \hat{T} - ip_\mu l - ip_\mu/2} - \delta_{\alpha\nu} \sum_{l=0}^{\hat{T}-1} e^{ip_\nu \hat{T} - ip_\nu l - ip_\nu/2} \right) \\
= &\sum_\alpha \int_{BZ} \frac{d^4p}{(2\pi)^4} A_\alpha(p) e^{ipn_0} \left(\delta_{\alpha\mu} \frac{e^{ip_\mu \hat{R}} - 1}{2i \sin(p_\mu/2)} + \delta_{\alpha\nu} \frac{e^{ip_\nu \hat{T}} - 1}{2i \sin(p_\nu/2)} e^{ip_\mu \hat{R}} \right. \\
&\left. -\delta_{\alpha\mu} \frac{e^{-ip_\mu \hat{R}} - 1}{-2i \sin(p_\mu/2)} e^{ip_\mu \hat{R} + ip_\nu \hat{T}} - \delta_{\alpha\nu} \frac{e^{-ip_\nu \hat{T}} - 1}{-2i \sin(p_\nu/2)} e^{ip_\nu \hat{T}} \right)
\end{aligned}$$

$$
\begin{aligned}
&= \sum_\alpha \int\limits_{BZ} \frac{d^4p}{(2\pi)^4} A_\alpha(p) e^{ip(n_0+\hat{\mu}\hat{R}/2+\hat{\nu}\hat{T}/2)} \left[\delta_{\mu\alpha} \frac{\sin(p_\mu \hat{R}/2)}{\sin(p_\mu/2)} \left(e^{-ip_\nu \hat{T}/2} - e^{ip_\nu \hat{T}/2} \right) \right. \\
&\quad \left. -\delta_{\nu\alpha} \frac{\sin(p_\nu \hat{T}/2)}{\sin(p_\nu/2)} \left(e^{-ip_\mu \hat{R}/2} - e^{ip_\nu \hat{R}/2} \right) \right] \\
&= -2i \sum_\alpha \int\limits_{BZ} \frac{d^4p}{(2\pi)^4} \sin(p_\mu \hat{R}/2) \sin(p_\nu \hat{T}/2) e^{ip(n_0+\hat{\mu}\hat{R}/2+\hat{\nu}\hat{T}/2)} \frac{A_\alpha(p)(\delta_{\mu\alpha} - \delta_{\nu\alpha})}{\sin(p_\alpha/2)}
\end{aligned} \tag{B.3}
$$

Using this, one immediately gets:

$$
\sum_l < A_l^A A_\beta^B(x) >_0 \tag{B.4}
$$

$$
= -2i \int\limits_{BZ} \frac{d^4p}{(2\pi)^4} \frac{\sin(p_\mu \hat{R}/2) \sin(p_\nu \hat{T}/2)}{\tilde{p}^2} e^{ip(n_0+\hat{\mu}\hat{R}/2+\hat{\nu}\hat{T}/2-x)} \frac{\delta_{\mu\beta} - \delta_{\nu\beta}}{\sin(p_\beta/2)}
$$

$$
\sum_{l_1,l_2} < A_{l_1}^A A_{l_2}^B >_0 \tag{B.5}
$$

$$
= +4\delta^{AB} \int\limits_{BZ} \frac{d^4p}{(2\pi)^4} \frac{\sin^2(p_\mu \hat{R}/2) \sin^2(p_\nu \hat{T}/2)}{\tilde{p}^2} \left(\frac{1}{\sin^2(p_\mu/2)} + \frac{1}{\sin^2(p_\nu/2)} \right)
$$

The last sum is the main ingredient of $< \omega^{(2)} >_0$ and is also crucial for calculating the vacuum polarization graphs.

B.2 Restricted sums

The following sum appears in $\omega^{(3)}$ as well as several times in $\omega^{(4)}$ and thus is needed often:

$$
\begin{aligned}
\sum_{l_1<l_2} [A_{l_1}, A_{l_2}] \;=\; & \int\limits_{BZ} \frac{d^4q}{(2\pi)^4} \int\limits_{BZ} \frac{d^4k}{(2\pi)^4} [A_\beta(q), A_\gamma(k)] \, e^{i(q+k)(n_0+\hat{\mu}\hat{R}/2+\hat{\nu}\hat{T}/2)} \\
& \cdot \left[\left\{ -2\delta_{\beta\mu}\delta_{\gamma\mu} \sin((k+q)_\nu \hat{T}/2) O_T(k_\mu, q_\mu) \right. \right. \\
& + i\delta_{\beta\mu}\delta_{\gamma\mu} \frac{\sin(k_\mu \hat{R}/2) \sin(q_\mu \hat{R}/2)}{\sin(k_\mu/2) \sin(q_\mu/2)} \sin((k-q)_\nu \hat{T}/2) \\
& + \delta_{\beta\mu}\delta_{\gamma\nu} \frac{\sin(k_\nu \hat{T}/2) \sin(q_\mu \hat{R}/2)}{\sin(k_\nu/2) \sin(q_\mu/2)} \\
& \left. \cdot \left(\cos(q_\nu \hat{T}/2 - k_\mu \hat{R}/2) + i \sin(q_\nu \hat{T}/2 + k_\mu \hat{R}/2) \right) \right\} \\
& \left. - \left\{ \mu \leftrightarrow \nu, \hat{R} \leftrightarrow \hat{T} \right\} \right]
\end{aligned} \tag{B.6}
$$

Appendix C

Some common integrals

In several calculations, integrals of the form

$$\int_{BZ} \frac{d^4p}{(2\pi)^4} \frac{\hat{p}_\mu \hat{p}_\nu \dots}{(\hat{p}^2)^n} \tag{C.1}$$

appear. All of them can be evaluated exactly, leaving only one constant which has to be determined numerically up to $n = 2$, and an additional constant for $n = 3$. For convenience, all results here will be given for arbitrary dimension d as well as for the relevant case $d = 4$. Hence the denominator is in general given by:

$$\hat{p}^2 = \sum_{\mu=0}^{d} \hat{p}_\mu^2. \tag{C.2}$$

Now first, the three most elementary integrals are:

$$\int_{BZ} \frac{d^dp}{(2\pi)^d} \frac{\hat{p}_\mu^2}{\hat{p}^2} = \frac{1}{d} \tag{C.3}$$

$$\int_{BZ} \frac{d^dp}{(2\pi)^d} \frac{1}{\hat{p}^2} =: \Delta_0 \tag{C.4}$$

$$\int_{BZ} \frac{d^dp}{(2\pi)^d} \frac{\hat{p}_\mu}{\hat{p}^2} = 0, \tag{C.5}$$

the first following from the symmetry of the lattice, the third from the fact that the integrand is odd, and the second simply being a definition of the one remaining constant Δ_0. This constant can be calculated more easily by noting that the corresponding integral can be rewritten in the following way:

$$\begin{aligned} \int_{BZ} \frac{d^dp}{(2\pi)^d} \frac{1}{\hat{p}^2} &= \int_0^\infty dt \int_{BZ} \frac{d^dp}{(2\pi)^d} e^{-t\hat{p}^2} \\ &= \int_0^\infty dt \int_{BZ} \frac{d^dp}{(2\pi)^d} \exp\left(-4t \sum_{\mu=0}^{d} \sin^2(p_\mu/2)\right) \end{aligned}$$

$$
\begin{aligned}
&= \int_0^\infty dt \left(\int_{-\pi}^{\pi} \frac{dp}{2\pi} \exp\left(-4t \sin^2(p/2)\right) \right)^d \\
&= \int_0^\infty dt e^{-2td} \left(\int_{-\pi}^{\pi} \frac{dp}{2\pi} e^{-2t\cos(p)} \right)^d \\
&= \frac{1}{2} \int_0^\infty dt\, e^{-td} I_0^d(t), \qquad \text{(C.6)}
\end{aligned}
$$

where it has been used that the integral

$$\int_{-\pi}^{\pi} dx\, e^{-t\cos(x)}$$

gives 2π times the Bessel function $I_0(t)$. The remaining one-dimensional integral can be evaluated using numerical integration routines much more easily than the original d-dimensional one. In the relevant case $d = 4$, the explicit result is:

$$\Delta_0 \approx 0.154933. \qquad \text{(C.7)}$$

From these three elementary integrals, one immediately gets:

$$\int_{BZ} \frac{d^d p}{(2\pi)^d} \frac{\hat{p}_\mu^2}{(\hat{p}^2)^2} = \frac{1}{d} \Delta_0. \qquad \text{(C.8)}$$

The general idea to treat the more complicated integrals can be found in appendix B of [37]; they can be evaluated using partial integration. For example:

$$
\begin{aligned}
0 &= \int_{BZ} \frac{d^d p}{(2\pi)^d} \frac{\partial}{\partial p_\mu} \frac{\sin(p_\mu)}{\hat{p}^2} \\
&= \int_{BZ} \frac{d^d p}{(2\pi)^d} \left(\frac{\cos(p_\mu)}{\hat{p}^2} - \frac{\sin(p_\mu) \cdot 4 \sin(p_\mu/2) \cos(p_\mu/2)}{(\hat{p}^2)^2} \right) \\
&= \int_{BZ} \frac{d^d p}{(2\pi)^d} \left(\frac{1 - 2\sin(p_\mu/2)^2}{\hat{p}^2} - 8 \frac{\sin^2(p_\mu/2)\cos^2(p_\mu/2)}{(\hat{p}^2)^2} \right) \\
&= \int_{BZ} \frac{d^d p}{(2\pi)^d} \left(\frac{1 - \frac{1}{2}\hat{p}_\mu^2}{\hat{p}^2} - 2 \frac{\hat{p}_\mu^2 - \frac{1}{4}\hat{p}_\mu^4}{(\hat{p}^2)^2} \right) \qquad \text{(C.9)}
\end{aligned}
$$

and therefore, using the elementary integrals mentioned above:

$$\int_{BZ} \frac{d^d p}{(2\pi)^d} \frac{\hat{p}_\mu^4}{(\hat{p}^2)^2} = \frac{4 - 2d}{d} \Delta_0 + \frac{1}{d}. \qquad \text{(C.10)}$$

Now make again use of the symmetry of the lattice:

$$
\begin{aligned}
1 &= \int_{BZ} \frac{d^d p}{(2\pi)^d} \frac{(\hat{p}^2)^2}{(\hat{p}^2)^2} \\
&= d \int_{BZ} \frac{d^d p}{(2\pi)^d} \frac{\hat{p}_\mu^4}{(\hat{p}^2)^2} + (d^2 - d) \int_{BZ} \frac{d^d p}{(2\pi)^d} \frac{\hat{p}_\mu^2 \hat{p}_\nu^2}{(\hat{p}^2)^2}
\end{aligned}
$$

with $\mu \neq \nu$ in the second term. This gives:

$$\int\limits_{BZ} \frac{d^d p}{(2\pi)^d} \frac{\hat{p}_\mu^2 \hat{p}_\nu^2}{(\hat{p}^2)^2} = \frac{2d-4}{d(d-1)} \Delta_0 \qquad \text{for } \mu \neq \nu. \tag{C.11}$$

Using the same methods, all integrals of the type (C.1) can be evaluated. The results up to $n = 2$ are given here:

$$\begin{aligned} \int\limits_{BZ} \frac{d^d p}{(2\pi)^d} \frac{\hat{p}_\mu^2 \hat{p}_\nu^2}{(\hat{p}^2)^2} &= \delta_{\mu\nu} \left(\frac{4-2d}{d} \Delta_0 + \frac{1}{d} \right) + (1 - \delta_{\mu\nu}) \frac{2d-4}{d(d-1)} \Delta_0 \\ &= \delta_{\mu\nu} \left(-\Delta_0 + \frac{1}{4} \right) + (1 - \delta_{\mu\nu}) \frac{1}{3} \Delta_0 \\ &= \left(\frac{4-2d}{d-1} \Delta_0 + \frac{1}{d} \right) \delta_{\mu\nu} + \frac{2d-4}{d(d-1)} \Delta_0 \\ &= \left(-\frac{4}{3} \Delta_0 + \frac{1}{4} \right) \delta_{\mu\nu} + \frac{1}{3} \Delta_0 \end{aligned} \tag{C.12}$$

$$\int\limits_{BZ} \frac{d^d q}{(2\pi)^d} \frac{\widehat{(p+q)}^2}{\hat{q}^2} = \hat{p}^2 \left(\Delta_0 - \frac{1}{2d} \right) + 1. \tag{C.13}$$

For $n = 3$, one needs an additional constant, which is defined in the following way:

$$\Delta_1 := (d-4) \int\limits_{BZ} \frac{d^d p}{(2\pi)^d} \frac{1}{\left(\hat{p}^2\right)^2} \tag{C.14}$$

Then one gets the following results:

$$\int\limits_{BZ} \frac{d^d p}{(2\pi)^d} \frac{\hat{p}_\mu^2}{(\hat{p}^2)^3} = \frac{1}{d} \Delta_1 \tag{C.15}$$

$$\int\limits_{BZ} \frac{d^d p}{(2\pi)^d} \frac{\left(\hat{p}_\mu^2\right)^2}{(\hat{p}^2)^3} = \frac{1}{2d} \Delta_0 - \frac{1}{d} \Delta_1 \tag{C.16}$$

$$\int\limits_{BZ} \frac{d^d p}{(2\pi)^d} \frac{\hat{p}_\mu^2 \hat{p}_\nu^2}{(\hat{p}^2)^3} = \frac{1}{2d(d-1)} \Delta_0 + \frac{1}{d(d-1)} \Delta_1 \qquad \text{for } \mu \neq \nu \tag{C.17}$$

$$\int\limits_{BZ} \frac{d^d p}{(2\pi)^d} \frac{\left(\hat{p}_\mu^2\right)^3}{(\hat{p}^2)^3} = \frac{3-2d}{d} \Delta_0 + \frac{1}{d} - \frac{4}{d} \Delta_1 \tag{C.18}$$

$$\int\limits_{BZ} \frac{d^d p}{(2\pi)^d} \frac{\left(\hat{p}_\mu^2\right)^2 \hat{p}_\nu^2}{(\hat{p}^2)^3} = \frac{1}{d(d-1)} \Delta_0 + \frac{4}{d(d-1)} \Delta_1 \qquad \text{for } \mu \neq \nu \tag{C.19}$$

$$\int\limits_{BZ} \frac{d^d p}{(2\pi)^d} \frac{\hat{p}_\mu^2 \hat{p}_\nu^2 \hat{p}_\lambda^2}{(\hat{p}^2)^3} = \frac{2d-6}{d(d-1)(d-2)} \Delta_0 - \frac{8}{d(d-1)(d-2)} \Delta_1 \tag{C.20}$$

$$\text{for } \mu \neq \nu \neq \lambda$$

For $d \to 4$, the additional constant Δ_1 can be calculated exactly by extracting the infrared divergence: The integral

$$\int_{BZ} \frac{d^d p}{(2\pi)^d} \frac{1}{(\hat{p}^2)^2}$$

is divergent for $p \to 0$. But in that limit, $\hat{p}^2$ can be replaced by p^2:

$$\lim_{d\to 4} \Delta_1 = \lim_{d\to 4} (d-4) \int_{BZ} \frac{d^d p}{(2\pi)^d} \frac{1}{(p^2)^2}.$$

Additionally, the region of integration can be restricted to a (small) sphere around the origin:

$$\lim_{d\to 4} \Delta_1 = \lim_{d\to 4} (d-4) \int d\Omega_d \int_0^R p^{d-1} \frac{dp}{(2\pi)^d} \frac{1}{p^4} = \lim_{d\to 4} \frac{\Omega_d}{(2\pi)^d} R^{d-4},$$

where Ω_d is the surface of the d-dimensional sphere. Taking the limit and inserting the explicit value $\Omega_4 = \frac{1}{2}(2\pi)^2$, one finally gets:

$$\lim_{d\to 4} \Delta_1 = \frac{1}{2(2\pi)^2}. \tag{C.21}$$

Appendix D

Fourier transform of the potential

In section 2.1, the following expression for the quark-antiquark potential in momentum space was given:

$$\begin{aligned} V(\vec{q}^2) &= -\frac{g_0^2(a)}{\vec{q}^2} C_2(F) \\ &\quad \cdot \left[1 + g_0^2(a) \left[\beta_0 \left(\ln \frac{\pi^2}{a^2 \vec{q}^2} - \gamma + \frac{31}{33} \right) - \frac{\bar{A}(1,0,N)}{4\pi} + R(N) \right] \right]. \end{aligned} \tag{D.1}$$

In order to get the dependance of the potential on $\hat{R}$, one has to perform a Fourier transformation. In the literature usually only the result is given; here I explain explicitly how the calculation can be done. The first term is easy—simply use the residual theorem:

$$\begin{aligned} & \int \frac{d^3q}{(2\pi)^3} \frac{1}{\vec{q}^2} e^{i\vec{q}\cdot\vec{R}} \\ = & \lim_{\alpha\to 0} \int \frac{d^3q}{(2\pi)^3} \frac{1}{\vec{q}^2 + \alpha^2} e^{i\vec{q}\cdot\vec{R}} = \lim_{\alpha\to 0} \frac{1}{(2\pi)^2} \int_0^\infty q^2 dq \int_{-1}^{1} dx \frac{1}{q^2+\alpha^2} e^{iqRx} \\ = & \lim_{\alpha\to 0} \frac{1}{(2\pi)^2 iR} \int_{-\infty}^{\infty} \frac{q}{q^2+\alpha^2} e^{iqR} dq = \lim_{\alpha\to 0} \frac{1}{4\pi R} e^{-\alpha r} \\ = & \frac{1}{4\pi R}. \end{aligned} \tag{D.2}$$

In the second term, additional to the pole, there is a branch cut on the positive imaginary axis because of the logarithm. Thus one has to use a more complicated path of integration:

$$\int \frac{d^3q}{(2\pi)^3} \frac{\ln\left(\frac{\vec{q}^2}{\mu^2}\right)}{\vec{q}^2} e^{i\vec{q}\cdot\vec{R}} = \lim_{\alpha,\beta\to 0} \int \frac{d^3q}{(2\pi)^3} \frac{\ln\left(\frac{\vec{q}^2+\beta^2}{\mu^2}\right)}{\vec{q}^2+\alpha^2} e^{i\vec{q}\cdot\vec{R}}$$

$$
\begin{aligned}
&= \lim_{\alpha,\beta\to 0} \frac{1}{(2\pi)^2 iR} \int_{-\infty}^{\infty} \frac{q}{q^2+\alpha^2} \ln\left(\frac{q^2+\beta^2}{\mu^2}\right) e^{iqR} dq \\
&= \lim_{\alpha,\beta\to 0} \frac{1}{(2\pi)^2 iR} \Bigg[\int_{\text{⌒}} \frac{q}{q^2+\alpha^2} \ln\left(\frac{q^2+\beta^2}{\mu^2}\right) e^{iqR} dq \\
&- \int_{\text{⌒}} \frac{q}{q^2+\alpha^2} \ln\left(\frac{q^2+\beta^2}{\mu^2}\right) e^{iqR} dq \\
&- \int_{\text{‖}} \frac{q}{q^2+\alpha^2} \ln\left(\frac{q^2+\beta^2}{\mu^2}\right) e^{iqR} dq \Bigg]
\end{aligned} \tag{D.3}
$$

The first term can again be evaluated using the residual theorem, the second vanishes, and the third gives a contribution from the discontinuity across the branch cut:

$$
\begin{aligned}
&= \lim_{\beta\to 0} \frac{1}{4\pi R} \ln\left(\frac{\beta^2}{\mu^2}\right) - \lim_{\epsilon,\beta\to 0} \frac{1}{(2\pi)^2 iR} \int_{i\beta-\epsilon}^{i\infty-\epsilon} \frac{2i\mathrm{Im}\ln\left(\frac{q^2+\beta^2}{\mu^2}\right)}{q} e^{iqR} dq \\
&= \lim_{\beta\to 0} \frac{1}{4\pi R} \ln\left(\frac{\beta^2}{\mu^2}\right) + \lim_{\beta\to 0} \frac{1}{2\pi R} \int_{i\beta}^{i\infty} \frac{1}{q} e^{iqR} dq \\
&= \lim_{\beta\to 0} \frac{1}{4\pi R} \ln\left(\frac{\beta^2}{\mu^2}\right) + \lim_{\beta\to 0} \frac{1}{2\pi R} \int_{\beta R}^{\infty} \frac{1}{x} e^{-x} dx
\end{aligned} \tag{D.4}
$$

Now the second term gives a modified Gamma function, which can be evaluated exactly in the limit $\beta \to 0$:

$$
\begin{aligned}
&= \lim_{\beta\to 0} \frac{1}{4\pi R} \ln\left(\frac{\beta^2}{\mu^2}\right) + \lim_{\beta\to 0} \frac{1}{2\pi R} \Gamma(0, \beta R) \\
&= \lim_{\beta\to 0} \frac{1}{4\pi R} \ln\left(\frac{\beta^2}{\mu^2}\right) - \lim_{\beta\to 0} \frac{1}{2\pi R} \left(\ln(\beta R) + \gamma\right) \\
&= -\frac{\ln(\mu^2 R^2) + 2\gamma}{4\pi R}.
\end{aligned} \tag{D.5}
$$

Putting everything together, the potential in coordinate space is given by:

$$
\begin{aligned}
V(R) &= -\frac{g_0^2(a)}{4\pi R} C_2(F) \\
&\quad \cdot \left[1 + g_0^2(a) \left[\beta_0 \left(\ln\frac{\pi^2 R^2}{a^2} + \gamma + \frac{31}{33}\right) - \frac{\bar{A}(1,0,N)}{4\pi} + R(N)\right]\right].
\end{aligned} \tag{D.6}
$$

Bibliography

[1] J. D. Bjorken, S. D. Drell, *Relativistic Quantum Mechanics*, McGraw-Hill (1964); R. E. Marshak, E. C. G. Sudarshan, *Introduction to Elementary Particle Physics*, John Wiley (1961).

[2] M. Gell-Mann, Phys.Rev. **125**, 1067 (1962); Phys.Lett. **8**, 214 (1964).

[3] G. Zweig, CERN Report TH 401 (1964), TH 412 (194); published in *Developments in the Quark Theory of Hadrons, A Reprint Collection*, Hadronic Press, Nonamtum, Ma. (1980).

[4] W. Panofsky, in *Proceedings of the International Symposium on High Energy Physics*, Vienna (1968).

[5] J. D. Bjorken, E. A. Paschos, Phys.Rev. **185**, 1975 (1969).

[6] F. E. Close, *An Introduction to Quarks and Partons*, Academic Press (1979).

[7] H. Fritzsch, M. Gell-Mann, in *Proc. XVI'th Intern. Conf. on High Energy Physics*, Chicago-Batavia (1972).

[8] H. Fritzsch, M. Gell-Mann, H. Leutwyler, Phys.Lett. **47B**, 365 (1973).

[9] W. Marciano, H. Pagels, Phys.Rep. **36C**, 137 (1978).

[10] H. Meyer, AIP Conf. Proc. 74, 338 (1981).

[11] G. Flugge, in *Quarks and nuclear forces*, Springer (1982).

[12] G. Morpurgo, Acta Physica Austriaca, Suppl. **21**, 5 (1979).

[13] S. Kratochvila, P. de Forcrand, Contribution to the 20th International Symposium on Lattice Field Theory (LATTICE 2002), Boston, Massachusetts, 24-29 Jun 2002 [hep-lat/0209094].

[14] K. G. Wilson, Phys.Rev. **D10**, 2445 (1974).

[15] J. Kogut, L. Susskind, Phys.Rev. **D11**, 395 (1975).

[16] H. J. Rothe, *Lattice Gauge Theories*, Second Edition, World Scientific (1997).

[17] H. B. Nielsen, M. Ninomiya, Nucl. Phys. **B185**, 20 (1985).

[18] F. J. Wegner, J.Math.Phys. **12**, 2259 (1971).

[19] L. S. Brown, W. I. Weisberger, Phys. Rev. **D20**, 3239 (1979).

[20] D. Gromes, Phys.Rep. **200**(Part II), 186 (1991).

[21] C. Michael, Nucl.Phys. **B280**[FS18], 13 (1987).

[22] H. G. Dosch, O. Nachtmann, M. Rueter [hep-ph-9503386].

[23] H. J. Rothe, Phys.Lett. **B355**, 260 (1995).

[24] H. J. Rothe, Phys.Lett. **B364**, 227 (1995).

[25] C. Michael, Phys.Rev. **D53**, 4102 (1996).

[26] X. Ji, Phys.Rev. **D52**, 271 (1995).

[27] J. Collins, A. Dunkan, S. D. Joglekar, Phys.Rev. **D16**, 438 (1977).

[28] S. Caracciolo, P. Menottie, A. Pelissetto, Nucl.Phys. **B375**, 195 (1992).

[29] G. S. Bali, K. Schilling, Ch. Schlichter, Phys.Rev. **D51**, 5165 (1995).

[30] E. Kovacs, Phys.Rev. **D25**, 871 (1982).

[31] W. Celmaster, R. Gonsalves, Phys.Rev. **D20**, 1420 (1979).

[32] A. Hasenfratz, P. Hasenfratz, Phys.Lett. **93B**, 165 (1980).

[33] P. Weisz, Phys.Lett. **100B**, 331 (1981).

[34] L. Susskind, in *Weak and Electromagnetic Interactions at High Energy*, Les Houches (1976); J. B. Kogut, in *Recent Advances in Field Theory and Statistical Mechanics*, Les Houches (1982).

[35] W. Fischler, Nucl.Phys. **B129**, 157 (1977).

[36] B. E. Baaquie, Phys.Rev. **D16**, 2613 (1977); A. Hasenfratz, P. Hasenfratz, Phys.Lett. **93B**, 165 (1980); A. Di Giacomo, G. Paffuti, Nucl.Phys. **B205**[FS5], 313 (1982).

[37] H. Kawai, R. Nakayama, K. Seo, Nucl. Phys. **B189**, 40 (1981).

[38] T. Reisz, Commun.Math.Phys. **116**,81 (1988); **117**, 79, 639 (1988).

[39] U. Heller, F. Karsch, Nucl.Phys. **B251**, 254 (1985).

[40] U. Heller, *personal communication*

[41] W. H. Press et al, *Numerical Recipes in C*, Second Edition, Cambridge University Press (1992).

[42] F. Karsch, Nucl.Phys. **B205**, 285 (1982).

[43] H. G. Dosch, Phys.Lett. B **190**, 177 (1987); H. G. Dosch, Y.A. Simonov, Phys.Lett. B **205**, 339 (1988).

[44] A. I. Shoshi, F. D. Steffen, H. G. Dosch, H. J. Pirner [hep-ph/0211287].

Acknowledgements

First I would like to thank Prof. H. J. Rothe for offering this interesting topic for my dissertation to me, for his friendly supervision and support and the intensive discussions about crucial points of the thesis. It was an interesting experience to check and to validate the lattice sum rules he himself had derived.

Next I am very grateful to Prof. W. Wetzel, who helped me checking some of my calculations for errors and who suggested both the proof of the transversality of the vacuum polarization and the proof of the gauge invariance of the expectation value of the Wilson loop to me. He invested many hours of his time on this and gave me lots of valuable hints and suggestions.

Many thanks go also to Prof. U. Heller, who provided me with some of his notes on his calculations of the potential on the lattice, using lattice perturbation theory. I got several crucial clues from these notes which helped me to understand his paper written in collaboration with Prof. F. Karsch.

I thank Prof. D. Gromes for his friendly interest and readiness to referee this thesis.

The great working atmosphere at the Institute for Theoretical Physics in Heidelberg, especially in the "Westzimmer", also has to be mentioned. I would like to thank Tanja Robens, Markus Müller, Christian Müller, Felix Schwab, Martin Pospischil, Sebastian Diehl, Kai Müller, Hendrik Ballhausen, Ewald Puchwein, Felix Nagel, Filipe Pacetti, Lala Adueva and Raffi Kasarcan for interesting and enlightening discussions, cheerful conversations and also lots of fun.

Special thanks go to Kai Schwenzer and Frank Steffen for the many hours we spent together discussing and proofreading the contribution of Prof. J. Zinn-Justin to the workshop "Topology and Geometry in Physics" of the Graduiertenkolleg "Physical Systems with many Degrees of Freedom". In these discussions, I learnt lots about toplogy, geometry and Quantum Field Theory in general, and despite the amount of work which had to be done, in our meetings there was always time left for fun.

Many thanks go to the above mentioned Graduiertenkolleg, too, for supporting me financially during my last third months working on my thesis, and for providing several interesting workshops. Additionally to the workshop on topology and geometry, the ones on Biophysics and Quantum Information were both very interesting and valuable.

Also I would like to thank the Landesgraduiertenförderung Baden-Württemberg for financial support during most of the time I worked on my dissertation and for an interesting evening in the Alte Aula of the University of Heidelberg in December 2002.

Schlussendlich danke ich auch allen meinen Freunden innerhalb und ausser-

halb der Physik, als da wären Hannes Klehr, Max Urban, Wouter Kornelis, Martina Keller, Vera Spillner und Michael Elser, für ihre jahrelange Freundschaft und Unterstützung. Besonderer Dank geht an meine Freundin Kristin Warnick und meine Familie für ihre Liebe und Geduld mit mir.